Analysis of the quantity of CPTs in relation to the inner slope stability

S. Joosten

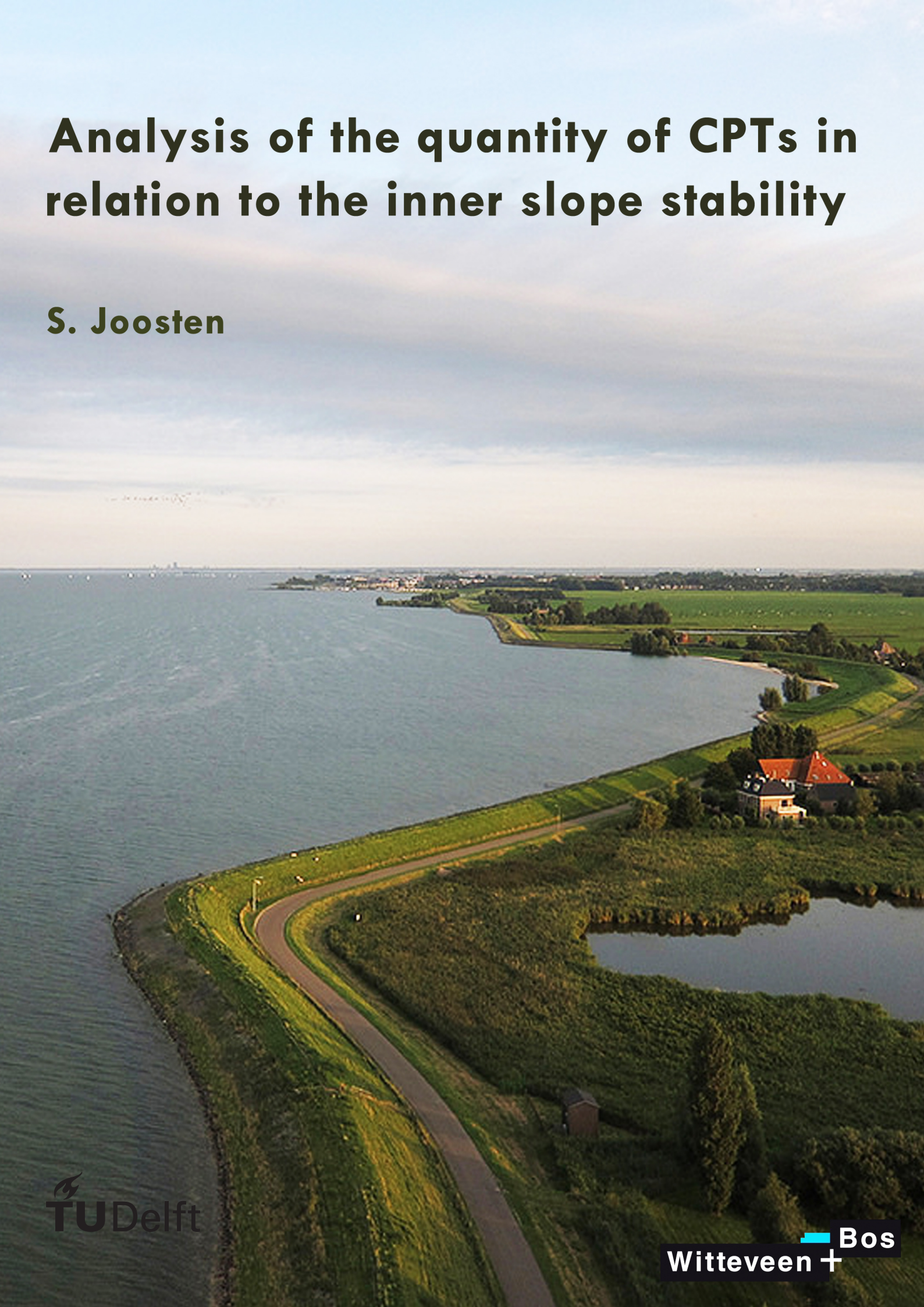

TU Delft

Witteveen + Bos

Cover photo: https://www.flickr.com/photos/de_kist/29446836193/

Analysis of the quantity of CPTs in relation to the inner slope stability

by

S. Joosten

to obtain the degree of Master of Science
at the Delft University of Technology,
to be defended publicly on Tuesday June 19, 2018 at 14:00.

Student number: 4174070
Project duration: September, 2017 - June, 2018

Thesis committee:

Prof. dr. ir. M. Kok,	TU Delft, chairman
Ir. K.J. Reinders,	TU Delft
Dr. A. Askarinejad,	TU Delft
Ir. J. de Greef,	Witteveen + Bos

An electronic version of this thesis is available at `http://repository.tudelft.nl/`.

TU Delft Delft University of Technology

Witteveen + Bos

"Information is the resolution of uncertainty"
C.E. Shannon

Preface

This thesis is part of the master program Hydraulic Engineering at Delft University of Technology. I performed this research at Delft University of Technology, Witteveen + Bos and the Markermeerdijken Alliantie. First of all I would like to thank the Markermeerdijken Alliantie for providing all the required data for this research.

I would like to thank Witteveen + Bos for the opportunity to execute this research. Particularly I would like to thank my company supervisor Jos de Greef, and part time supervisor Joost van der Meer for several fruitful discussion, positive feedback and their help throughout the last nine months. Additionally, I appreciate the willingness of all other colleagues at the Hydraulic and Geotechnical department of Witteveen + Bos to help me.

Completing this thesis would not have been possible without my supervising committee. In would like to thank Kristina Reinders particular, for her support and always useful and constructive feedback on my report. Furthermore I appreciate all the help of Mark van der Krogt regarding the use of the Probabilistic Toolkit.

I would like to thank my fellow students and friends for all joyful moments throughout the past seven years. Especially I am very grateful to Julian, Roel and Jochem since they did part of the proofreading. Finally I would like to thank Wilke and my family for supporting me throughout my entire study period.

Stan Joosten
Delft, June 2018

Abstract

The introduction of the new 'Waterwet' led to the retesting of a lot of primary flood defences within the Netherlands, sequentially certifying a lot of levees as unsafe regarding inner slope stability. To test or design a levee an adequate amount of soil investigation is required to indicate the presence of different soil types, stratification and to estimate the relevant soil parameters. The spatial spreading and the fact that the number of cone penetration tests (CPT) and boreholes within a levee to determine geotechnical parameters and stratification are limited, means that the estimated parameters always contain uncertainties.

Whereas previous studies regarding spatial uncertainty in levee design mainly focus on the identification of various soil types, this study focusses on the spatial distribution of soil parameters [22] [29] [53]. The unit weight and undrained shear strength (referred to as s_u) are two soil parameters that have a significant influence on the inner slope stability. The unit weight can be determined relatively accurately whereas s_u can show large fluctuations in longitudinal direction within the same soil type, as a result this thesis will focus on s_u. The main research question is: *How does the quantity of CPTs in longitudinal direction affect the estimation of the undrained shear strength and how is that related to the probability of failure regarding inner slope stability?*

Based on existing soil investigation the undrained shear strength amongst other soil parameters is determined. These parameters are implemented in a semi-probabilistic and probabilistic stability model. The probabilistic stability analysis provides insight in the relative influence of the undrained shear strength on the probability of failure regarding inner slope stability. A stability analysis is performed in cross sectional direction and is independent of the quantity of CPTs in longitudinal direction, therefore the theory of entropy is used to analyse the effect of changing CPT interval sizes on the estimation of the undrained shear strength.

The S_u-measured method allows to determine the undrained shear strength based on the cone tip resistance obtained from a CPT with a cone factor. The cone factor resembles the relation between the undrained shear strength determined in laboratory test and the cone tip resistance of CPTs. Linearisation of the cone tip resistance is required to decrease the number of layers in the stability analysis. A combination of two variation coefficients cover the uncertainty in the cone factor and in the linearisation. The design values of the undrained shear strength, equal to the 5% characteristic values implemented in the semi-probabilistic stability analysis, depends on these variation coefficients.

This thesis is based on one specific case of a primary flood defence along the Markermeer. All data used in this thesis is obtained from the Markermeerdijken project, within which a 5 km long research area is chosen containing a continuous peat and clay layer. Four CPTs are conducted every 100 m in longitudinal direction, linear interpolation in between CPTs is used to set up 51 cross sections. The inner slope stability of each cross section is analysed with the limit equilibrium methods of Bishop and Spencer in D-Geo Stability, which is a level I reliability method. Although simplifications within the model ensure that only layer thickness and s_u vary in longitudinal direction, the calculated safety factors still show a lot of variation, indicating that a proper estimation of s_u is important.

In contrast to a level I reliability method the relative influence of each stochastic parameter can be found by performing a FORM analysis with the Probabilistic Toolkit, requisite to quantify the influence of s_u along the critical slip surface on the probability of failure. Four scenarios are composed to quantify the influence of the undrained shear strength in cross sectional and longitudinal direction of the levee and analyse the influence of layer thickness and unit weight. The mean and standard deviation of s_u in cross sectional direction are based on the uncertainty in the determination of the cone factor, whereas the distribution in s_u the longitudinal direction is based on a combination of s_u measurements in all 51 cross sections. In the considered case study the undrained shear strength has a larger influence on the probability of failure in comparison to layer thickness, unit weight and outside water level.

A lot of guidelines are present to ensure sufficient safety within the estimation of the characteristic undrained shear strength, however barely any guidelines include the spatial variability of s_u in longitudinal direction [40],[11],[34]. As a matter of fact no guidelines are available to cover uncertainty in the estimation of the undrained shear strength in longitudinal direction.

Historical events show that the inner slope often fails over a length of 50 to 100 meter due to the presence of a weak layer [21]. In this thesis it is assumed that all weak layers that potentially can cause failure of the inner slope are characterised when a 50 m CPT interval size is conducted. As the CPT interval size increases in longitudinal direction, the minimum value in safety factor can be overseen, which can lead to optimistic estimations of the reliability. Intuitively additional CPTs lead to more information, it is however hard to quantify this assumption. As a result the theory of entropy is used to analyse the effect of changing CPT interval sizes on the estimation of the undrained shear strength. Entropy measures the amount of uncertainty/information in a dataset. Normalizing the entropy provides a measure of relative uncertainty. The available CPTs are divided into multiple datasets representing interval sizes of 100, 200, 300 and 400m. Sequentially s_u at the top and bottom of each layer is used to determine the (normalized) entropy. In general the normalized entropy decreases with decreasing interval size.

In this thesis a new partial factor (referred to as 'spatial factor') that accounts for the uncertainty in s_u in longitudinal direction is proposed. The proposed spatial factor accounts for spatial uncertainty in the undrained shear strength and assigns additional safety when the CPT interval size would be larger than 100 m for the specified research area.

Contents

List of Figures

List of Tables

List of Symbols

Abbreviations

AHN	Actueel Hoogtebestand Nederland
AL	Hinterland ('Achterland')
BI	Inner Berm ('Binnenberm')
CPT	Cone Penetration Test
CS	Cross Section
DHW	Design High Water
DSS	Direct Simple Shear test
Field	Soil investigation in and near the levee
FORM	First Order Reliability Method
KR	Crest ('Kruin')
LD	Longitudinal Direction
LEM	Limit Equilibrium Method
LRFD	Load and Resistance Factor Design
MHW	Mean High Water
MMD	Markermeerdijken
NAP	Normaal Amsterdams Peil
OI2014v4	OntwerpInstrumentarium 2014 version 4
PDF	Probability Density Function
PL	Phreatic Line
SF	Safety Factor
SLS	Serviceability Limit State
Testing field	Location where borehole and CPT are close to one another
TT	Triaxial Test
ULS	Ultimate Limit State
W	Water
WBI2017	WettelijkBeoordelingsInstrumentarium 2017

Nomenclature

α_H	Angle based on H_{nor100} to determine $\gamma_{su,ld}$	°
$\bar{q}_{net}$	Mean q_{net} over all measurements in one layer	MPa
$\bar{z}$	Mean depth over all measurements in one layer	m
β	Reliability index	–
$\beta_{req,cs}$	The required reliability index for the considered cross section as defined in OI2014v4	–
β_{uw}	Measure for the inclination of the equal unit weight contours	–
Δx	Difference in interval sizes	m
Γ	Remaining vertical reduction factor	–
γ_b	Schematisation factor	–
γ_d	Model factor	–
γ_m	Material factor	–
γ_n	Loss factor	–
γ_S	Partial factor for the strength	–
γ_v	Vertical reduction factor	–
$\gamma_{sat,ref}$	Reference unit weight at which the cone resistance is constant	kN/m^3
$\gamma_{su,ld}$	Spatial factor: Partial safety factor that accounts for uncertainty in $s_{u,ld}$	–
γ_{unsat}	Unsaturated unit weight of soil	kN/m^3
μ_x	The mean of X	–
$\mu_{ln(x)}$	The mean of X for a log normal distribution	–

ϕ'	Angle of internal friction	°
σ'_{vi}	in-situ effective vertical stress	kN/m^2
σ'_{vy}	Pre-consolidation pressure	kN/m^2
σ_n	normal stress	kN/m^2
σ_x	The standard deviation of X	–
$\sigma_{ln(x)}$	The standard deviation of X for a log normal distribution	–
$\sigma_{su,ent}$	Adapted standard deviation of s_u based on relative entropy and interval size	kPa
σ_{vo}	in-situ total vertical stress	kN/m^2
τ_f	Shear strength	kN/m^2
a	The ratio of the cone base cross section and the total cross section	–
B_q	Normalized pore pressure parameter	–
c'	Cohesion	kN/m^2
c_i	Constant	m
D_{cone}	Cone diameter	mm
f_s	Sleeve friction	MPa
$H(X)$	Discrete entropy	nat
H_{max}	Maximum discrete entropy	nat
H_{nor100}	Normalized entropy for 100 m CPT interval size	–
H_{nor}	Normalized entropy	–
I_p	Measure of information/uncertainty	nat
k_n	Statistical coefficient equal to 1.645 for the 5% quantile with n=∞	–
m	exponent for the increase in strength	–
n	Number of samples	–
$N_{kt,k}$	The characteristic value of the cone factor	–
N_{kt}	Cone factor	–
$n_{m,cpt}$	Number of measurements in one CPT	–
$n_{m,reg}$	Number of measurements in all CPTs used for cone factor determination	–
OCR	Over Consolidation Ratio	–
p_i	Probability of occurrence	%
POP	Pre Overburden Pressure	kN/m^2
Q	Normalized cone penetration resistance	–
q_c	Cone tip resistance	MPa
q_t	Corrected cone tip resistance for pore water pressure	MPa
q_{net}	Normalized cone tip resistance	MPa
$q_{t,ref}$	Reference cone resistance at which the unit weight is constant	Mpa
R_d	Design value of the resistance	–
R_f	Friction ratio	%
R_k	Characteristic value for resistance	–
$R_{f,ref}$	Reference friction ratio at which the apex of all lines of equal unit weight is located	–
r_{sys}	The systematic error	–
S	Normal consolidated undrained shear strength ratio	–
S_d	Design value of the strength	–
S_k	Characteristic value for strength	–
s_u	Undrained shear strength	kN/m^2
$s_{u,lin,i}$	Linearised undrained shear strength	kPa
u_0	Equilibrium pore pressure	MPa
u_2	Pore water pressure	MPa
VC_x	The variation coefficient of X	–
VC_{Nkt}	The variation coefficient for the difference between $s_u - q_{net}/N_{kt}$	–
VC_{reg}	Regional variation coefficient	–
VC_{tot}	The total variation coefficient of the undrained shear strength	–
VC_{trans}	The transformation variation coefficient	–
x	Interval size	m
X_k	Characteristic value	–
Z	Limit State Function	–
z	Depth	m

1 Introduction

1.1. Background information

The protection of people and assets against a potential flood is a topic that has been of great importance within delta areas such as the Netherlands for a long time. This directly involves the probability of failure of the water retaining structures along the primary water ways. Most of these structures are levees that mainly consist of soil. The calculated safety of a levee depends on the considered failure mechanisms, the variation in soil types and profile, the geotechnical parameters, the applied loads and assumed water levels.

In 2017 a new law, the 'Waterwet', was introduced in the Netherlands. This resulted in a new standard to assess the safety of levees and structures regarding floods, the WBI2017 (Wettelijk Beoordelingsinstrumentarium 2017). The WBI2017 uses a 'probability of flooding' in comparison to the old method that uses a 'probability of exceedance'. The introduction of the new law led to retesting of a lot of levees within the Netherlands, sequentially certifying a lot of levees as unsafe.

In order to be able to design or test a levee sufficient data should be available. The water level of the adjacent water body and traffic loads are often well known as is their probability of occurrence. The soil profile and the soil characteristics give rise to the largest uncertainties within the design. In order to gain as much information as possible within the given budget it is of importance that the soil investigation is conducted properly.

Depending on the governing failure mechanisms the soil investigation can be specified, in this thesis the inner slope stability is the only considered failure mechanism. The purpose of soil investigation is to gain more insight in the subsoil at a certain location. It helps to give an indication of the presence of different soil types and their stratification, moreover soil investigation can give information regarding a lot of soil parameters. The purpose to conduct soil investigation within a levee design can therefore be divided in soil profile and soil parameters, see figure 1.1. It has to be emphasized that this division does not suggests that soil parameters and soil profile are completely independent. The occurrence of soil types and the stratification belong to the soil profile while the strength and density are soil parameters. Obviously there are many more soil parameters, however these are the most important within levee design.

The uncertainty regarding the soil profile and the presence of certain soil types is covered, up to a certain extent, within WBI-SOS. For a more precise estimation either in-situ soil investigation with Cone Penetration Tests (CPTs) are required or a geologist (with knowledge of the area) can provide more insight. It is stated that the inner slope can fail, when a weak layer of usually more than 50 meter is present in longitudinal direction [21]. Examination of historical slope failures showed that a slope often fails over a length of approximately 50-100 meters and therefore layers shorter than 50 meters do not cause the levee to fail on its own. The probability that a weak layer, which can cause slope instability, will not be indicated when the interval between CPTs in longitudinal direction is 50 m is very small. Although theoretically this may be true, this interval size is seldom applied in practice, which therefore includes some spatial uncertainty within the design. It is however uncertain which CPT interval size is sufficient for practical applications, or what the advantages are when the interval size is decreased.

Spatial uncertainty in the subsoil often focusses on the occurrence of different soil types and profiles, whereas certain soil properties, e.g. the undrained shear strength, variates in longitudinal direction as well. The

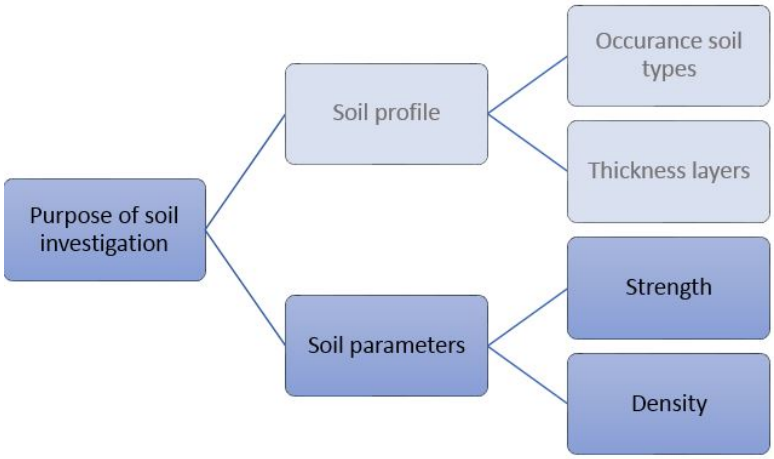

Figure 1.1: Purpose of soil investigation within a levee design considering Limit Equilibrium Methods (LEM)

undrained shear strength often provides a significant part of the resistance regarding inner slope stability, if the subsoil consists of predominantly cohesive layers. Furthermore the density/unit weight can either influence the driving moment or the resisting moment depending on the position in the cross section. The unit weight can be determined with more accuracy than the undrained shear strength and therefore this thesis focusses on the undrained shear strength.

The probability of failure is often based on one representative cross section within a levee segment. The choice of this cross section is often (not necessarily) based on the CPT profile, the stratification and the geometry that represent the most unfavourable situation. It is however uncertain if this unfavourable cross section is a good representation of the levee in longitudinal direction, because there are hardly any guidelines regarding the interval size between the successive cross sections. The spatial uncertainty that arises when the interval length is increased, is not considered within the process of a levee design. Therefore the selected unfavourable cross section could either be conservative or unsafe.

From an engineers perspective the purpose of soil investigation is to gain more knowledge and thereby to improve the design in terms of cost and safety. Additional soil investigation within a levee design often results in increasing reliability however simultaneous the cost increase as well due to the discovery of a more unfavourable cross section.

As indicated some research has been done on the distance between CPTs within a levee design. These studies often consider the variation in soil profile and hardly ever consider the spatial distribution of soil parameters within a layer [22] [29] [53]. This research will mainly focus on the spatial distribution of the undrained shear strength within one geological deposit. As the undrained shear strength depends on the stratification this cannot be neglected completely.

1.2. Problem description

The spatial spreading and the fact that the number of CPTs and boreholes within a levee to determine geotechnical parameters are limited, means that the estimated parameters always contain uncertainties. Intuitively it seems obvious that data densification results in less uncertainty. It is however still hard to quantify the effect or added value of this additional data, specifically additional CPTs. The way a soil investigation is set up is therefore of importance to diminish these uncertainties as much as possible.

The problem description can be summarized as follows: It is uncertain what the benefit of additional CPTs within a levee project is with respect to the determination of the undrained shear strength and how this relates to the inner slope stability. In other words, it is uncertain how the quantity of CPTs affects the final levee design.

1.3. Research objective and questions

The objective is to gain more insight in the relation between the undrained shear strength and the inner slope stability and thereby take the amount of soil investigation into account. The uncertainty regarding parameter determination as well as the spatial uncertainty of the undrained shear strength is considered. The research will be conducted based on the information available in a case study. Based on the problem description and the objective the main research question is:

How does the quantity of CPTs in longitudinal direction affect the estimation of the undrained shear strength, and how is that related to the probability of failure considering inner slope stability?

This question can be answered by answering the following sub-questions.

- What is the current way to deal with the uncertainty regarding inner slope stability and how does this relate to engineering practice?
- How does the quantity of CPTs and laboratory tests influence the uncertainties within the estimation of the cone factor (N_{kt})?
- How does the amount of soil investigation (CPTs) influence the calculated inner slope stability?

1.4. Methodology and report structure

To answer the proposed research questions the Markermeerdijken project is used as a case study. Equally to practice, the steps shown in figure 1.2 succeed each other in this thesis. These steps also represent the chapter sequence. The information and tools which are used to complete these steps are presented on the right side of the figure.

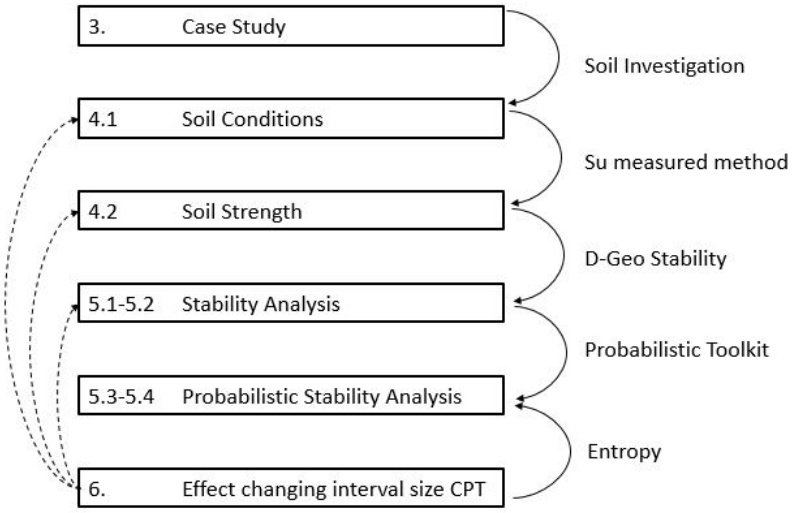

Figure 1.2: Methodology

The answer to the research question can be divided into two parts:

1. The effect of the undrained shear strength on the probability of failure considering inner slope stability will be answered with chapter 3 to 5. At first the Markermeerdijken project is chosen as a case study. Within that case soil investigation is conducted, consisting of CPTs, boreholes and laboratory tests, that are used to determine the soil conditions and soil strength. Thereafter a slope stability analysis is performed. In chapter 5 the relative influence of the undrained shear strength on the slope stability is determined with a probabilistic stability analysis.

2. How the quantity of CPTs in longitudinal direction affect the undrained shear strength is answered in chapter 5 and 6. The theory of entropy is used to determine the uncertainty in the available data and the effect of changing CPT interval sizes. A combination of chapter 6 and 5 can help to answer the question

how the quantity of CPTs influences the slope stability. The amount of available data influences chapter 4 and 5 as well, which is indicated with the dotted lines in figure 1.2.

The chapters as shown in figure 1.2 are succeeded by the conclusion, discussion and recommendations.

1.4.1. Boundary conditions and limitations

The major boundaries and limitations within this research can be listed as follows:

- The inner slope stability is the only failure mechanism that is considered.
- It is stated that the inner slope fails, when a weak layer of usually more than 50 meter is present in longitudinal direction [21]. A CPT interval length of 50 meters will therefore be considered as the minimum interval length to safely design a levee considering inner slope stability.
- This research mainly focusses on the spatial variability of the undrained shear strength and to a lesser extent on the variability of the soil profile.
- Within this research the Markermeerdijken Project is used as a case study. Therefore the results are only based on this location.

2
Background Information

Within this chapter the mechanisms, models and soil investigation that is required for the determination of the inner slope stability is elaborated on. At first the considered safety philosophy is presented, resulting in the required probability of flooding. The theoretical background concerning slope stability is explained, herein the focus lies on the method that is currently applied in the Netherlands. The soil conditions and soil strength can be determined with the results from in-situ and laboratory test. The Critical State Soil Mechanics (CSSM) and the associated SHANSEP and S_u-measured method are explained. In practice often a combination of SHANSEP and the S_u-measured method is applied. Finally the requirements regarding the required reliability are presented.

2.1. Safety philosophy

All dunes, river and lake levees are subjected to the standard formulated in the 'Waterwet'. This standard is based on the requirement that all people that live behind a dune or levee have a probability of at most 1/100.000 per year to pass away as a cause of inundation. Areas where consequences are large, in terms of assets or due to a large number of people, have stricter requirements. To ensure that the required safety is obtained the WBI2017 can be consulted [41].

The WBI2017 uses a probability of flooding, which is the probability that inundation occurs. A levee can fail due to a lot of different failure mechanism, some of which are listed in figure 2.2. The failure mechanisms which are most relevant regarding the safety of a levee are: overtopping, piping, inner slope stability and damage to the revetment [23]. These failure mechanisms are accounted for in the estimation of failure probability ('faalkansbegroting'), each with their own share in the total probability of failure, figure 2.1. By default the inner slope stability, the only considered failure mechanism within this thesis, has a share of 4% within the estimation of probability of failure. It therefore seems of minor importance at first, however a lower share within the total probability of flooding will result in stricter requirements for the failure mechanism. In case the probability of flooding is equal to 1/5.000 for the entire levee and all failure mechanisms combined, a 4% share within the estimation of probability of failure for inner slope stability will result in probability of failure equal to 1/125.000. Furthermore inner slope stability is a failure mechanism which is less predictable

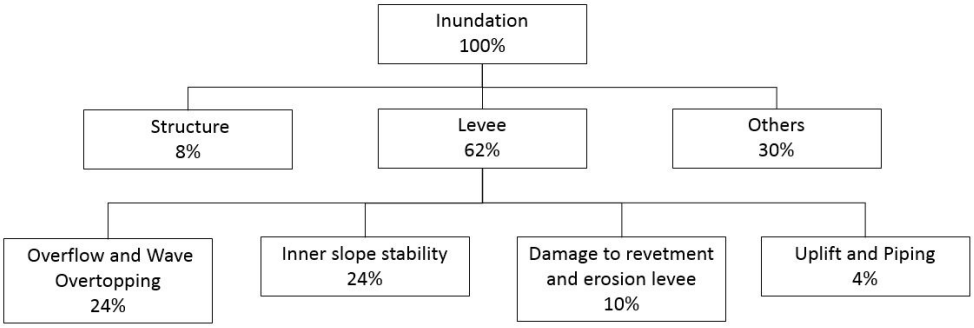

Figure 2.1: Maximum allowable failure probability in percentages of the total probability of inundation

in comparison with for instance overtopping (24% of total probability of failure) and therefore requires just as much attention.

For each levee project it can be decided to deviate from the default standards, for the Markermeerdijken project a share of 24% is implemented for the inner slope stability, figure 2.1 [2]. This reclassification is made because the probability that piping occurs is minimal, while the probability regarding failure of the inner slope is significant.

2.2. Theory inner slope stability

A slope fails if the resisting moments along a slip surface are smaller than the driving moments caused by the soil weight under the crest. The shear forces along this sliding plane are overruled, which results in a volume of soil sliding down a slope as is visualized in figure 2.3 [55]. This mechanism is often triggered after or during a long period of high water. In such a case the driving forces exceed the resistance forces due to the decrease of effective stress within the levee.

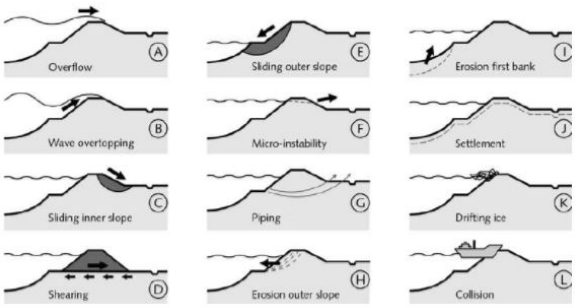

Figure 2.2: Failure modes of levees [60]

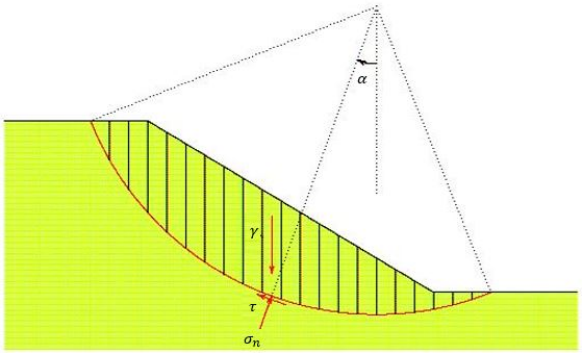

Figure 2.3: Inner slope stability with method of Fellenius [58]

2.2.1. Limit equilibrium methods

Several methods are available to describe the mechanism of slope failure. Some examples of Limit Equilibrium Methods (LEM) are: Bishop, Spencer and Uplift Van [13]. These methods differ due to the shape of slip surface and the distribution of shear stresses along the slip surface. The limit equilibrium method describes the process of a piece of soil sliding down a slope because gravitational forces overcome the shear stress capacity within the soil body. Deformations of the soil body that occur due to the instability are not considered in the limit equilibrium method. Such deformations can be analysed using a finite element method, Which is not considered within this thesis. In the following paragraphs the methods of Bishop, Spencer and Uplift Van are briefly elaborated.

Method of Fellenius and Bishop The stability is described as the driving and resisting moments around a point above the levee. Within the resisting moment, the shear forces along a potential sliding surface are considered. The slip surface is divided into multiple slices that each have there own weight, these cause the driving moment. The methods described by Fellenius and Bishop are based on the described phenomena, see figure 2.3. Bishop includes a reduction factor to cohesion and friction, whereas Fellenius neglects this factor [13].

Method of Spencer Spencer came up with a method that describes a total equilibrium. He took into account the equilibrium of both horizontal and vertical forces. Furthermore the slip surface does not necessarily have to be circular, but could also obtain other shapes. The Spencer method therefore seeks for the slip surface with the least resistance, this often causes a vast part of the slip surface to be situated in relatively weak layers. Because the slip surface is not restricted to a round shape the safety determined with this method will always be equal or lower than the safety determined with Bishop.

Method Uplift Van As the name of the method describes, this method accounts for uplift within a cross section. Uplift occurs when upward water pressures in the hinterland, caused by high water levels in the river or lake, exceed the downward force induced by the weight soil. This method differs from the others due to its shape and is characterised by a horizontal line in between to half circular shapes. Uplift could occur in the horizontal part in between the two half circles. The two slip circles are described similarly as the Bishop method, in the horizontal part only horizontal equilibrium is considered.

Depending on the considered cross section, different LEMs can be applied. In the OI2014v4 the LEM of Spencer is recommended [40], since it best represents the critical slip surface. As a result of numerical problems/inaccuracies in the method of Spencer also the Uplift Van method is often used in practice. In case the critical slip surfaces of Spencer and Uplift Van are almost circular it can be justified to use the LEM of Bishop.

2.3. Soil investigation

The subsoil contains a lot of variability in soil types, stratification and soil parameters. In order to properly design a levee this variability needs to be quantified and mapped with soil investigation. The design process of a levee, in specific the soil investigation, can be rather complicated due to several aspects. There is no standard framework to set up a soil investigation. Although there are guidelines available which provide some relieve, every levee project is unique and requires special attention. In 2017 a new law, the 'Waterwet', was introduced in the Netherlands that obligates the use of new calculation methods, which require a different approach to set up soil investigation. The expertise on which decisions regarding soil investigation were mainly based on in the past seem to be of less use with the new standard. The set up of soil investigation becomes even more complex considering that a lot of failure mechanism require different set ups.

In the new standard (WBI2017) the WBI-SOS model is used as a stochastic underground model and can be used in the preliminary stages of the design. The WBI-SOS can give a good indication of the expected soil variability and the probability of occurrence for a particular soil profile along a levee [20]. Nevertheless in further design stages the in-situ and laboratory data will be governing. Several in-situ measurement equipment is available nowadays of which the Cone Penetration Test (CPT) is most used in the Netherlands. The results from the laboratory tests and CPTs can directly be coupled when they are conducted close to another (see section 2.3.4)[39].

The reason to set up a soil investigation will be elaborated on in this chapter. Furthermore the required CPTs and laboratory test are described and how the results of these test can be combined. Subsequently a spatial overview of a typical soil investigation is presented. The main information soil investigation has to provide in order to determine the inner slope stability is:

- Presence of different soil types
- Stratification of the subsoil
- Undrained shear strength
- Over Consolidation Ratio (OCR)
- Unit weight, water level and thereby soil stresses in the levee
- Parameters S and m (see section 2.4)

2.3.1. Reason for soil investigation

As figure 1.1 indicates, a distinction can be made in between the different variabilities that are present in the subsoil. Soil investigation or geological knowledge is required to map this variability. The purpose of soil investigation is to indicate the difference in soils, stratification and soil parameters. In this thesis the focus lies on the fluctuations of the undrained shear strength and to a lesser extend on the variability of the soil profile.

Over the years different materials are deposited, resulting in the current stratification. In the Netherlands the subsoil conditions can differ a lot over a short distance due to the large diversity in soil deposits. This diversity is caused by, among other things, sea level rises and river divergences [25]. The different deposits cause the subsoil to be heterogeneous; a soil body that contains at least two elements or layers with different physical properties. The depositions over time led to the anisotropic properties of most soil bodies. Anisotropy means

that the properties within the layer are directional dependent. As an example, the undrained shear strength shows much more fluctuations on a small scale in vertical direction in comparison to the horizontal direction and is therefore anisotropic. The regional variation in the soil is caused by different processes in the past, e.g. ice ages. These processes can cause the considered subsoil to be over consolidated due to the presence of loads in the past. The undrained shear strength is dependent on such processes and therefore fluctuates in horizontal direction within the same material [8].

The first dozens of meters of soil, originating from the Pleistocene and Holocene era, are of most interest regarding levee design. Besides the vast variability in the subsoil, the levee itself tends to contain an even bigger variability in stratification and parameter determination because it is a man-made structure. The levee can contain several different types of materials that were used throughout the years to construct the levee. The variability and thereby the uncertainty of this anthropogenic soil body is less predictable in comparison with geological deposits. For inner slope stability calculations the characterisation of anthropogenic material and the weakest layers are most important, figure 2.4.

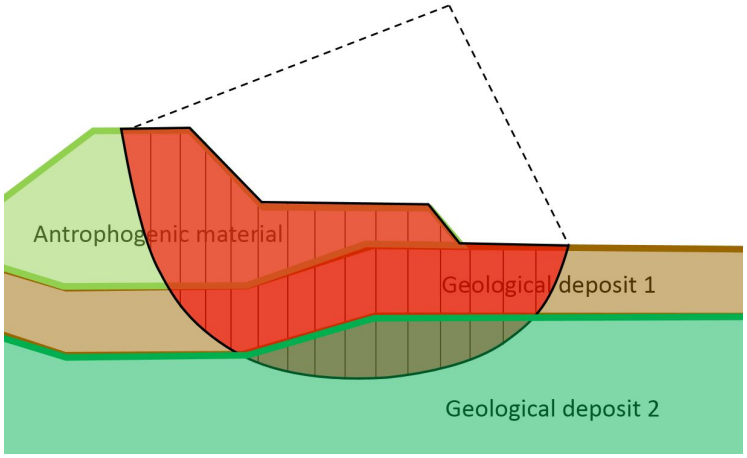

Figure 2.4: Example of cross section containing anthropogenic material

2.3.2. Cone Penetration Test (CPT)

As the name indicates the basic technique of the Cone Penetration Test (CPT) is driving the cone vertically through the soil with a constant velocity. The force required to penetrate the soil is measured and is an indication of strength/stiffness. Based on this strength/stiffness the soil can be classified, a higher strength coincides with more dense soils like sand, whereas a lower strength coincides with soft soils like peat.

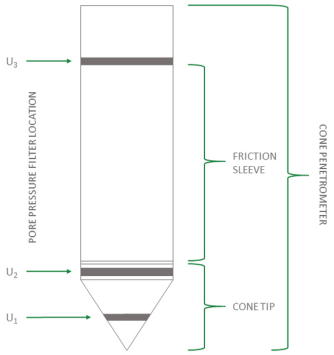

Figure 2.5: Terminology for cone penetrometers [31]

A cone as shown in figure 2.5 is most often used in a CPT and consist of two load cells which measure the cone tip resistance and the sleeve resistance. The cone is pushed into the soil at constant rate which results in a nearly continuous measured profile of the resistance. During a CPT both the cone tip resistance (q_c) and the sleeve resistance (f_s) are measured every 2, 5 or 10 cm, an example of the results are given in figure A.6. The results give a detailed overview of the stratigraphic profile and can be used for the estimation of geotechical parameters. In a CPTu also the pore water pressures are measured, depending on the location of the equipment within the cone the pore water pressure is indicated with u_1,u_2 or u_3. u_2 is measured directly behind the cone and is the most common in the Netherlands. The main advantages of a CPT are fast and nearly continous measurments, it is repeatable and provides reliable data[43]. The disadvantage of a CPT is that no soil samples is obtained.

Researchers tried to estimate a lot of parameters from raw CPT data of which some are listed here: soil unit weight, undrained strain shear, soil sensitivity, over consolidation ratio, in-situ stress ratio, relative density, friction angle and stiffness [43]. The complexity of soil causes these parameters to be obtained with the help of empirical formulas. Although a lot of parameters can be estimated with a CPT, depending on the size and risk of a project soil samples are required to test in the laboratory in order to improve the accuracy.

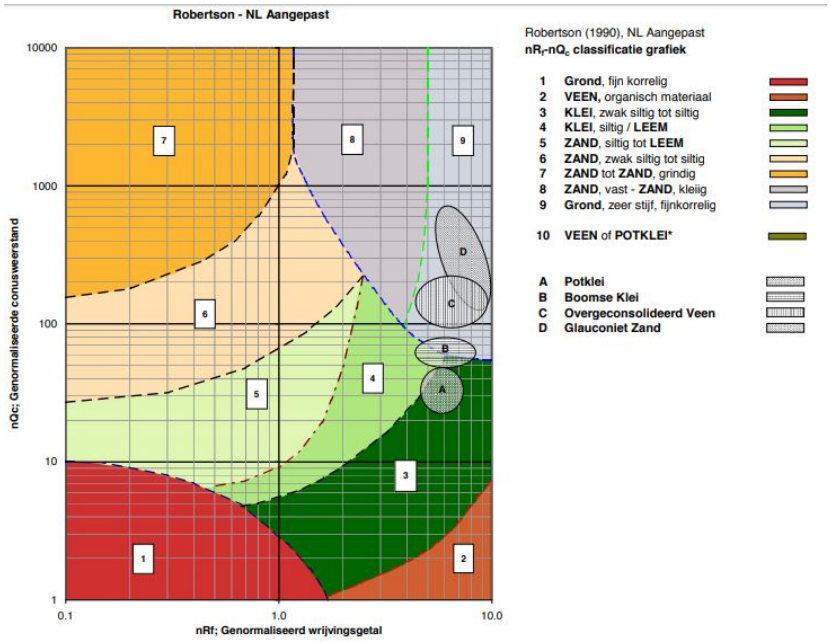

Figure 2.6: Normalized SBT chart Robertson adapted for Dutch soil conditions [18]

In the Netherlands the subsoil conditions can differ a lot over a short distance due to the large diversity in soil, see section 2.3.1. An indication of the variation in the subsoil that is present and the stratification is of importance to indicate the stability of a levee. The CPT is very useful to determine the stratification and the presence of different soil types. Soils can be characterised by their difference in behaviour which is expressed in strength (q_c) and friction (f_s). The soil type is often indicated with a Soil Behaviour Type (SBT), which can be displayed in a SBT chart. Several researchers developed a SBT chart, but the normalized chart of Robertson is the most popular one, see appendix A. A specially adapted version to account for typical Dutch soils is presented in figure 2.6 [18]. The chart is divided into 9 different zones, which each represent different soil types based on their behaviour. Despite the Dutch SBT version, typical Dutch soils, e.g. peat and organic soils are often misclassified. A more extensive explanation of the CPT is provided in Appendix A.

Although one single CPTs can provide a good insight in variability in vertical direction, the horizontal variability has to be covered with multiple CPTs. Since the number of CPTs (and boreholes) within a levee are limited, the estimated parameters always contain uncertainty. The spatial set up of a soil investigation is of importance to reduce this uncertainty as much as possible. Horizontal variability can be divided in cross sectional and longitudinal direction of the levee.

The stratification can show large variations on a small scale. These large variations can partly be devoted to the anthropogenic material in the levee and due the compressed underlying geological layers, figure 2.4. Consequently at least 3 CPTs are required to properly map the stratification in cross sectional direction.

Since the fluctuations in stratifications and parameters are larger in cross sectional direction than the longitudinal direction the spatial spreading CPT is large in the longitudinal direction. The distance between the successive cross sections is often equal to 100 meters as indicated in figure 2.11, but can differ per project.

2.3.3. Laboratory tests

Laboratory test are required to determine the undrained shear strength amongst other parameters. Before the laboratory test can be conducted samples have to be obtained from boreholes at a specific location and depth. The retrieved soil from such a borehole can also be used to determine the presence of different soils and the stratification. This soil classification method is dependent on the experience of the operator and is therefore prone to errors.

The most common laboratory test to determine the undrained shear strength are the Direct Simple Shear test (DSS) or the Triaxial Test (TT). Furthermore compression test are required to determine certain parameters which are required for the SHANSEP method (S and m), see section 2.4.1. Within the DSS and triaxial test also the unit weigth and water content are determined.

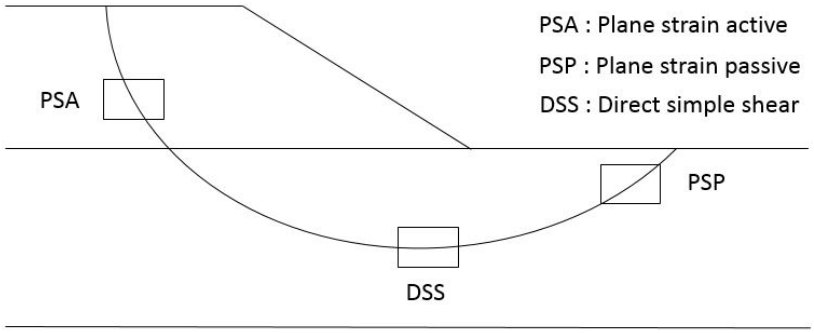

Figure 2.7: Laboratory test depending on the position in the failure plane [27]

Although the DSS test and the Triaxial Test have a lot in common, there are still some key differences and therefore it is important to know which test is most suitable to determine the shear strength within a levee. In figure 2.7 a slip surface is shown on which the appointed laboratory test are projected at different locations in the slip surface. Within a triaxial test (PSA in figure) the specimen will fail under a certain angle and therefore this figure suggest this test should be used on the steep part of the slip surface, while the DSS test (DSS in figure) fails horizontally and thus should be used in the bottom part of the slip surface. If the average of the undrained shear strength over a slip surface is required the DSS test gives a good or slight conservative estimation, moreover the bottom of the slip circle is most critical regarding slope stability [27]. The plane strain passive (PSP) shown in figure 2.7 is not considered in this thesis.

The undrained shear strength obtained from a DSS test is generally lower in comparison to the results from the triaxial tests. The type of test thereby influences the obtained undrained shear strength which is used within the project. This concludes that the results cannot simply be compared and moreover that the have to be used with care, especially results from triaxial test.

The undrained shear strength can also be determined with the help of Field Vane tests, however according to Ladd these often show divergent results to the actual shear strength. Furthermore there are not sufficient tests within the case study and therefore the field vane is not considered [27].

Direct Simple Shear Test The Direct simple shear test is used to determine the undrained shear strength of a soil specimen and is most often performed on soft soils such as peat and clay. The sample has to be consolidated before the test is conducted. The consolidation stress needs to be chosen with care, because it can affect the undrained shear strength. In case the consolidation stress is too low, the soil will behave as a over consolidated soil. In this case negative pore pressures can accumulate in the sample which lead to higher undrained shear strengths. A consolidation stress equal to, or higher than the yield strength causes the soil to behave normal consolidated (OCR = 1) [19]. In case DSS test are combined with CPT results, to estimate the undrained shear strength locally as explained in section 2.4.2, the in-situ stress has to be used as consolidation stress.

A round specimen is placed within a box, which is divided in a upper box and a lower box, these boxes can move separately. The specimen is closed with a porous stone on both the top and bottom, this prevents excess pore pressure during the test. During the test a constant vertical force (F_v) is applied at the top of the specimen, while a increasing horizontal force (F_h) is applied at the upper box, see figure 2.8. This will eventually lead to failure of the soil specimen. During the process both the vertical and the horizontal movements are measured, these can be translated to axial and shear stresses respectively.

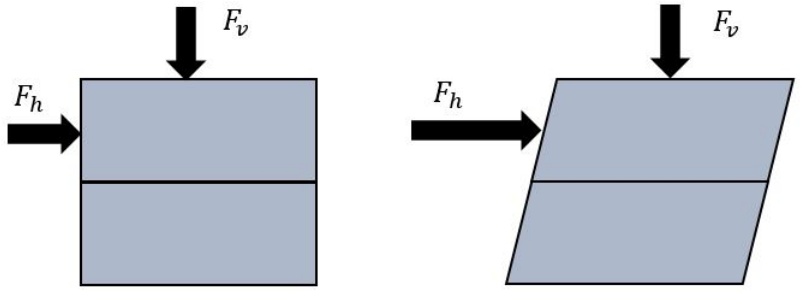

Figure 2.8: Set up DSS test

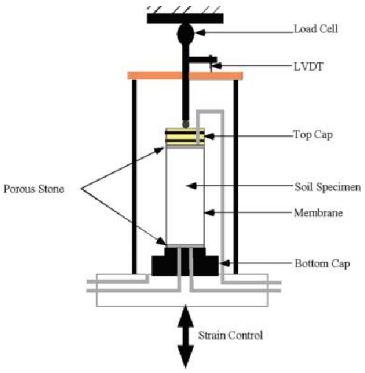

Figure 2.9: Set up Triaxial Test [63]

Triaxial Test Similar to the DSS test the triaxial test is used to measure the shear strength of a specimen. A cylindrical specimen is covered with a membrane and sequentially a load is applied to the top of the specimen. A valve is used to regulate the water pressures during the test. A triaxial test can be divided into two stages, the consolidation phase and the shear phases. In total there are 3 different types of traixial test.

- Consolidated-Drained (CD): The valve is always open during this test. This is a effective stress test because no excess pore pressures can accumulate. This test generally takes very long.
- Consolidated-Undrained (CU): During shear the pore pressures are measured, in this case both the effective and the total stresses can be computed.
- Uncosolidated-Undrained (UU): The valve is always closed. This a total stress test because excess pore pressures can accumulate during the test. Because the specimen does not have to be consolidated this test can be performed very quick.

The use of CSSM requires the shear strength in undrained conditions, only the CU and the UU test fulfil these requirements, section 2.4. The Consolidated-Undrained test is most suitable since both the total as well as the effective stresses can be computed. The choice for the consolidation stress is similar to the DSS test and therefore depends on which method will be used to determine the undrained shear strength, see section 2.4.2.

The triaxial test can fail either due to shear, by barrelling (distributed shearing) or due to both mechanisms simultaneously. In case the sample fails by barrelling it is expanded in horizontal direction and compressed in vertical direction. Although the barrelling does not have a typical failure plane often small failure planes are present within the specimen. In general all three possible failure mechanism are used to determine the undrained shear strength.

Test results As can be seen in figure 2.10, stress strain profiles can be different depending on the soil history or how dense a soil is packed. An over consolidated clay has a peak stress higher than the critical stress (residual stress in the figure). Such a soil specimen expands during a DSS test, while a normal consolidated sample contracts during the test. It is important to notice that both over consolidated and normal consolidated soils (within the same geological deposit) have similar critical stresses. In practice these critical stresses can differ due to inaccurate measurements or sample disturbance. In the CSSM large strains are assumed to be present during failure and therefore the critical strength is used within the stability analysis, see section sec:CSSM. For peat and clay the large strain requirements are 25% and 40% strain respectively, independent of the performed test.

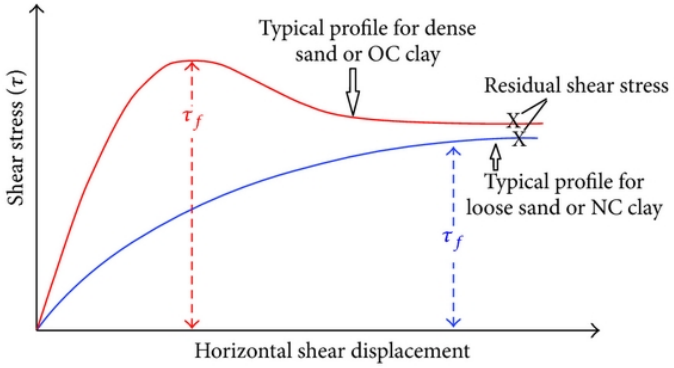

Figure 2.10: Typical result from a DSS test [10]

2.3.4. Combination CPTs and laboratory test

A spatial overview of how CPTs and boreholes are generally situated within a levee design is presented within figure 2.11. Often a CPT interval of 100 m in longitudinal direction is conducted in levee projects.

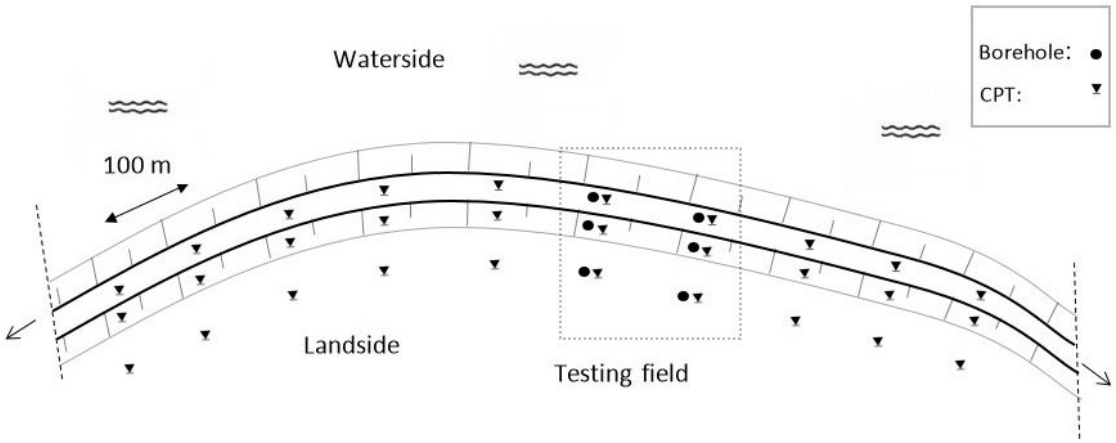

Figure 2.11: Typical spatial overview of soil investigation in a levee project

Results of the laboratory test can be combined with CPT data to estimate the undrained shear strength at each CPT location. This method, referred to as the S_u-measured method is described in section 2.4.2. Combining CPT data with laboratory test can only be done in case the borehole, which contained the considered (tested) soil sample, is close[1] to the conducted CPT [39]. Often multiple borehole-CPT combinations are conducted in a so called testing field. In the testing field the correlation between the cone tip resistance and the undrained shear strength obtained from laboratory test is determined (see section 2.4.2). As figure 2.11 indicates the testing field is partly located on the levee, this is however not essential.

[1] Whereas the distance between borehole and CPT was approximately 0.5 m in Schematiseringshandleiding Macrostabiliteit 2015 [57], the distance is defined as 'close' in the version released in december 2016 [39]

2.4. Critical Soil Strength Mechanics (CSSM)

Within the new standard (Waterwet) it is mandatory to calculate slope stability according to the Critical State Soil Mechanics (CSSM). In the old standard, the Mohr Coulumb method was used to determine the shear strength based on the angle of internal friction and the cohesion as in equation 2.1.

$$\tau_f = c' + \sigma_n \cdot tan(\phi') \tag{2.1}$$

The CSSM is internationally acknowledged to calculate slope stability. The main differences between the Mohr Coulomb method and the CSSM are:

- Within the CSSM the soil history (the over consolidation ratio) is taken into account. Loads that where present in the past and caused the soil to be densified, influence the estimated undrained shear strength in case CSSM is applied.
- Within the CSSM peat and clay like soils are considered to be undrained during slope failure.
- The CSSM makes use of large strains, while the Mohr Coulomb method assumes that small strains are representative during failure. With the use of critical undrained shear strengths it is assumed that the undrained shear strength is mobilized along the entire slip surface. The use of critical undrained shear strengths leads to another interpretation of laboratory test, like DSS and triaxial test. In figure 2.10 it is shown that at large strains samples in similar geological deposits will have similar undrained shear strengths independent of the soil history.

Within the Netherlands there are two methods that can help to describe the slope stability based on the CSSM, the SHANSEP method (or WBI-Method) and the S_u-measured method (or Dijken op Veen method). Within the following sections the two methods and the corresponding parameters are briefly discussed [14].

2.4.1. SHANSEP method

In the SHANSEP method, the undrained shear strength, for clay and peat, can be determined with equation 2.2. This equation can be explained with the help of figure 2.12. When the over consolidation ratio is equal to 1, a linear relation between the undrained shear strength and the in-situ vertical stress(σ'_{vi}) can be described by the normal consolidated undrained shear strength ratio (S). The linear relation presented by the orange line is called the critical state line, all stress paths will end up on this line.

In case the soil is over consolidated the dotted line (OCR^m) replaces the critical state line. This means that over consolidation causes the soil to have a higher undrained shear strength with equal effective stresses in comparison to soils that are normal consolidated, implying that the SHANSEP method accounts for soil history. All stress paths originating from soil samples obtained from similar geological deposits and similar depths will theoretically end up in the same point on the critical state line, also known as the critical strength.

The OCR of the soil can be determined based on the Pre Overburden Pressure (POP) or the pre-consolidation pressure (σ'_{vy}), equation 2.3.

$$s_u = \sigma'_{vi} \cdot S \cdot OCR^m \tag{2.2}$$

$$OCR = \sigma'_{vy} / \sigma'_{vi} = (\sigma'_{vi} + POP) / \sigma'_{vi} \tag{2.3}$$

Where:

s_u	=	Undrained shear strength	$[kN/m^2]$
σ'_{vy}	=	Pre-consolidation pressure	$[kN/m^2]$
σ'_{vi}	=	In-situ effective vertical stress	$[kN/m^2]$
OCR	=	Over Consolidation Ratio	$[-]$
S	=	Normal consolidated undrained shear strength ratio	$[-]$
m	=	Exponent for the increase in strength	$[-]$
POP	=	Pre Overburden Pressure	$[kN/m^2]$

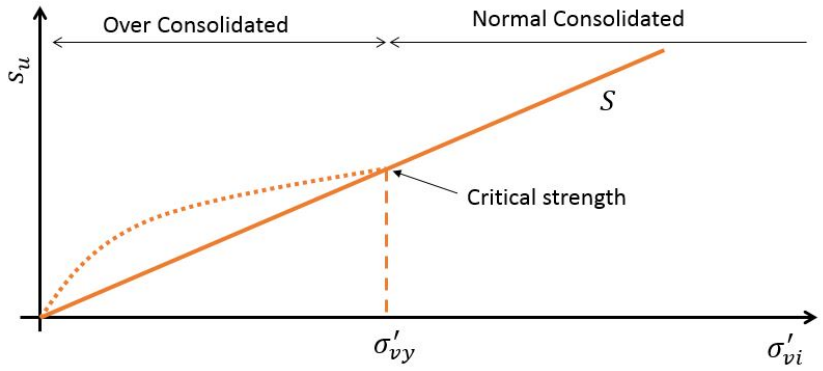

Figure 2.12: Shear strength vs effective stress according to CSSM with the SHANSEP method

A first estimation of the undrained shear strength can be made with the default values in combination with the in-situ effective stress (0.8 and 8 kN/m^2 for m and POP respectevily, default for S depend on the material and can be found in 'Schematiseringshandleiding Macrostabiliteit' [57]). The in-situ effective vertical stress (σ'_{vi}) is estimated based on the depth, the estimated volumetric weight of the above soil minus the pore pressure. If a levee is considered to be safe while default values are implemented no further assessment is required.

In case default values do not result in the required safety, laboratory test can provide relieve. The pre consolidation stress, the S and m parameters can be determined with direct simple shear, triaxial or a compression test. The derivation of the parameters in laboratory test leads to a higher accuracy in comparison to the default values.

2.4.2. S_u-measured method

The S_u-measured method provides a direct correlation between the cone tip resistance and the undrained shear strength, see equation 2.4. In the preliminary stages of the project a default value (N_{kt} = 20) for the cone factor can be used. However if necessary or appropriate a project specific N_{kt} value for each soil type can be determined with the help of direct simple shear of triaxial test. A correlation between the cone tip resistance and the undrained shear stress determined with laboratory test, results in a N_{kt} value. To link the cone tip resistance to the undrained shear strength, the borehole that contained the tested soil sample has to be close to the CPT [57]. The N_{kt} value is set per geological deposit, subsequently it can be used to determine the undrained shear strength for each CPT in the field.

$$s_u = q_{net}/N_{kt} \tag{2.4}$$

$$q_{net} = q_c + (1-a)u_2 - \sigma_{v0} \tag{2.5}$$

In which:

q_{net}	=	Corrected cone tip resistance	$[MPa]$
N_{kt}	=	Cone factor	$[-]$
q_c	=	Cone tip resistance	$[MPa]$
a	=	The ratio of the cone base cross section and the total cross section	$[-]$
u_2	=	Pore water pressure	$[MPa]$
σ_{v0}	=	In-situ total vertical stress	$[kN/m^2]$

As a soil is more compressed due to historical events the cone tip resistance will increase. Without any additional laboratory test the soil history will directly be accounted for in the S_u-measured method. In figure 2.13 multiple cone tip resistance divided by the cone factor are visualised with black triangles on the CSSM frame. When the soil is over consolidated the undrained shear strength obtained from equation 2.4 follows the dotted line presented in 2.12. Since soils naturally always contain some over consolidation in the value for the undrained shear strengths are only presented in the over consolidated region of the CSSM framework.

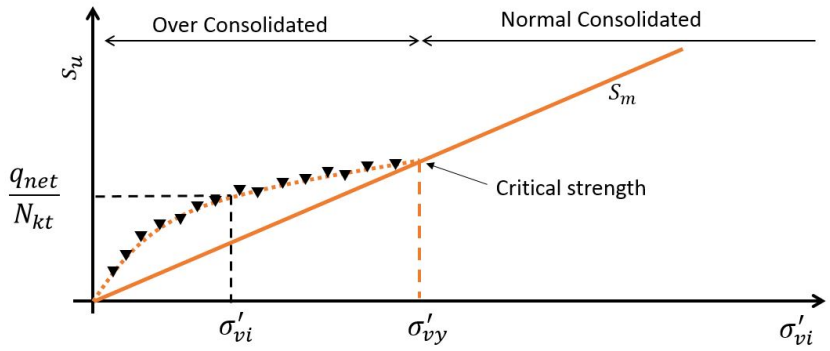

Figure 2.13: Undrained shear strength based on cone factor presented on the CSSM framework

2.4.3. Combination SHANSEP and S_u-measured methods

Although the SHANSEP and the S_u-measured methods can be described as two different methods, in practice they are complementary to one another. The SHANSEP method is convenient for a first estimation of the undrained shear strength, while the S_u-measured method provides a better local estimation. Furthermore the normalized cone tip resistance directly includes the over consolidation ratio in the S_u-measured method. A main advantage of the SHANSEP method is that it uses effective stresses and therefore can account for difference in water level, while the S_u-measured method cannot. High water levels are often the reason for failure to occur and are therefore important to take into consideration.

In this thesis the S_u-measured method is used to determine the undrained shear strength in each cross section. However the undrained shear strength (s_{u*}) determined with the S_u-measured method is rewritten to POP values in a model that accounts for different water levels, see equation 2.6. In this equation the S_u-measured is combined with the SHANSEP method.

$$POP = \sigma'_{vi} \cdot ((\frac{s_{u*}}{S \cdot \sigma'_{vi}})^{(1/m)} - 1) \tag{2.6}$$

Both the SHANSEP as well as the S_u-measured method make use of similar types of CPTs and laboratory test. However the SHANSEP method emphasizes the use of normal consolidated test and the S_u-measured method emphasizes over consolidated test.

The S_u-measured method is in general more accurate in comparison with the SHANSEP method, but is also of practical use due to it's simplicity. The undrained shear strength can be determined with the help of only one parameter (N_{kt}) at every CPT location. Uncertainty within the S_u-measured method is described with a variation coefficient as shown in section 4.2 [64].

2.5. Reliability

As part of the safety philosophy it is important to determine if the levee (design) meets the required safety. In the design process it is important to ensure that the actual reliability of the levee exceeds the required reliability. The reliability can be expressed with the probability of failure. To ensure sufficient reliability, uncertainties in the design have to be quantified. A lot of different uncertainties are present in a levee design, but in general two different types of uncertainties can be distinguished [37]:

- **Aleatory uncertainties** are uncertainties caused by randomness. A good example is the annual maximum discharge of a river. A probability density function can be determined based on daily measurements. Additional measurements hardly diminish the uncertainty towards the prediction of future water levels.
- **Epistemic uncertainties** are uncertainties that in principle could be known, for instance the undrained shear strength or other soil parameters which are based on a number of measurements. Due to limited accuracy or resolution the actual value can stay uncertain. However additional data can provide relieve

in reducing uncertainty, while this is not the case with aleatory uncertainty. Uncertainties in simplifications, measurements errors, subjective judgement or inaccurate schematisations can also be classified as epistemic uncertainties.

Both types of uncertainties are of importance within a levee design. In the semi probabilistic stability analysis, characteristic values in combination with partial factors result in design values, which are assume to cover most of the uncertainty. Whilst in the probabilistic analysis the probability density function (PDF) is implemented as a stochastic parameter. The difference between these two reliability approaches are analysed in section 2.5.1 and 2.5.2

2.5.1. Semi Probabilistic analysis (Level I reliability approach)

In the Netherlands the Load and Resistance Factor Design (LRFD) is often used for semi probabilistic analysis [16]. The characteristic value is used in Serviceability Limited State (SLS) while the design values are used in Ultimate Limit State (ULS). Within the design of a levee only the ULS is of interest and therefore always the design values are required as input values. The characteristic values are equal to the 95% and 5% quantile for the strength and the resistance respectively. Within a semi probabilistic approach partial factors are implemented to cover the uncertainties. The characteristic values of the strength are divided by a partial factor and the characteristic value of the loads is multiplied with partial factors, these thereby result in the design values, equation 2.7. Failure can be described with the limit state function and occurs when the design strength exceeds the design resistance, equation 2.8. 'A limit state is a condition of a structure beyond which it no longer fulfils the relevant design criteria' [24].

$$R_d = \frac{R_k}{\gamma_m} = SF \qquad S_d = \gamma_S S_k = \gamma_n \gamma_d \gamma_b \tag{2.7}$$

$$Z = R_d - S_d \quad SF \geq \gamma_n \gamma_d \gamma_b \tag{2.8}$$

In which:

R_k	=	Characteristic value of the resistance	[−]
R_d	=	Design value of the resistance	[−]
S_k	=	Characteristic value of the strength	[−]
γ_S	=	Partial factor for the strength	[−]
S_d	=	Design value of the strength	[−]
SF	=	Safety Factor	[−]
γ_m	=	Material factor	[−]
γ_n	=	Loss factor	[−]
γ_d	=	Model factor	[−]
γ_b	=	Schematisation factor	[−]
Z	=	Limit State Function	[−]

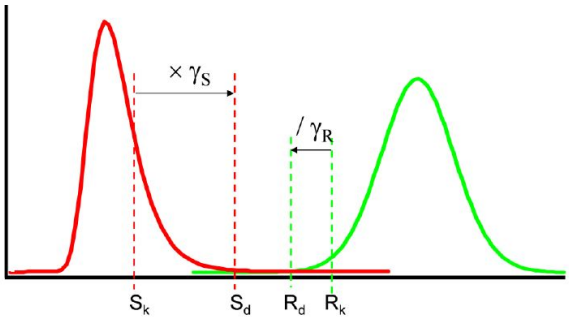

Figure 2.14: Probability density function of strength and resistance [24]

In a levee design the resistance and the strength depend on multiple parameters. In a semi probabilistic design the design value for the resistance is characterized with the Safety Factor (SF). A material factor is used within the Mohr Coulomb method to determine the design value for the resistance. For the CSSM the material factor is set to 1.0, the characteristic value of the resistance is therefore equal to the design value. The partial factor on the right hand side of equation 2.7 consist of a model factor, a schematization factor and a loss factor ('schadefactor'). Multiplication of these factors determines the required safety factor [34] [15]. The advantage of several partial safety factors is that the uncertainty can be pinpointed, resulting in a less conservative design. The partial factors are required to cover part of the epistemic uncertainty. Since CSSM will be applied throughout this thesis, the associate partial factors for this method will be presented in this section.

Model factor (γ_d) The model factor is introduced to take into account uncertainties regarding the imperfect reproduction of reality in models. The model factor as presented in table 2.1 depend on the chosen limit equilibrium method, described in section 2.2.1 [38]. The different limit equilibrium methods are assumed to reflect reality with different accuracy. This can mainly be devoted to the shape of the slip surface.

Table 2.1: Model factors per limit equilibrium method [38]

Method	Model Factor (γ_d)
Bishop	1.11
Spencer	1.07
Uplift Van	1.06

Schematization factor (γ_b) The semi probabilistic model is a schematization of the reality and therefore the schematization factor is introduced. One cross section represents a few hundred meters of a levee in longitudinal direction, 3D-effects are not considered implying that the model is a simplification of reality. Furthermore the use of Limit Equilibrium Methods is a simplification since these methods do not account for deformations in the levee. The schematization factor ranges from 1.0 till 1.3. If sufficient data is available this factor can be diminished to 1.0. Hence, a schematization of the most unfavourable cross section has to made in that case. In practice 1.1 is most often used as minimum. The schematization contains a large part of the total uncertainty within the design [16].

Loss factor (γ_n) The loss factor links the regulation regarding the semi probabilistic method to the length of a considered levee (or the considered segment), the estimation of the probability of failure ('faalkansbegroting') and the design water level. The loss factor is based on a calibration study but is slightly more conservative introduced within the OI2014v4 [38] [23]. The loss factor for the CSSM model is determined with equation 2.9.

$$\gamma_n = 0.15(\beta_{req,cs}) + 0.41 \tag{2.9}$$

$\beta_{req,cs}$ is the required reliability index regarding the probability of flooding. The required reliability index originates from a probabilistic stability analysis, it depends on the maximum allowable probability of failure and differs per location along the primary flood defences within the Netherlands, see section 2.5.2. In appendix A of OI2014v4 these required indexes are determined per levee trajectory [38].

Characteristic value normal distribution The characteristic value can be determined in many different ways. In this thesis the method presented in equation 2.10 is used. The statistical coefficient (k_n) is 1.645 for the inferior characteristic value, equal to the 5% quantile of the normal distribution, see figure 2.15.

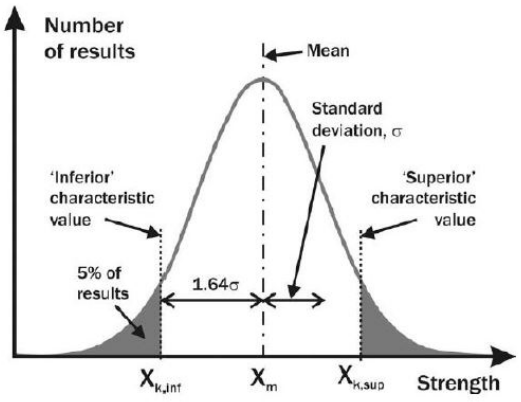

Figure 2.15: Characteristic values for a normal distribution [7]

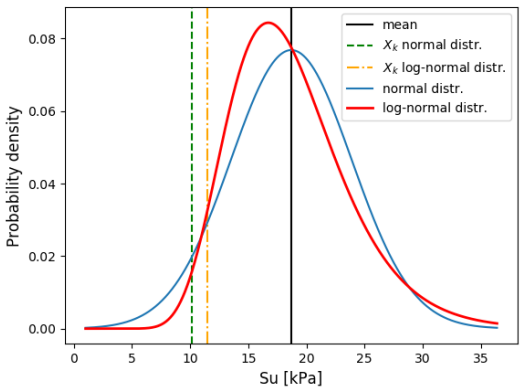

Figure 2.16: Comparison normal vs log normal distribution

$$X_k = \mu_x \pm k_n \sigma_x = \mu_x(1 \pm k_n VC_x) \tag{2.10}$$

$$VC_x = \frac{\sigma_x}{\mu_x} \tag{2.11}$$

In which:

VC_x	The variation coefficient of X	[−]
μ_x	The mean of X	[−]
σ_x	The standard deviation of X	[−]
X_k	Characteristic value	[−]
k_n	Statistical coefficient equal to 1.645 for the 5% quantile with n=∞	[−]

Characteristic value log-normal distribution Physically some of the implemented variable, e.g. the undrained shear strength, cannot be lower than zero. Implementation of a log-normal distribution ensures that the considered variable will not become negative. Equations 2.12 and 2.13 show how the average variation coefficient can be rewritten to a standard deviation for a log-normal distribution and how this results in a mean value. In equation 2.14 eventually the characteristic value, X_k is determined.

$$\sigma_{ln(x)} = \sqrt{ln(1 + VC_x^2)} \tag{2.12}$$

$$\mu_{ln(x)} = ln(\mu_x) - \frac{1}{2}\sigma_{ln(x)}^2 \tag{2.13}$$

$$X_k = e^{\mu_{ln(x)} - k_n \cdot \sigma_{ln(x)}} \tag{2.14}$$

In which:

$\mu_{ln(x)}$	The mean of X for a log normal distribution	[−]
$\sigma_{ln(x)}$	The standard deviation of X for a log normal distribution	[−]

In figure 2.16 a comparison between a log-normal and normal distribution of the undrained shear strength is made as an example; both distributions have a mean value of 18.7 kPa. The characteristic values are 10.2 and 11.5 kPa for the normal and log-normal distribution, as is indicated in figure 2.16. The distribution has to be chosen with consciousness since the application of a log-normal distribution versus a normal distribution leads to a higher reliability. However in practice seldom enough test are conducted to make a finite choice of the best distribution [5].

2.5.2. Probabilistic analysis (Level II reliability approach)

Modern applications provide the possibility to implement parameters stochastically and thereby determine the probability of failure instead of a safety factor. The probability that the strength exceeds the resistance is indicated with the red part in figure 2.17 and can be referred to as the probability of failure. Instead of partial factors the mean and standard deviations of the strength and load can be implemented in the calculation. In a perfect accurate model failure would occur in case SF < 1.0, however model uncertainty is present in a probabilistic analysis and therefore the limit state function is as presented in equation 2.15.

$$Z = SF \cdot m_d - 1 \tag{2.15}$$

Similar to the semi-probabilistic analysis the model factors depend on the applied limit equilibrium method, see table 2.2. However in a probabilistic analysis the model factors are implemented stochastically. As the method gives a better representation of reality the model factor decreases [50].

Table 2.2: Model factors and their uncertainty per limit equilibrium method

Soil type	μ_{md}	σ_{md}
Bishop	1.025	0.050
Uplift-Van	1.005	0.033
Spencer	1.008	0.035

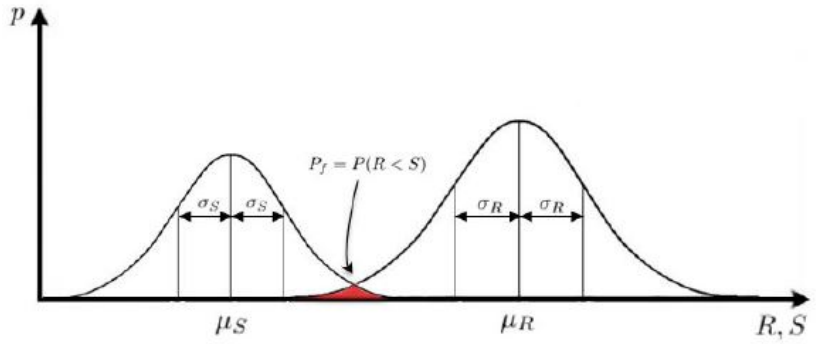

Figure 2.17: Probability density function of strength and resistance for probabilistic analysis [49]

A distinction between a level II and level III reliability approach can be made. Monte Carlo Simulation is an example of a level III reliability approach that can determine the exact probability of failure in the limit. A well known level II reliability approach is the First Order Reliability Method (FORM). This method is used in this thesis and will be referred to as the probabilistic stability analysis. Besides the probability of failure the reliability index (β) is often used to express safety. The cumulative normal distribution of the reliability index results in the probability of failure as is presented in figure 2.19. For a reliability function that is normally distributed it is relatively simple to determine the probability of failure and the reliability index. As β increases the failure probability decreases and thus safety increases. The reliability index originates from the FORM analysis and can be expressed as the shortest distance of the origin to the failure region [24].

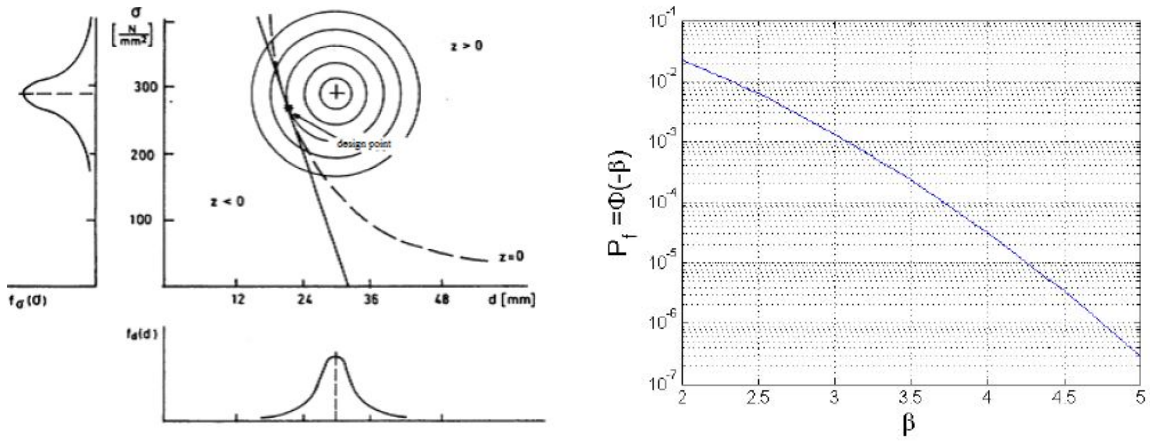

Figure 2.18: Example of linearisation of the limit state function in the design point [24]

Figure 2.19: Probability of failure P_f vs reliability index β [24]

Within this Level II reliability analysis, both the joint probability density function as well as the limit state function are linearised at the design point. The design point is characterized as the point of the limit state function with the highest probability density and it thereby is the point of the limit state function that is closes to the center of the joint probability density function (β). In case the limit state is non linear, it can be linearised. This linearisation has to take place in the design point. An example of the joint probability density function and the linearisation of the limit state function is presented in figure 2.18. An iteration process localizes the design, if sufficient convergence occurs. The convergence requirements and the number of iterations that are imposed can indicate if a calculation can be classified as successful.

In equation 2.9 the loss factor is based on a given reliability index, which is required for a certain levee trajectory. This required reliability index is based on a probabilistic stability analysis. The reliability index determined in a probabilistic analysis should be larger than the required reliability index for the considered cross section, as shown in equation 2.16.

$$\beta > \beta_{req,cs} \tag{2.16}$$

In which:

β	Reliability index	[−]
$\beta_{req,cs}$	The required reliability index for the considered cross section as defined in OI2014v4	[−]

3

Case Study

The goal of this thesis is to determine how the quantity of CPTs in longitudinal direction affects the estimation of the undrained shear strength and how it is related to the inner slope stability. A case study is required to provide sufficient data, particularly CPT data and CPT-borehole combinations. The Markermeerdijken is chosen as a case study. This case helps to answer the main research question because:

- A lot of data, both in-situ as well as laboratory data is available. Each cross section along the 33 km long levee consists of at least 4 CPTs. The successive cross sections have an interval size of approximately 100 m for the greater part of the Markermeer levee. The data can easily be obtained due to the involvement of Witteveen + Bos in the design process.
- The S_u-measured method is development based on the 'Dijken op Veen' project [47]. The project location is close to the Markermeerdijken project.
- The size of the project makes it possible to only investigate part of the levee in which the soil stratification is more or less constant in longitudinal direction.

The 33 kilometre long levee along the Markermeer, between Hoorn and Amsterdam, is classified as unsafe according to the new WBI2017, figure 3.1. Measures are required to ensure that the people and assets behind the levee remain safe, section 2.1.

The considered levee is part of the IJsselmeer and Markermeer system. The Markermeer drains water to the IJsselmeer which on its turn drains water to the Waddenzee. High precipitation rates in combination with a high discharge from the river IJssel result in an increase of the water level. Under extreme conditions the water level in the Waddenzee could rise due to North Western winds. Due to the high water levels the water from the IJsselmeer could not be drained, this also holds for the drainage from the Markermeer to the IJsselmeer. During this period of high water the levees become saturated, this could lead to stability problems. To prevent levee instability in the future reinforcement is required.

Figure 3.1: Location of Markeermeerdijken case study

3.1. Location within Markermeerdijken project

Within the 33 km long levee stretch a smaller area is selected, based on the requirements as described within this section:

- **A constant stratification along the longitudinal direction of the levee:** This means as little as possible diversity in the layer thickness, soil types and difference in surface level. A homogeneous soil profile is required to decrease the influence of the stratification on the final results, since the soil state and parameter are examined in this thesis.
- **A continuous peat and clay layer have to be present over a least 3 kilometres:** Since one cone factor is determined for each geological layer, continuous layers prevent the use of multiple cone factors. The use of 1 $N_k t$ value per geological layer ensures that all estimated s_u values share the same uncertainty. A 3 km long trajectory is required to ensure sufficient data is present when the effect of larger interval sizes is investigated.
- **Sufficient CPTs have to be conducted in both longitudinal as well as cross sectional direction:** In order to investigate the CPT density along a levee sufficient CPTs have to be available. A minimum longitudinal interval of 100 meter is chosen and at least 3 CPTs in cross sectional direction are required. Both requisites are fulfilled at almost every location within the Markermeerdijken project.

Only one location along the 33 km stretch fulfilled the requirements. A 5 kilometre long stretch is chosen, since the CPT interval size is 100 m, 51 cross sections are present in the selected area. Due to confidentiality the exact location is shown in Appendix E and is only visible if authorized.

3.2. Water level in Markermeer

As indicated the high waters in the Markermeer can lead to instability of the inner slope. In order to model the inner slope stability the 'high' water needs to be quantified. The water level in the Markermeer depends on the discharge of the river IJssel and the discharge to the IJsselmeer. The latter one can be regulated, the measured water levels can therefore not simply be extrapolated as is often done with water levels in rivers. For the inner slope stability analysis the mean high water level (MHW), the design high water (DHW) and the polder level are most important.

MHW in the Markermeer is equal to -0.40 m NAP and is based on measurements. A water level can be expressed with the probability of occurrence. The considered DHW is equal to 1.00 m NAP and is based on the maximum permissible failure probability which is equal to 1/1.000 years for the Markermeerdijken trajectory [40]. The polder level in the hinterland is -2.26 m NAP. The water levels in table 3.1 are obtained from a report provided by the Markermeerdijken Alliantie and are applicable to the considered 5 km research area [2].

Table 3.1: MHW, DHW and polder level

MHW	-0.40	m NAP
DHW	+1.00	m NAP
Polder level	-2.26	m NAP

3.3. Required reliability

The required reliability and safety factor are obtained from report 'Ontwerpbasis Dijken DO' from the Markermeerdijken Alliantie [2]. A distinction between a level I (semi-probabilistic) and level II (probabilistic) approach is made in this section.

3.3.1. Reliability in a semi probabilistic analysis (level I)

The partial factors used in the Markermeerdijken project are shown in table 3.2. These partial factors result in the limit state functions for the LEMs of Bishop and Spencer, as indicated in equation 3.1.

$$SF_{req,Bishop} = 1.24 \qquad SF_{req,Spencer} = 1.19 \tag{3.1}$$

Table 3.2: Partial factors used in MMD project for the method of Spencer

Model Factor Bishop	(γ_d)	1.11
Model Factor Spencer	(γ_d)	1.07
Schematization Factor	(γ_b)	1.10
Loss Factor	(γ_n)	1.02
Material Factor	(γ_m)	1.00

3.3.2. Reliability in a Probabilistic Analysis (level II)

The required reliability index for the considered trajectory ($\beta_{cs,req}$) is obtained from 'Ontwerpbasis Dijken DO' and is based on the 24% share within the estimation of failure probability as indicated in section 2.1, see equation 3.2 [2].

$$\beta_{cs,req} = 4.03 \tag{3.2}$$

The model factors are determined based on a calibration study and decrease when the LEM gives a better representation of the actual slip surface, table 2.2. Since the relative influence of the model is not of interest, the model factors are implemented deterministically. The 95% characteristic value of the model factors are used in the model, see table 3.3.

Table 3.3: 95% characteristic value of model factor for different LEMs

Model Factor Bishop	1.11
Model Factor Spencer	1.06
Model Factor Uplift Van	1.07

4

Parameters for determination undrained shear strength

In this chapter the soil investigation conducted in the Markermeerdijken project is elaborated, which consist of CPTs, boreholes and laboratory test. Furthermore the parameters required to determine the undrained shear strength based on the S_u-measured method are presented in this chapter.

4.1. Soil investigation for Markermeerdijken project

Soil investigation helps to quantify the soil conditions present along the Markermeer levee. The soil conditions are determined with the help of CPTs, boreholes and laboratory tests. CPT profiles are used to estimate the stratification present in the subsoil. A combination of CPT data and laboratory data can provide an estimation of several parameters of which the undrained shear strength and the unit weight are most important for the stability analysis.

4.1.1. CPT data

In the selected area every 100 meter, 4 CPTs within a cross section are present. In figure 4.1 the cross sectional locations of the CPTs are indicated: in the hinterland (AL), inner berm (BI), the crest (KR) and in the water (W).

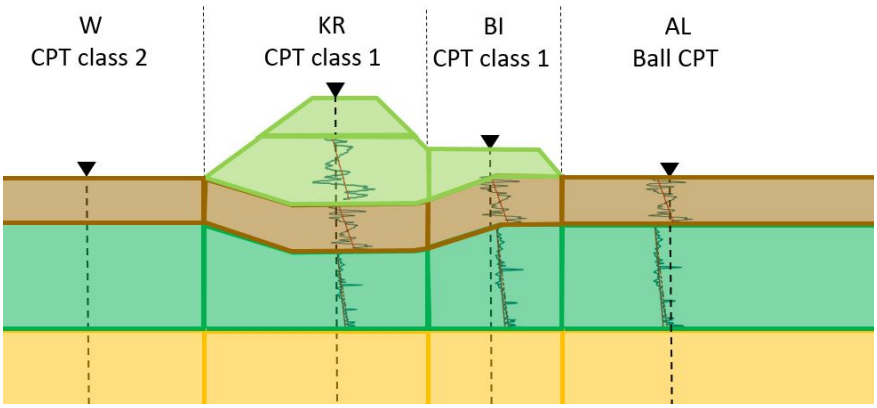

Figure 4.1: CPT types in cross section

The CPT profiles are used to estimate the stratification of the subsoil. Linear interpolation of these stratifications in cross sectional direction result in a cross section. In some cases boreholes are used as additional information towards the estimated stratification. Within the selected area the typical soil profile looks as presented in table 4.1 and figure 4.2. Only four layers are assumed to be present: Anthropogenic clay (Clay A) within the dike, peat (Peat), clay Calais (Clay C) and Pleistocene sand (Sand), see table 4.1. The names in between brackets is how the soils are referred to in the rest of this thesis. In table 4.1 and figure 4.2 the Antropogenic clay layer is divided into two layers; Clay A1 and Clay A2. This division has advantages in the stability analysis and is based on the drained vs undrained behaviour of the soil, this is clarified in section 5.1.2.

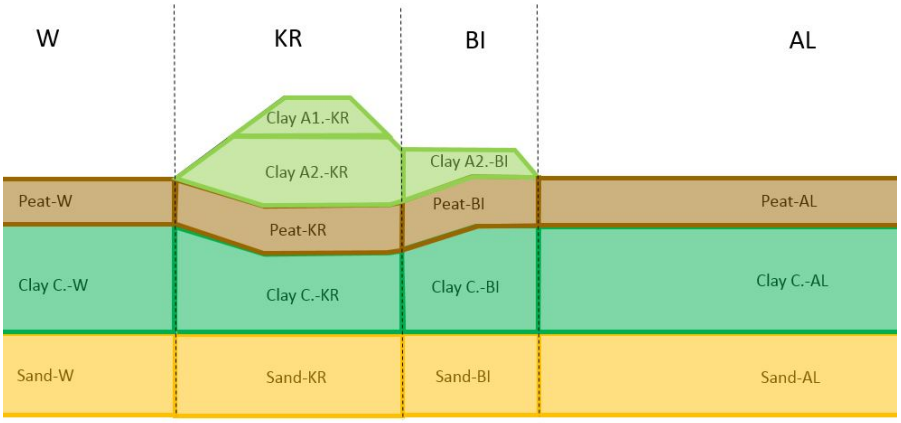

Figure 4.2: Stratification within the selected area

Table 4.1: Stratification in selected research area

	Water (W)	**Crest (KR)**	**Inner berm (BI)**	**Hinterland (AL)**
Layer 1	-	Clay A1.-KR	-	-
Layer 2	-	Clay A2.-KR	Clay A2.-BI	-
Layer 3	Peat-W	Peat-KR	Peat-BI	Peat-AL
Layer 4	Clay C.-W	Clay C.-KR	Clay C.-BI	Clay C.-AL
Layer 5	Sand-W	Sand-KR	Sand-BI	Sand-AL

In the specified research area the stratification is assumed to be constant in longitudinal direction. Thereby the layer thickness can differ per cross section and is based on CPT data in each cross section. Nevertheless the layer sequence in vertical direction remains similar in all 51 cross sections.

The cone tip resistance is normalized for both the water pressure as well as the total stress, to determine the normalized cone tip resistance q_{net}. Pore water pressures indicate that at least a second class CPT is required (see appendix A). In the Markermeerdijken project class 1 CPTs are performed in the crest and inner berm, these are the most suitable considering the soft soils that are present. To compare a CPT with the results of a DSS test the normalized cone tip resistance is averaged over 3 measurements or 6 cm, this is approximately equal to the height of a soil sample used in a DSS test (5 cm).

In the hinterland and parts of the water, CPTs with a ball cone are conducted (BCPT), see figure 4.1. This cone has a larger surface which results in more accurate measuring, however most of the times no friction ratio is measured in BCPTs, see Appendix A. The friction ratio is of great use regarding layer identification, lack of this information can cause complications. It is therefore assumed that the layer separation between peat and clay C in the hinterland is at equal depth as in the inner berm.

4.1.2. Unit weight determination

The cone tip resistance of both peat and clay C. in the Markermeerdijken project are low. Small changes in the total stress can have a large influence on the calculation of the normalized cone tip resistance, see equation 2.5. Moreover a proper estimation is required in case the in-situ stress is used as consolidation stress in a TT or DSS test. An accurate estimation of the total soil stress is therefore important. The total stress depends on the depth, the water level and the unit weight of the soil. The unit weight of soils can be determined in several ways. Robertson and Mayne both use CPT data for their estimation of the unit weight [45] [33]. Their empirical formulas give a good estimation for dense soils (15 kN/m^3 or higher). In softer soils such as peat and clay these formulas lack accuracy.

The unit weight of most soils are also listed in table 2.b in the Nen-en1997 (Eurocode 7). Based on the cone tip resistance the unit weight of a soil can be found within this table [34]. The effort to determine the unit weight for each measured cone tip resistance (every 2 cm) is significant.

Next to these methods the unit weight can also be determined based on laboratory test. The unit weight is determined in a lot of laboratory test, therefore in most projects sufficient data is available to give a good estimation. However if no or little laboratory data is available this estimation can lack accuracy, moreover the unit weight is determined on small samples, which represent an entire geological layer.

The author assisted in a research in which the unit weight of soft soil can more accurately be determined based on CPTs [28]. The proposed formula for the estimation can be seen in equation 4.1. As is shown within the article the estimation for soft soils is more accurate in comparison to Mayne and Robertson in the range between 10 to 15 kN/m^3 while its estimation is equally good for soils with a unit weights higher than 15 kN/m^3.

$$\gamma_{sat} = \gamma_{sat,ref} - \beta_{uw} \cdot \frac{log(\frac{q_{t,ref}}{q_t})}{log(\frac{R_{f,ref}}{R_f})} \tag{4.1}$$

In which:

$\gamma_{sat,ref}$	Reference unit weight at which the cone resistance is constant[19.0]	$[kN/m^3]$
$q_{t,ref}$	Reference cone resistance at which the unit weight is constant[5.0]	$[Mpa]$
$R_{f,ref}$	Reference friction ratio at which the apex of all lines of equal unit weight is located [30.0]	$[-]$
β_{uw}	Measure for the inclination of the equal unit weight contours [4.12]	$[-]$

The required total stress for the calculation of q_{net} can now be determined based on the unit weight obtained with equation 4.1. An advantage is that the estimation of the unit weight can be more easily be automated in comparison to the Eurocode or laboratory tests.

4.1.3. Laboratory test

DSS and triaxial test are used to determine the undrained shear strength and thereby the cone factor (N_{kt}) for each geological deposit. In order for laboratory test to be used in the cone factor determination they have to meet certain requirements, ranging from quantity of tests to the spacing in a CPT-Borehole combination [57]. These requirements are listed below and are elaborated on in this section:

- Quantity laboratory test
- Spacing CPT-Borehole
- Strain requirements
- Remaining requirements

The laboratory test are performed on samples retrieved from boreholes in a testing field. The testing field can either be located within the levee or next to it as long as the same soils are present as in the levee, see figure 4.3. In the Markermeerdijken project the testing fields are located along the levee as shown in figure 4.3 and in Appendix E.

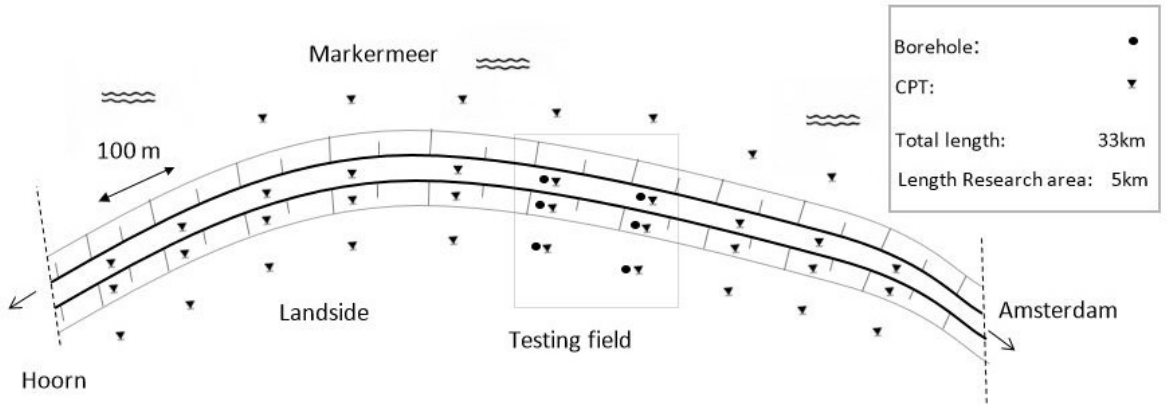

Figure 4.3: A schematic spatial overview of the Su-measured method applied in the Markermeerdijken project

Quantity laboratory test In this thesis the undrained shear strength in the peat, clay C, and the clay A. layers are determined based on the Su-measured method. It is stated that at least 10 borehole - CPT combination give good results [14]. Within these combinations at least 50 laboratory test have to be performed for each layer. In total 285 DSS and 142 triaxial test are performed that could be used to determine the cone factor. In the peat and clay C. layer sufficient soil samples are obtained, however in the Anthropogenic clay layer not sufficient tests are performed to determine the cone factor for this layer.

Spacing CPT-Borehole The CPT-borehole combination and the laboratory tests have to fulfil certain requirements. In order to link the cone tip resistance with the results obtained from laboratory test these two have to be performed close to one another, approximately 0.5 m [14]. In the Markermeerdijken project multiple testing fields are present. These testing fields have a spacing between CPTs and boreholes ranging from 0.81 m up to 18.8 m. To properly estimate the cone factor only the boreholes and CPT combinations that are close to one another can be used. None of the combinations fulfil the requirement of 0.5 m spacing, therefore a new project specific requirement is set:

- All combination within a 5 meter range are accepted after a quick check.
- All combinations with a spacing of 5 to 10 meters are discarded unless examination proves that the soil sample agrees to the cone tip resistance and friction ratio in the CPT.
- All combinations with a 10 meter spacing or more are eliminated.

In this thesis the class 1 CPTs present in the crest and inner berm are used to determine the cone factor N_{kt}, the cone factor determined from BCPTs is obtained from the Markmermeerdijken project, see section sec:Soilstrength.

Strain requirements According to the CSSM the undrained shear strength has to be determined at a strain of 25 and 40% (large strains) for clay and peat respectively. In some cases the sample in a DSS or triaxial test has failed before this strain is reached. Therefore all the shear stress-strain graphs available are validated based on the axial stress - shear stress graphs. As can be seen in figure 4.5 the decay of the shear stress indicates that the sample has failed. The strain which was present at the moment of failure is used to determine the undrained shear strength.

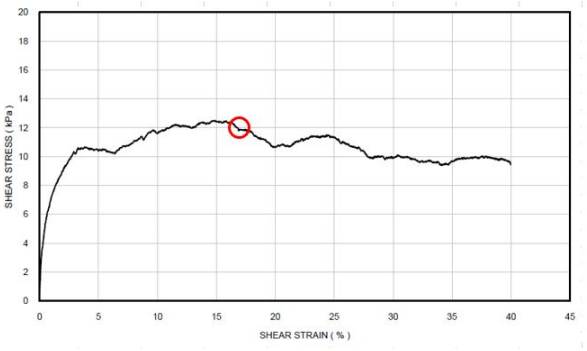

Figure 4.4: DSS test shear stress vs strain

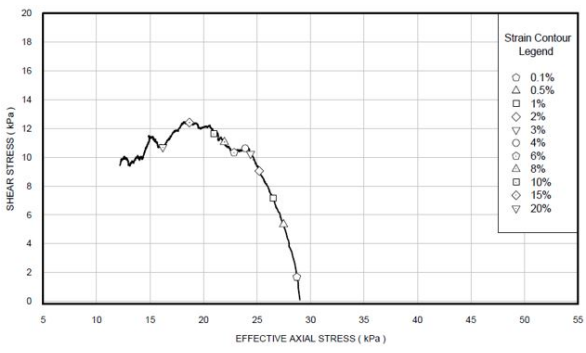

Figure 4.5: Axial stress vs shear stress DSS test

Remaining requirements Apart from the requirements mentioned in the previous paragraphs there are some other reasons to reject laboratory tests. The reason for this rejection originates from sample disturbance or inaccurate measurements. Samples are rejected in case one of the following criteria were applicable:

- Deviant bulk density of the specimen: In case a specimen had a significant lower bulk density than specimens from the same material.
- Deviant water content of the specimen: In case a specimen had a significant lower water content than specimens from the same material.

- Deviant stress: In case the path of the axial stress vs shear stress or the strain vs shear stress deviated from the expected path. The reason for this deviation could be caused by an incorrect preparation of the sample, or the sample could contain a small piece of wood etc.. Besides that a comparison is made with the torvane test in the soil. If the undrained shear strength obtained from the test is significantly lower/higher than the torvane test the sample is rejected.
- Softening: Softening describes the behaviour in case the peak stress is much higher than the critical stress. In this thesis it is assumed that softening occurs in case the peak strength is 10 % higher than the critical stress.

Summary The flow chart presented in figure 4.6 shows how the requirements cause a total of 285 available DSS test to decrease to only 45 DSS accepted test. The number of tests are shown in between brackets for each step in figure 4.6. The figure show that 20 and 25 DSS test are used for the cone factor determination of peat and clay C. respectively. The results of the accepted laboratory tests are shown in appendix B.

The requirement regarding the amount of laboratory tests are therefore not fulfilled for both peat and clay Calais [57]. Both the number of laboratory test (50) as well as the number of CPTs (10) that are prescribed are not met, moreover the test are divided over only two different testing fields. Although both triaxial and DSS test are conducted in the Markermeerdijken project only the DSS test are used to determine the cone factor. Not enough triaxial test meet the requirements and therefore the cone factor is only based on DSS test. Moreover in section 2.3.3 it is underlined that DSS give a better representation of the average undrained shear strength over the slip surface. The flow chart for the traixial test is shown in Appendix B.
The cone factor (N_b) for BCPTs is not calculated in this thesis as indicated in figure 4.6, instead the values determined in the Markermeerdijken project are used.

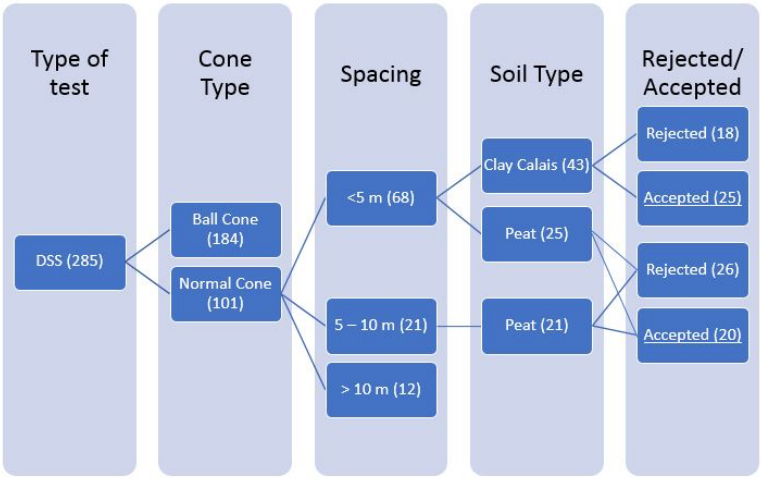

Figure 4.6: Flow chart representing the requirements regarding laboratory test

4.2. Determination design values undrained shear strength

Although the two methods to determine the undrained shear strength are already briefly discussed in chapter 2, a more thorough explanation of the S_u-measured method is given in this section. This method is preferred in contrast to the SHANSEP method because the S_u-measured method directly uses the CPT data and therefore the OCR in the subsoil. This method could therefore more easily give insight in the gain of additional data as is addressed in the research questions. However as indicated in section 2.4.3, a combination between the SHANSEP and the S_u-measured method is required when changes in effective stress are of importance and is therefore considered in this chapter as well.

The parameter determination and thereby the formulas presented in this chapter are based on 'Dijken op Veen II, DOV werkwijze voor bepaling macrostabiliteit Markermeerdijk' [64], which will be referred to as the DOV method. In the meanwhile the applied formulas are slightly alternated in more recent reports [59] [65].

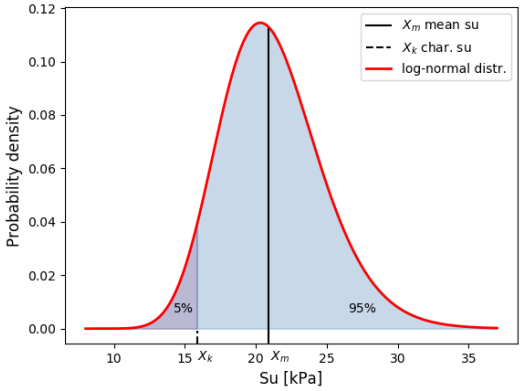

Figure 4.7: Requirements regarding the probability density function for semi probabilistic analysis

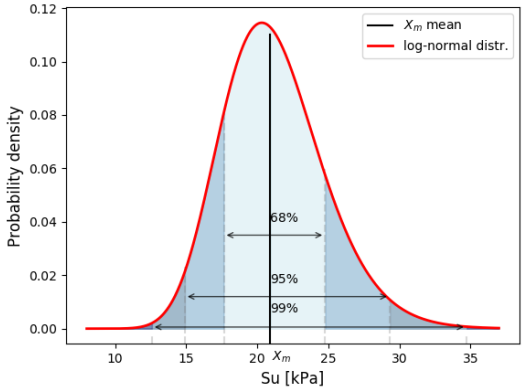

Figure 4.8: Requirements regarding the probability density function for probabilistic analysis

The major changes in calculation method are discussed in the conclusion.

For each measured q_{net} (every 2 cm) the undrained shear strength can be determined when the S_u-measured method is applied. The undrained shear strength can be represented as a log-normal distribution and contains a mean and standard deviation. The mean X_m, the standard deviation and thereby the characteristic value X_k for the undrained shear strength are determined in this chapter, see figure 4.7. For the probabilistic analysis the entire distribution is required as indicated in figure 4.8. The standard deviation of these log-normal distributions depends on a variation coefficient as in equation 2.12.
In order to determine the undrained shear strength from CPT class 1 data the following steps are required, which are elaborated on in the subsequent paragraphs:

1. Cone factor (N_{kt})
2. Transformation uncertainty (VC_{kt})
3. Linearisation of the undrained shear strength
4. Regional uncertainty ($VC_{av,reg}$)
5. Total variation coefficient (VC_{tot})

At first the cone factor is determined based on the accepted laboratory test in combination with CPT data for both peat and clay C. in the crest and inner berm. The variation coefficient required to determine the standard deviation of the undrained shear strength as in equation 2.10 is based on two separate variation coefficients; the transformation and regional variation coefficient. These result in the total variation coefficient which is presented in step 5. For modelling convenience the undrained shear strength is linearised per layer in step 3.

As figure 4.6 indicates, BCPTs are not considered in the cone factor determination, these values are adopted from the Markermeerdijken project. In the hinterland only BCPTs are conducted and therefore these values are required to determine the undrained shear strength at this location. The cone factor (N_b) and its variation coefficients are presented in table 4.2.

Table 4.2: Cone factor and variation coefficients for BCPTs

	Clay C	Peat
N_b	18.00	19.80
VC_{trans}	0.24	0.24
$VC_{av,reg}$	0.14	0.14
VC_{tot}	0.28	0.28

4.2.1. Cone Factor

In figure 4.9 and 4.10 the undrained shear strength measured in the laboratory, coupled to the normalized cone tip resistance is presented for clay C. and peat respectively. The observations are shown in different colors, these represent the different boreholes from where the samples are obtained. Only the laboratory test that are accepted (figure 4.6) are used to determine to determine the cone factor. In table B.2 and B.1 in Appendix B the results of the laboratory test that are used for the determination of the cone factor are presented together with the normalized cone tip resistances. As an example the cone factor is determined with all laboratory test as well in Appendix B.

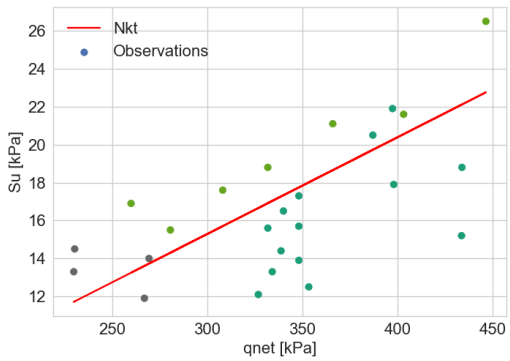

Figure 4.9: N_{kt} determination for clay C.

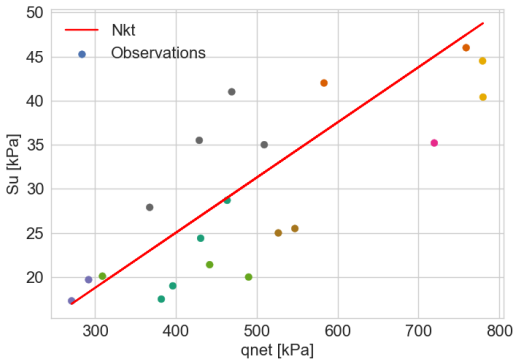

Figure 4.10: N_{kt} determination for peat

There are multiple methods to determine the 'best' fit based on the combination of laboratory test and cone tip resistance. In this thesis the method presented in the DOV research and WBI is used, in appendix B a comparison of multiple linear and non linear fits is made.

The cone factor can be determined with linear regression. The least square error method is a standard approach for linear regression. As the name indicates the solution minimizes the sum of the squares. The method will search for the value of N_{kt} which minimizes the outcome (F_{kt} in equation 4.2). The cone factors indicated in figure 4.9 and 4.10 are not necessarily the best fit of the considered dataset. The intersection of the cone factor with zero is based on equation 2.4 ($N_{kt} = q_{net}/s_u$); if the cone tip resistance is zero the undrained shear strength will be zero and vice a versa. The application of equation 2.4 prevents negative estimations for the undrained shear strength. The cone factors for both deposits are presented in table 4.3.

$$F_{kt} = \sum_i (s_{u,i} \frac{N_{kt}}{q_{net,i}} - 1)^2 \tag{4.2}$$

Table 4.3: Cone factor for peat and clay C.

	Clay C	Peat
N_{kt}	19.62	15.98

The cone factor of peat is lower in comparison with the cone factor of clay C.. The main cause for this difference is the higher undrained shear strength in peat which causes the cone factor to decrease. Based on these results it can be concluded that the average strength of the clay C. will be lower than peat. It stands out that in figure 4.9 almost all the samples from borehole B3 (dark green) are situated below the red line, whilst the samples obtained from borehole B4 (light green) are all situated above the red line. Since insufficient laboratory tests are present to determine a cone factor in the clay A2. layer, the same cone factor for clay C. is used for clay A2.. This is also done in the Markermeerdijken project, were it is validated that this method results in conservative estimations of s_u in clay A2..

In the 'Schematisatie Handleiding Macrostabiliteit' it is stated that at least 10 CPT-Borehole combination are required with at least 50 laboratory tests [57]. In both cone factor determinations fewer test are used. Sufficient test are performed in the field, however only 25 and 20 DSS test fulfilled the requirements stated

in section 4.1.3. A student-t factor can be used to indicate and adjust for the fact that too few laboratory test are used in the cone factor determination. Although this is a valuable and accepted method it is not applied within this thesis since the difference in N_{kt} minimum, see appendix B.

4.2.2. Transformation uncertainty

Transformation uncertainty can be classified as an epistemic uncertainty and is introduced when laboratory test ($s_{u,i}$) in combination with field test ($q_{net,i}$) are transformed into input parameters, as is the case for the cone factor. Since the CPT-sample combinations presented in figure 4.9 and 4.10, do not lie in a straight line, uncertainty is present in the determination of the cone factor. Similar as the determination of the cone factor, the uncertainty in the cone factor can be determined and represented in multiple ways. The DOV method is considered in this thesis, other methods are elaborated in Appendix B.

Low undrained shear strengths often coincide with low values for the normalized cone tip resistance, this leads to the ascending line for the cone factor in figure 4.9 and 4.10. A variation coefficient (VC_{Nkt}) is used to define the uncertainty in N_{kt} instead of a standard deviation, since it is proportional to the mean value [11]. The use of variation coefficients prevents the undrained shear strength to become negative. Similar to the cone factor, the least square error method is used to determine VC_{Nkt} in equation 4.3. For clay C. VC_{Nkt} is equal to 0.17, while for peat it is equal to 0.21, see table 4.4.

In section 2.5, equation 2.10 indicates how the characteristic values can be determined based on a variation coefficient. In equation 4.4 the characteristic values of N_{kt} are determined with variation coefficient, VC_{Nkt}. The statistical coefficient k_n is kept constant to 1.645 in the DOV method (in BEEM k_n depends on the number of samples). This is presented in figure 4.11 and 4.12 with the 90 % confidence interval, the blue and green line represent the 5% and 95 % quantile respectively. The inferior $N_{kt,k}$ (blue lines) are 28.37 and 19.13 and the superior $N_{kt,k}$ (green lines) values are 14.99 and 13.73 for clay C. and peat respectively.

$$VC_{Nkt} = \sqrt{\sum_{j=1}^{n} \frac{(\frac{s_{u,i} - \frac{q_{net,i}}{N_{kt}}}{\frac{q_{net,i}}{N_{kt}}})^2}{n-1}} \tag{4.3}$$

$$N_{kt,k} = N_{kt}(1 \pm k_n VC_{Nkt}) \tag{4.4}$$

In which:

VC_{Nkt}	The variation coefficient for the difference between $s_u - q_{net}/N_{kt}$	[−]
n	Number of CPT - laboratory sample combinations	[−]
$N_{kt,k}$	Characteristic value of the cone factor	[−]

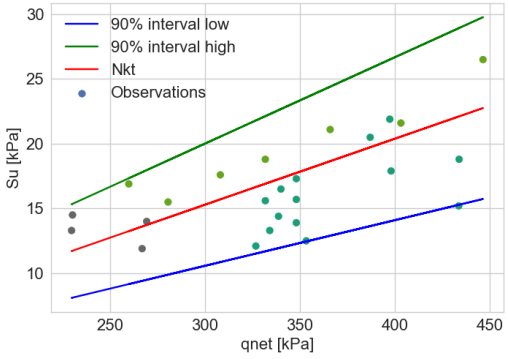

Figure 4.11: VC_{Nkt} determination for clay C.

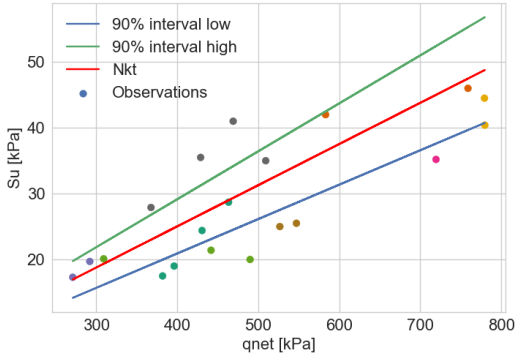

Figure 4.12: VC_{Nkt} determination for peat

The use of the least square error as a linear regression, results in the linear ascending $N_{kt,k}$ lines in figure 4.11 and 4.12. As is clearly visible in figure 4.12 there are hardly any points on the right top part of the figure,

this can indicate that there is a limitation in maximum undrained shear strength for the peat layer. At some point an increasing cone tip resistances will no longer coincide in an increasing undrained shear strength. It is therefore questionable if the linear regression is the most suited method. A quadratic regression could perhaps bring relieve in this case, this is discussed in appendix B.

Part of the uncertainty present in the determination of the cone factor cannot be devoted to epistemic uncertainty, and is referred to as the systematic error. This part of the uncertainty cannot be averaged over VC_{nkt} and will not diminish with additional measurements. It is assumed that this 'behaviour' can be devoted to the soil and can therefore not be labelled as uncertainty, the implementation of this systematic error will result in a reduction of the transformation coefficient. The value for the systematic error lies between 0 and 1.

The relationship between the undrained shear strength and the cone tip resistance can be presented by an ascending line (N_{kt}). However it can occur that laboratory test obtained from the same borehole give different results for the undrained shear strength, while the cone tip resistance is almost constant. This results in a systematic error, an example of such an error is indicated with vertical arrows in figure 4.13. This figure is adopted from the 'Dijken op Veen' project [11]. The systematic error is assumed to be equal to 0.75, this value is also used in this thesis and in the Markermeerdijken project.

In figure 4.13 the points have different colours which represent different testing fields. The blue lines represent the cone factor and VC_{Nkt}. It is interesting to notice that the data of each single testing field presented in figure 4.13 will result in a lower VC_{Nkt}, compared to the VC_{Nkt} of all testing fields combined. In a large project, where sufficient data is available, it could perhaps be interesting to determine a local N_{kt} and VC_{Nkt}, that depend on the data of two or three testing fields.

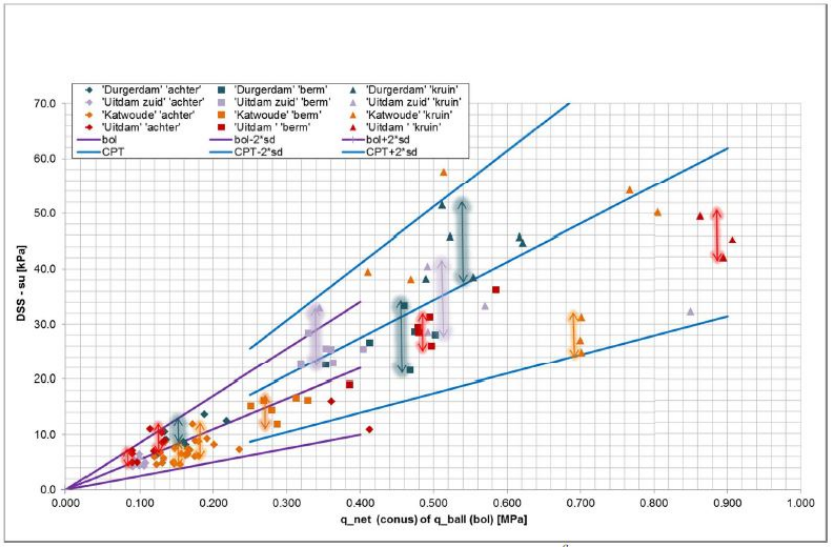

Figure 4.13: An indication of the systematic error determined in the DOV project [11]

The correction for the systematic error on VC_{Nkt} results in the transformation variation coefficient, equation 4.5. Within this equation also the number of measurements is considered. In a CPT every 2 centimetres a measurement is present and therefore $1/n_{m,cpt}$ is approximately equal to zero.

$$VC_{trans} \approx \sqrt{r_{sys} + \frac{1}{n_{m,cpt}}} \cdot VC_{N_{kt}} \approx \sqrt{r_{sys}} \cdot VC_{N_{kt}} \tag{4.5}$$

In which:

VC_{trans}	The transformation variation coefficient	[−]
r_{sys}	The systematic error	[−]
$n_{m,cpt}$	Number of measurements in 1 CPT (every 0.02 cm)	[−]

Table 4.4: Variation coefficient and systematic error

	Clay C.	**Peat**
r_{sys}	0.75	0.75
$\frac{1}{n_{m,CPT}}$	0.00	0.00
VC_{Nkt}	0.17	0.21
VC_{trans}	0.15	0.19

4.2.3. Linearisation undrained shear strength

To implement the estimated undrained shear strength in a model it is convenient to linearise all measurements (every 2 centimetres) in a layer. The linearisation of the undrained shear strength is a practical solution to decrease the number of layers in vertical direction within the model. A linearisation is preferred over the average since the undrained shear strength often shows a trend with increasing depth. The linearisation is performed with equation 4.6 and 4.7. The part of the cone tip resistance present near layer transitions is not considered since it can cause distortion in the linearisation. Therefore 3·*cone diameter* (D_{cone}) is added to the bottom of a layer and D_{cone} mm is subtracted from the top of a layer [64]. The class 1 CPT cone diameter used in the Markermeerdijken project is 43 mm.

$$z = c_2 + c_1 \cdot q_{net} \tag{4.6}$$

$$c_1 = \frac{\sum(z-\bar{z})^2}{\sum((q_{net}-\bar{q}_{net})(z-\bar{z}))} \qquad c_2 = \bar{z} - c_1 \cdot \bar{q}_{net} \tag{4.7}$$

In which:

z	=	Depth	$[m]$
$\bar{z}$	=	Mean depth over all measurements in one layer	$[m]$
$\bar{q}_{net}$	=	Mean of q_{net} over all measurements in one layer	$[MPa]$
c_i	=	Constant	$[-]$

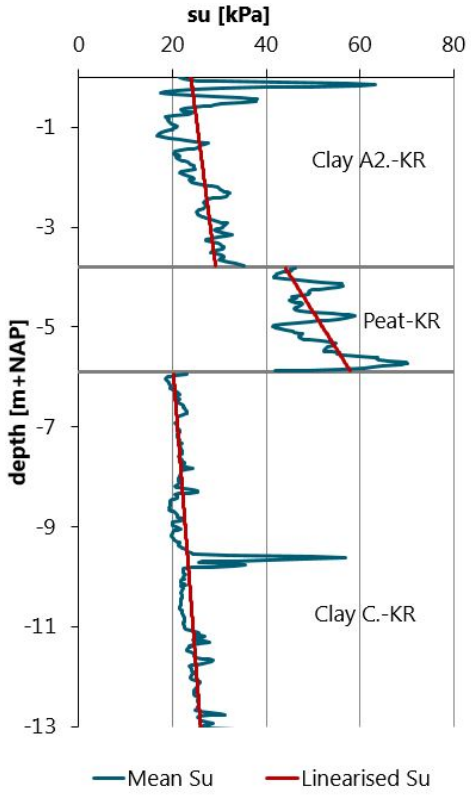

Figure 4.14: Example of linearised undrained shear strength for different soils

In figure 4.14 an example of a linearisation for three different layers is shown. In blue the undrained shear strength obtained with the cone factor is shown and in the red line is the linearised undrained shear strength.

The stratification and the enormous variability within the subsoil can cause problems regarding the linearisation. Small sand or clay lenses could for instance be present in a thicker layer. Modelling all lenses separately would be inconvenient and would hardly effect the stability within the model in most cases. The linearisation is adapted (if needed) to create the best representation for the considered cone tip resistance. The 'best representation' is a linearisation in which the major part of the undrained shear strength coincides with the linearisation. The small lenses can cause the linearisation to be translated or can affect the angle. Adjustment for large peaks can lead to a conservative or progressive linearisation.

4.2.4. Regional uncertainty

Besides the transformation uncertainty a regional uncertainty is present, the analogy behind the regional uncertainty is explained in this section. Geotechnical parameters, such as the undrained shear strength, differ in space. The undrained shear strength is anisotropic, in vertical direction there are much more fluctuations on a small scale in comparison to the fluctuations in horizontal direction. The undrained shear strength is expected to vary along the x coordinate (horizontal) and the z coordinate (vertical) as presented in figure 4.15. In figure 4.15 the fluctuations of the undrained shear strength vary along a mean value. The mean and standard deviation depend on the geological deposit and the chosen layer thickness. Both the local variation (each CPT) as the regional variation (set of CPTs) in one geological deposit are considered in the regional variation coefficient [8].

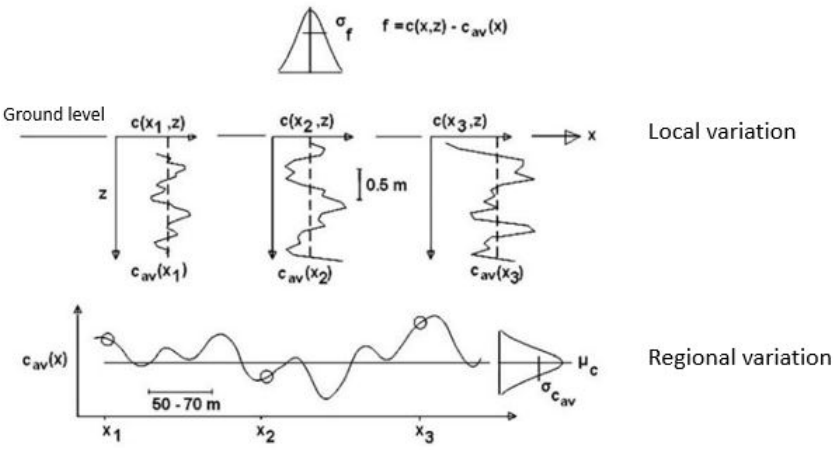

Figure 4.15: Spatial variation in undrained shear strength [8]

The regional variation coefficient does not really account for uncertainty in s_u in vertical and horizontal direction. In a model the undrained shear strength is linearised over each layer, see section 4.2.3. The linearisation is an approximation of the actual undrained shear strength and will therefore result in an error. The error originating from this linearisation is used to quantify the local uncertainty. Combining the errors of multiple CPTs will result in the regional variation coefficient, equation 4.8. The regional variation coefficient adjusts for the over- and underestimation due to the linearisation of the undrained shear strength.

The regional variation coefficient is determined based on the CPTs that are used in the testing field. A large regional variation coefficient, originating from large errors regarding the linearisation of CPTs in the testing field, affects the uncertainty in the entire project. Local q_c peaks in the CPTs of the testing field could lead to a misleading regional uncertainty, see appendix B. In this thesis the regional variation coefficient adjustment for local peaks is not taking into consideration.

$$VC_{reg} = \sqrt{\frac{\sum_{i=1}^{n_{CPTs}} \sum_{j=1}^{n_{meas,j}} \left(\frac{q_{net}}{N_{kt} \cdot s_{u,lin,i}} - 1\right)^2}{n_{m,reg}}} \tag{4.8}$$

The regional variation coefficient has to be multiplied with multiple factors that correct for the layer thickness, number of measurements and the ratio between the regional and the transformation uncertainty [64]. This results in the average regional variation coefficient, shown in equation 4.9. The determination of these factors are elaborated in appendix B. The average regional variation coefficient and the associated parameters are shown in equation 4.9 and presented in table 4.5.

$$VC_{av,reg} = \sqrt{\frac{1}{n_{m,reg}} + \Gamma^2 + \gamma_v \cdot (1 - \Gamma^2)} \cdot VC_{reg} \tag{4.9}$$

In which:

$s_{u,lin,i}$	=	Linearised undrained shear strength	$[kPa]$
$n_{m,reg}$	=	Number of measurements in all CPTs used for cone factor determination	$[-]$
Γ^2	=	Variation reduction factor of local average	$[-]$
γ_v	=	Vertical variation reduction factor	$[-]$
VC_{reg}	=	Regional variation coefficient	$[-]$
$VC_{av,reg}$	=	Average regional variation coefficient	$[-]$

Table 4.5: Regional variation coefficients and associated parameters

	Clay C	**Peat**
Γ^2	0.93	0.87
γ_v	0.17	0.10
$\frac{1}{n_{m,reg}}$	0.0	0.0
VC_{reg}	0.08	0.16
$VC_{av,reg}$	0.08	0.15

4.2.5. Total variation coefficient

The total variation required to determine the standard deviation and thereby the characteristic value of the undrained shear strength depends on a combination of the average regional ($VC_{av,reg}$) and transformation (VC_{trans}) variation coefficients, see equation 4.10. In general the contribution of the transformation uncertainty to the total uncertainty is 90%. The contribution of the transformation uncertainty is less than 90% in this thesis, but still governing with 78% and 62% for clay C. and peat respectively. The cone factors for peat and clay C. and the different variation coefficients are summarized in table 4.6

$$VC_{tot} = \sqrt{VC_{av,reg}^2 + VC_{trans}^2} \tag{4.10}$$

Table 4.6: Cone factors and variation coefficients

Parameter	**Clay C.**	**Peat**
N_{kt}	19.62	15.98
VC_{trans}	0.15	0.19
$VC_{av,reg}$	0.08	0.15
VC_{tot}	0.17	0.24

Example: Determination characteristic value of undrained shear strength
In figure 4.7 an example of the log-normal distribution for the undrained shear strength in the clay C.-KR layer is presented. This log-normal distribution is based on a single measurement in a CPT at a depth of -7.2 m NAP. As an example the required calculations and the corresponding values for this example are presented in equations 4.11 till 4.14. The input for this calculation are cone factor ($N_{kt,clay}$ = 19.62) and total variation coefficient ($VC_x = VC_{tot,clay}$ = 0.17) determined in this chapter. Furhtermore the cone tip resistance is required as an input value (q_{net} = 416kPa).

The characterized undrained shear strength over a CPT profile is shown in figure 4.16. In this CPT three different layers are indicated with the horizontal gray lines. The red line is the linearised mean

undrained shear strength and the dotted red line is the linearised characteristic value of the undrained shear strength over the depth. The measured example is taken at a depth of -7.2 m NAP as indicated with the green line in figure 4.16.

$$X_m = s_{u,mean} = \frac{q_{net}}{N_{kt}} = \frac{416}{19.62} = 21.20kPa \tag{4.11}$$

$$\sigma_{ln(x)} = \sqrt{ln(1+VC_x^2)} = \sqrt{ln(1+0.17^2)} = 0.169 \tag{4.12}$$

$$\mu_{ln(x)} = ln(s_{u,mean}) - \frac{1}{2}\sigma^2_{ln(x)} = ln(21.2) - \frac{1}{2}\cdot 0.169^2 = 3.04 \tag{4.13}$$

$$X_k = s_{u,k} = e^{\mu_{ln(x)} - 1.64\cdot\sigma_{ln(x)}} = e^{3.04-1.64\cdot 0.169} = 15.84kPa \tag{4.14}$$

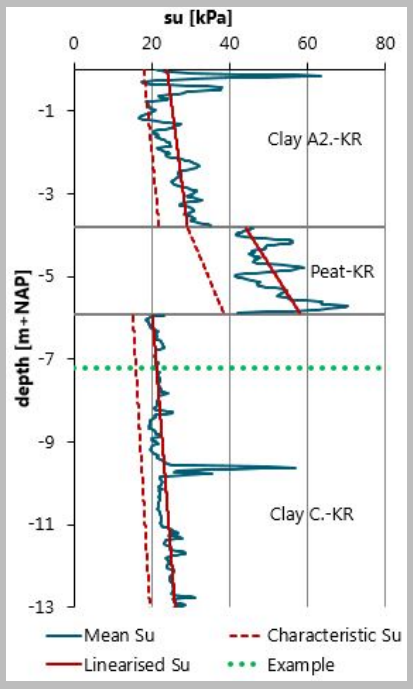

Figure 4.16: Example of $s_{u,k}$ over the depth

4.3. Reflection of S_u-measured method

In section 4.2 the cone factor and the corresponding variation coefficients were determined to calculate the characteristic undrained shear strength, however in most projects the influence of changing effective stresses on the s_u has to be accounted for. This effect can be considered with a combination between the SHANSEP and S_u-measured method as will be explained in this section. Furthermore the most important conclusions and remarks are listed here.

4.3.1. Combination SHANSEP and S_u-measured methods

In most projects it is of interest how the undrained shear strength changes when the effective stress changes, because an increasing water level is often a major cause of inner slope failure. In section 2.4.3 an explanation is given to combine SHANSEP and the S_u-measured method to account for different effective stresses.

The input parameters to determine the undrained shear strength during different conditions (SHANSEP) in a model are the unit weight, S, m, σ'_{vi} and a state parameter; σ'_{vy} or POP. The unit weight, S and m are adopted

Table 4.7: Parameters required for the SHANSEP method and friction angle [12]

	S_m	S_k	m_m	m_k	ϕ
Clay A1 and A2	-	0.22	-	0.80	-
Peat	0.47	0.45	0.88	0.85	-
Clay C	-	0.22	-	0.80	-
Sand	-	-	-	-	30.0

from the Markermeerdijken Alliantie, the unit weight will be elaborated on in section 5.1.2. In table 4.7 both the mean and characteristic values of S and m are shown. Similar to the S_u-measured method the SHANSEP method makes use of characteristic values as indicated in equation 4.15. For the clay layers the available data did not lead to a proper estimation of S and m and therefore characteristic values are obtained from literature [12]. Sand is modelled with the Mohr Coulomb model and therefore the S, m parameters are not applicable for this soil. The friction angle (ϕ) of 30 degrees is adapted from the Markmermeerdijken project [2].

$$s_{u,k} = \sigma'_{vi} \cdot S_k \cdot (\frac{\sigma'_{vy,k}}{\sigma'_{vi}})^{m_k} \tag{4.15}$$

In figure 4.17 the effect of characteristic values is visualised on the CSSM frame. In theory the POP or σ'_{vy} can be determined when both the SHANSEP and S_u-measured methods are combined. The combination of these two methods is based on mean values for all input parameters. An incorrect use of characteristic values in this combination can lead to wrong estimations of the POP or σ'_{vy}. Implementation of both the characteristic value for S (S_k) as well as N_{kt} ($N_{kt,k}$)[1] leads to an negligible error in the estimation of $\sigma'_{vy,k}$. This thereby ensure that the soil state does not change when the characteristic values are implemented. In figure 4.17 m_m is used, the characteristic value m_k is implemented in the model after $\sigma'_{vy,k}$ is determined.

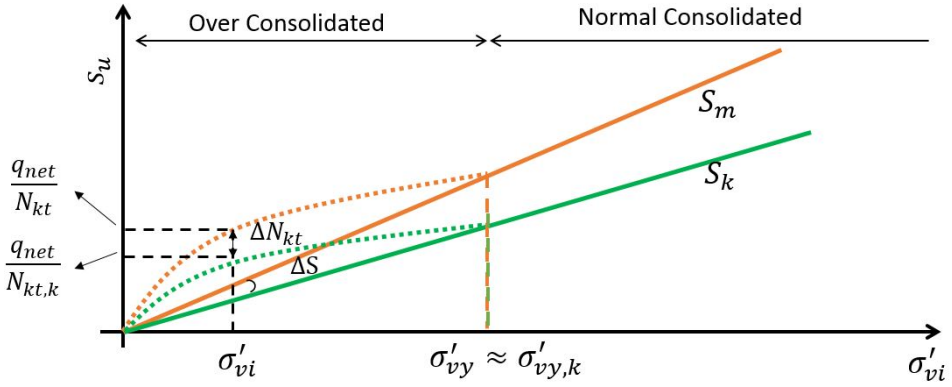

Figure 4.17: Combination of SHANSEP and S_u-measured method in the CSSM frame

Figure 4.17 indicates that X_k in equation 4.14 is only a part of the considered safety and the determination of S_k is of equal importance. In this chapter the focus lies in the determination of the cone factor and the corresponding variation coefficients to determine the undrained shear strength. However as indicated in this section differences in effective stress have to be taken into account in most calculations. Therefore an equal amount of effort and data should be used to determine S_k.

4.3.2. Conclusions and Remarks

The parameter determination and formulas presented in this chapter are based on 'Dijken op Veen II, DOV werkwijze voor bepaling macrostabiliteit Markermeerdijk' [64]. Additionally, the applied formulas to determine the variation coefficients of the cone factor are slightly alternated in more recent reports [59] [65].

[1] The characteristic cone factor ($N_{kt,k}$) is used for convenience in figure 4.17 Note: $N_{kt,k}$ is based on VC_{tot} whereas in equation 4.4 $N_{kt,k}$ is only based on VC_{Nkt}

It is remarkable that equation 2.10 used to determine the characteristic value of s_u, assumes that the statistical coefficient (k_n) is always equal to 1.645, which implies that infinite number of samples are present within the dataset. In the new presented method k_n is based on the number of samples [59] [65].

Despite striving for an objective execution of the calculations in this chapter, some subjectivity is present in the selection of the laboratory test and the linearisation of the undrained shear strength. The subjectivity partially results from the fact that the calculation of the cone factor along with the corresponding variation coefficient can be executed in several ways. Nevertheless these assumptions and applied methods are thought to be necessary and are further elaborated in appendix B.

The methods in more recent reports do not include $VC_{av,reg}$ [59] [65]. Since the contribution of $VC_{av,reg}$ to VC_{tot} is generally close to 10% it seems logical to exclude this part of the variation coefficient, especially since the effort of understanding and calculating this parameter is significant in comparison to its contribution in VC_{tot}. In this chapter the contributions of $VC_{av,reg}$ to VC_{tot} are equal to 22% and 38% for clay C. and peat respectively and therefore the contribution of $VC_{av,reg}$ is more relevant.

VC_{reg} is determined for one geological layer with multiple CPTs. The layer thickness for this considered geological layer can vary over the considered CPTs. The vertical reduction factor γ_v depends on the layer thickness and can therefore vary for each CPT. Nevertheless γ_v is multiplied with VC_{reg} in equation 4.9. This can to lead to misunderstanding and inaccurate estimations of $VC_{av,reg}$.

5
Stability Analysis

In this chapter the levee stability for the presented case study is assessed. In a semi-probabilistic analysis the safety factors for each cross section within the research area are determined. Furthermore a probabilistic stability analysis is performed to determine the relative influence of each input parameter on the probability of failure. The input parameters and results of both the semi probabilistic as well as the probabilistic stability analysis are given in this chapter.

5.1. Semi probabilistic stability analysis (Level I reliability approach)

In this section the safety of each cross section within the considered research area is computed and analysed. As in figure 4.2 the CPTs can be used to determine the stratification, with linear interpolation between successive CPTs a cross sectional model can be created. To analyse the stability of a cross section a calculation method is chosen, the water and phreatic level are required and furthermore the undrained shear strength, the unit weight, the S and m parameter of each deposit are required. All parameters are already addressed in chapter 3 and 4. A semi probabilistic stability analysis results in a safety factor; depending on the limit state function the cross section is classified as safe or unsafe. The stability analysis are performed with D-Geo Stability.

5.1.1. Software and calculation methods

The semi-probabilistic stability analysis are performed with the software D-Geo Stability provided by Deltares. D-Geo Stability is a tool that makes use of the Limit Equilibrium Methods discussed in section 2.2.1. All LEMs within D-Geo Stability make use of an algorithm that searches for the critical slip surface in the therefore assigned area in the cross section [13]. At first a stability analysis is performed with the LEM of Bishop to give an indication of the safety factor and location of the slip surface within the considered cross section. Additionally a stability analysis is performed with the LEM of Spencer to determine the actual critical slip surface and minimum safety factor. The execution of both methods helps to validate their results.

In D-Geo Stability the 'Default Shear Strength' has to be designated, this indicates how the undrained shear strength is implemented in the software, e.g. $s_{u,top}$ and $s_{u,bottom}$, POP_{top} and POP_{bottom} or σ'_{vy}. $s_{u,top}$ and $s_{u,bottom}$ could be obtained from CPT data with the cone factor. D-Geo Stability interpolates between the top and bottom value to determine s_u at any depth in the considered layer. With POP_{top} and POP_{bottom} a value for the over consolidation is implemented in D-Geo Stability. Interpolation between the top and bottom determines the degree of OCR at any depth in the considered layer. A pre-consolidation pressure (σ'_{vy}) is implemented per layer, D-Geo Stability calculates s_u based on the effective stress at any location in the layer. For this thesis the so called 'DOV calculated' method is used in the semi-probabilistic analysis, which requires the POP values to be quantified at the top and bottom of each layer, see section 5.1.2.

5.1.2. Input parameters

In this section all input parameters required to perform a stability analysis with D-Geo Stability are presented. The main goal is to determine the influence of the undrained shear on the safety factor. Therefore the stability in 51 cross sections along the 5 km long research area are analysed. The undrained shear strength is implemented with POP_{top} and POP_{bottom}. Simplifications within the model help to diminish the influence of other variables on the safety factor. These simplifications are listed below and are discussed throughout

Table 5.1: Parameters assumed to vary or be constant along 51 cross sections

Category	Parameter	Variation in longitudinal direction
Undrained shear strength	POP_{top} and POP_{bottom}	Varies in longitudinal direction
Stratification	Layer thickness	Varies in longitudinal direction
	Presence of layers in vertical	Constant
Ground level	Ground level	Constant
Phreatic lines	MHW	Constant
	DHW	Constant
Remaining parameters	γ_{sat} and γ_{unsat}	Constant
	S_k	Constant
	m	Constant

this section. In table 5.1 it is indicated which input parameters vary in longitudinal direction and which are assumed to be constant.

Pre Overburden Pressure (POP) The safety of the levee is assessed in ULS, as a result design values for s_u are required. Because the material factor (γ_m) is 1.0, the characteristic value of the undrained shear strength is equal to the design value, see equation 5.1.

$$\frac{s_{u,k}}{\gamma_m} = s_{u,d} \tag{5.1}$$

For the stability analysis in D-Geo Stability the 'DOV calculated' method which requires the POP value at the top and bottom of each layer is used. $s_{u,k}$ values are rewritten to characteristic POP values at the top and bottom of each layer with equation 5.2. This measure helps to account for difference in effective stress. The POP_{top} and POP_{bottom} have to be determined for each layer in 51 cross sections. As an example the POP value at the bottom of the peat-KR layer for 1 cross section is determined at the end of section 5.1.2.

$$POP_k = \sigma'_{vi} \cdot ((\frac{s_{u,k}}{S_k \cdot \sigma'_{vi}})^{(1/m)} - 1) \tag{5.2}$$

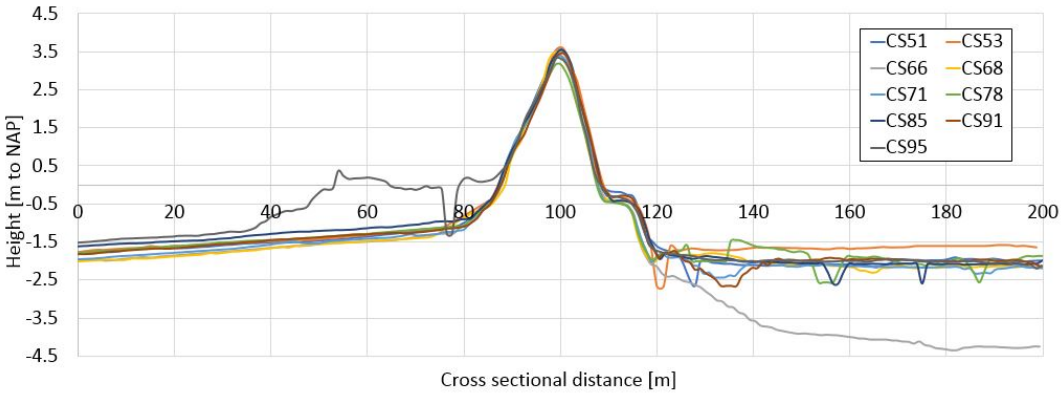

Figure 5.1: Comparison of 9 surface levels within the research area

Ground level The ground level describes the height of the levee relative to the NAP (Normaal Amsterdams Peil). A cross sectional profile of the ground level is composed with multiple consecutive measurements that are obtained from AHN (Actueel Hoogtebestand Nederland). For the Markermeerdijken 9 cross sectional profiles are constructed within the proposed research area. These 9 ground level profiles are shown in figure 5.1 and are thought to be most critical regarding the failure of the inner slope. The ground levels of cross section (CS) 66 and 95 stand out compared to the rest; In CS 95 a foreshore (voorland) is present and the ground level profile of CS 66 is characterized by a low lying hinterland.

In this thesis the ground level profile is assumed to be constant in longitudinal direction. The ground level profile of CS 91 is chosen as the representative ground level in the D-Geo Stability model. The number of AHN data points in the ground level profile is decreased to 15 points for the representative cross section, see figure 5.2. The influence of the ground level on the safety factor can be significant and therefore the effect of this simplification is examined in appendix C.

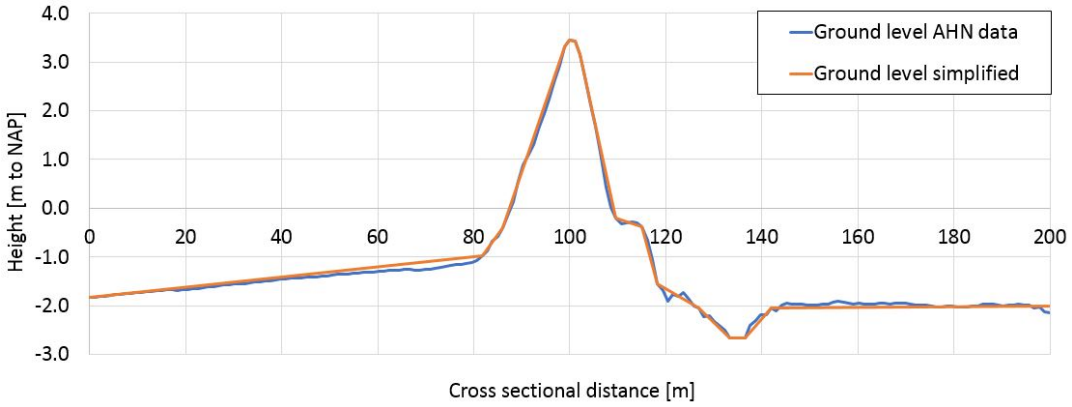

Figure 5.2: Representative ground level profile simplified

Stratification The stratification implemented in the model is shown in figure 5.3. The stratification is a simplification in comparison to reality but can still serve as a good representation. The layer sequence in vertical direction is assumed to be constant in longitudinal direction, whereas the layer thickness (t_{layer}), indicated with vertical arrows in figure 5.3 varies in longitudinal direction and is based on CPT data. Since the unit weight and undrained shear strength/OCR differs under and next to the levee there are vertical separations in geological deposits. As indicated in section 4.1.1 the layer separation in vertical W and AL are at equal depth as in the inner berm.

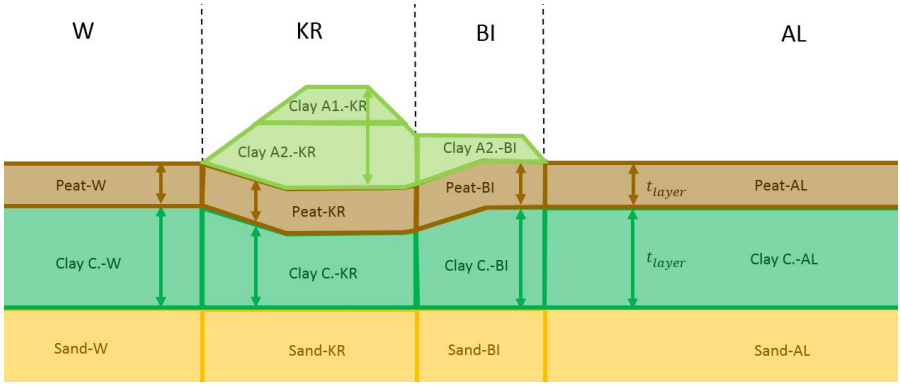

Figure 5.3: Stratification within the selected area

Under the crest, above the phreatic level, a part of the soil is not fully drained which causes the soil behaviour to deviate compared to undrained soil. Therefore the clay A. layer is divided into two layers, clay A1.-KR and clay A2.-KR, that are assumed to behave drained and undrained respectively. The division of these layers is below the phreatic level (0.54 m NAP). A major difference is that the POP in the clay A2.-KR is based on CPT data, whereas the POP in the clay A1.-KR is obtained from the Markermeerdijken project and assumed to be constant at 20 kN/m^2.

Phreatic lines The water level within the levee is based on the water level in the Markermeer and can be of significant influence on the inner slope stability. A good insight in the height of the phreatic lines is crucial to properly design a levee. The MHW, DHW and the polder level are obtained from the Markermeerdijken

project as indicated in chapter 3 and are shown in table 5.2. Based on the water levels in the Markermeer in combination with measurements of the water level in the levee, the phreatic lines are determined. The phreatic lines are obtained from the Markermeerdijken project as well.

The phreatic lines in the Markemeerdijken are based on measurements performed in 3 monitoring wells along the research area and are schematised as indicated in the Technical Report 'Waterspanning bij dijken' [56].The PL-lines differ along the 5 kilometre long research area and can be divided into three areas: CS 50-84 (red), CS 85-92 (green) and CS 93-100 (yellow) as shown in figure 5.4. The phreatic lines differ for MHW and DHW as well. The phreatic lines are compared and a representative phreatic line for the considered research area is chosen.

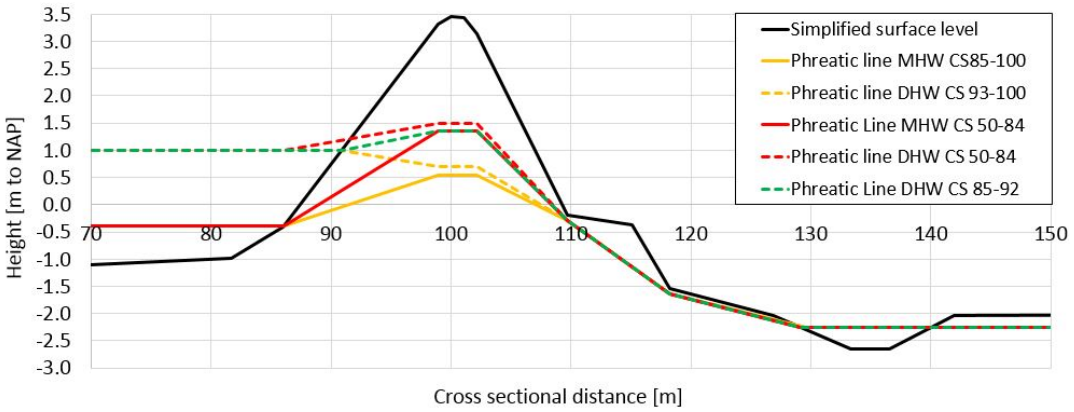

Figure 5.4: The different phreatic lines assumed to be present along the 5 km research area for MHW and DHW

Since cross section 50-84 covers most of the 5 km long area and the calculated phreatic lines and hydraulic heads are the highest these are assumed to be present over the entire research area (CS 50-100), see table 5.2. The assumption causes cross sections 85 till 100 to be modelled in a slightly conservative manner. The effect of this assumption on the safety factor is analysed in the sensitivity analysis in appendix C. Moreover the hydraulic heads in the sand layer is defined in table 5.2 and obtained from the Markermeerdijken Alliance as well.

Table 5.2: Assumed phreatic line in each cross section along the considered research area

	CS 50-100 [m to NAP]
MHW	-0.40
DHW	1.00
Polder level	-2.26
Water level KR MHW	1.35
Water level KR DHW	1.50
Hydraulic head in sand layer MHW	-2.40
Hydraulic head in sand layer DHW	-1.81

Unit weight, S and m In this thesis the unit weight, S and m of each layer are obtained from the Markermeerdijken project and are assumed to be constant in longitudinal direction [12]. In cross-sectional direction however, the unit weight of the clay C. and peat layers differ and are assumed to be lower in the hinterland than under the levee, see table 5.3. The weight of the levee compresses the soil layers underneath, which causes the unit weight to increase. The mean and characteristic values for S and m are already shown in table 4.7.

Table 5.3: Unit weight of layers

	KR $[kN/m^3]$	BI$[kN/m^3]$	W and AL $[kN/m^3]$
$\gamma_{sat}/\gamma_{unsat}$ Clay A1 and A2	14.3	14.3	-
$\gamma_{sat}/\gamma_{unsat}$ Peat	10.4	10.4	10.0
$\gamma_{sat}/\gamma_{unsat}$ Clay C	14.3	14.3	14.0
$\gamma_{sat}/\gamma_{unsat}$ Sand	18-20	18-20	18-20

Example: Determination characteristic POP value
As an example the POP value at the bottom of the peat-KR layer in one cross section is calculated. The CPT profile of figure 4.16 is used. The characteristic undrained shear strength at the bottom of the peat-KR layer is 35.8 kPa (at a depth of -5.8 m NAP). The effective stress is calculated based on the unit weight of the clay A1., clay A2. and the peat layer above the considered point and is equal to 71.5 kPa. The input values and the resulting $POP_{k,bottom}$ are shown here.

- $\sigma'_{vi} = 71.5kPa$
- $S_k = 0.45$
- $m_k = 0.85$
- $su_k = 35.8kPa$

$$POP_{k,bottom} = 71.5 \cdot ((\frac{35.8}{0.45 \cdot 71.5})^{(1/0.85)} - 1) = 9.5kPa \tag{5.3}$$

5.2. Results stability analysis

Along the 5 km specified research area, the inner slope stability is analysed with the LEMs of Bishop and Spencer in 51 cross sections. Calculations using the method of Bishop are calculated prior to the Spencer models. As an example, figure 5.5 shows the calculated undrained shear strength along the critical slip surface using Bishop, for cross section 67. In figure 5.5 it can be observed that the undrained shear strength along the critical surface is highest in the peat layer present under the crest. In figure 5.6 the calculated critical slip surface using Spencer for cross section 67 is shown. The two slip surfaces are fairly similar although the slip surface determined with Spencer is not circular, the stress distribution along the slip surface is comparable to Bishop's. The safety factors are 1.15 and 1.13 for the LEM of Bishop and Spencer respectively.

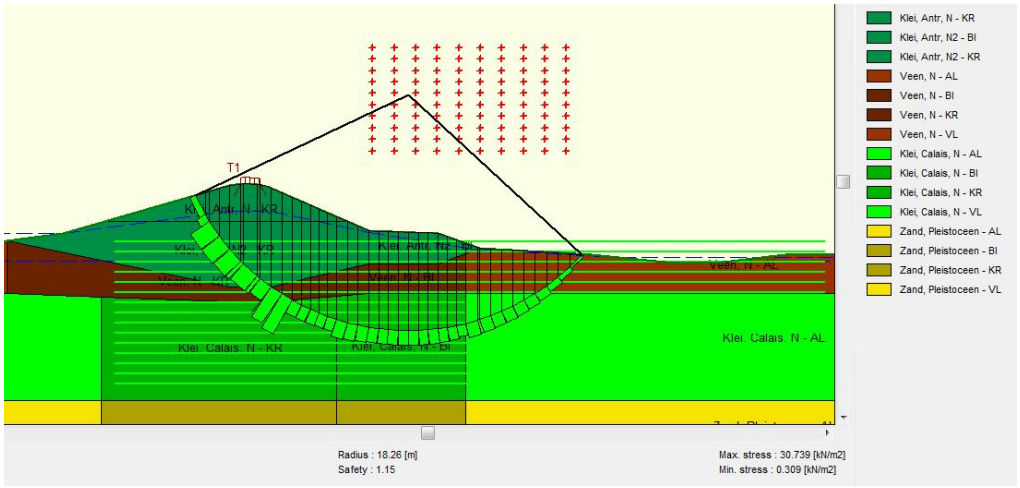

Figure 5.5: Undrained shear strength along the critical Bishop slip circle for cross section 67

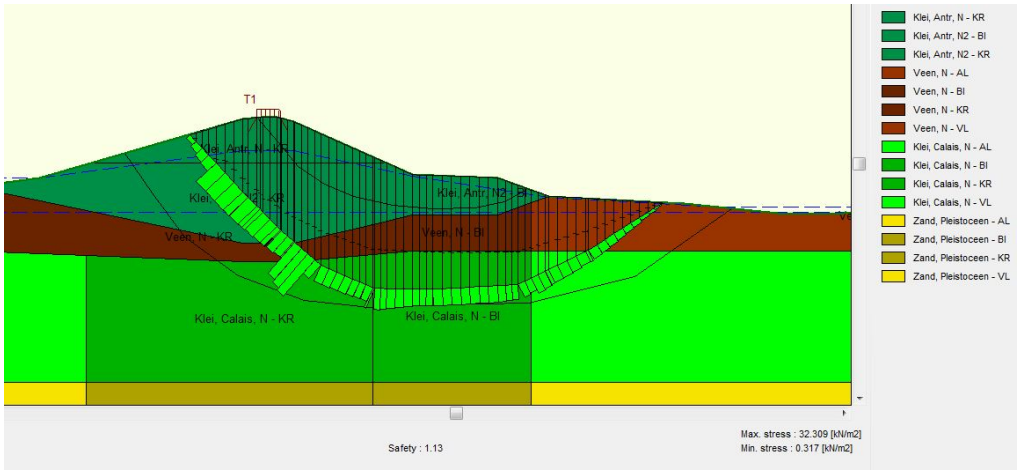

Figure 5.6: Undrained shear strength along the critical Spencer slip surface for cross section 67

Figure 5.7 shows the calculated safety factor (ULS) for each cross section determined with the method of Spencer, considering MHW. Due to the simplifications presented in section 5.1 the calculated safety factors only depend on the undrained shear strengths ($s_{u,d}$) and the layer thickness. The distance between successive cross sections is 100 m, the 51 cross sections cover a length of 5 km. The dotted line is used to improve visualisation and has no further meaning. Although most of the input parameters remain constant along the levee, still a lot of variation in safety factors along the levee is found. The stability analysis therefore gives an indication regarding the influence of s_u on the probability of failure of the inner slope. The required safety factor for Spencer ($SF_{req,spencer}$) is equal to 1.19, most cross sections are therefore classified as unsafe.

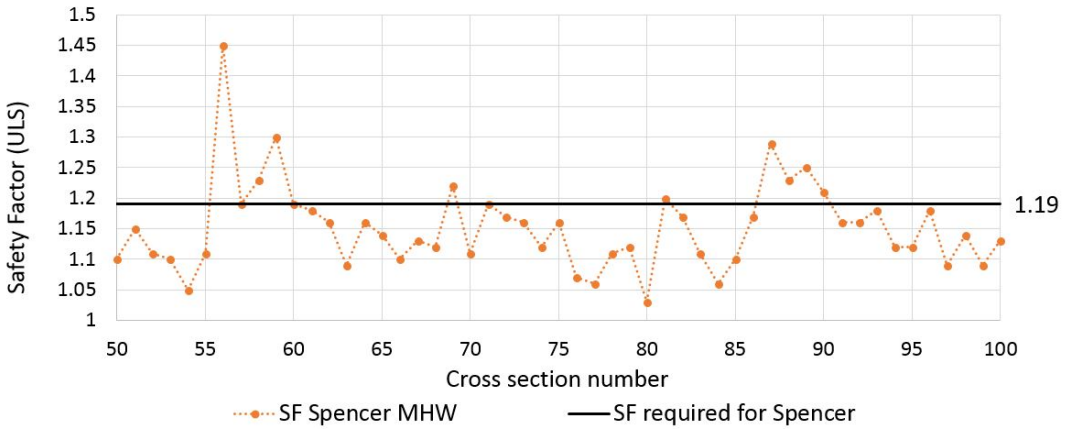

Figure 5.7: Safety factor (ULS) for 51 cross sections determined with the LEM of Spencer, considering MHW

The difference in safety factor considering MHW and DHW is minimal. In figure 5.8 the difference in safety factor for MHW and DHW for 51 cross sections for the LEM of Spencer is presented. On average the difference in safety factor is 0.03, whereas the difference in MHW and DHW is 1.4 m. The small change in safety factor is caused by a relatively small increase of 20 cm in PL-line within the levee. Implementing MHW and DHW conditions results in a small change in safety factor and therefore the water level is kept constant at MHW in the probabilistic analysis. MHW conditions are chosen since this does not require the undrained shear strength to be rewritten into POP values.

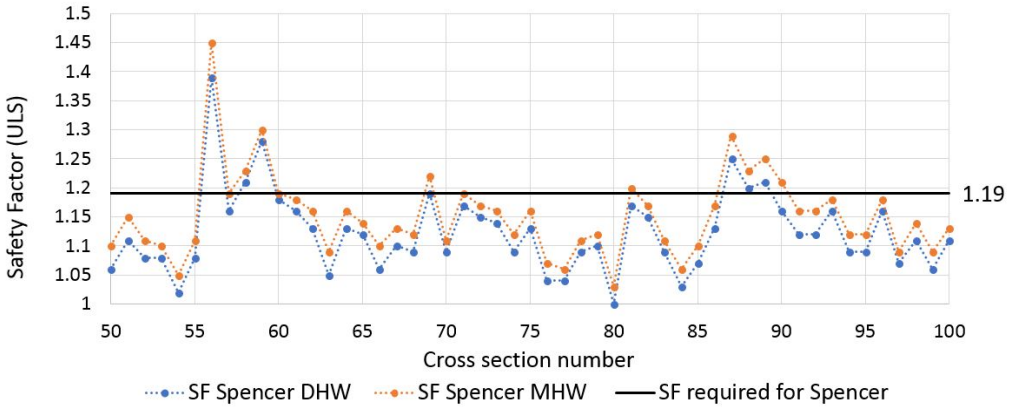

Figure 5.8: The difference in SF applying MHW and DHW calculated with Spencer

5.3. Probabilistic Stability Analysis (level II reliability approach)

In contrast to a semi-probabilistic stability analysis a probabilistic analysis provides more insight in the relative influence of stochastic parameters with respect to the estimated reliability of a levee. A probabilistic analysis results in a more realistic safety analysis compared to a semi-probabilistic analysis. Instead of characteristic values, which are implemented deterministically in a semi probabilistic stability analysis, distributions with a mean and standard deviation are used in a probabilistic analysis. With a probabilistic calculation the influence of each parameter on a given limit state function is presented in its alpha factor.

In this section the required software and calculation methods will briefly be addressed. The probabilistic analysis is conducted with the help of the Probabilistic Toolkit provided by Deltares, which imports D-Stability models. A sensitivity analysis prior to the probabilistic stability analysis is used to determine which scenarios are most essential to model in the Probabilistic Toolkit.

5.3.1. Software and calculation methods

The Probabilistic Toolkit provides multiple calculation methods such as Monte Carlo, Importance Sampling, Numerical integration, Numerical bisection, Directional sampling and a FORM analysis [1]. These available methods are all level III reliability methods except for the FORM analysis. In this thesis only the FORM analysis is used because the other methods require too much modelling time. The computation time in a Monte Carlo analysis depends on the probability of failure and the relative error, computation time increases with increasing number of stochastic parameters. The basic principles of a FORM are explained in section 2.5.2.

With a FORM analysis the relative influence of each stochastic parameter on the reliability can be determined, this is expressed in alpha factors (α) or influence factors. Although both the influence factor as well as the alpha factor represent the influence of stochastic parameters on the reliability index, they are expressed in different ways. The sum of the influence factors of all stochastic parameters is 100%, whilst the sum of the alpha factors squared is 1. Alpha factors can be positive and negative: a positive alpha value indicates that an increase of the corresponding variable results in non-failure or a higher reliability, vice versa for negative alpha factors.

Although FORM is relatively quick, there are some disadvantages. The iteration process can define a local design point instead of the actual design point. The local design point is different from the actual design point as it has a higher reliability index. Numerical problems may occur, because the limit state function needs to be continuous. In the probabilistic analysis the critical slip surface is locked within the first iteration. The following consecutive iterations make use of the same slip surface. It can occur that the locked slip surface is not the critical slip surface. Validation with a semi-probabilistic analysis has to determine if the considered slip surface is indeed the critical slip surface.

For each calculation the numerical input parameters as shown in table 5.4 are used as starting values. These values are adopted from 'Handreiking Faalkansanalyses Macrostabiliteit' [50], except for the number of iterations and the relaxation factor.

Table 5.4: Numerical input parameters Probabilistic Toolkit

Relaxation factor	1.0
Max iterations	6
Gradient step size	0.30
Conv. requirements: Difference β	0.05
Conv. requirements: Difference failure definition	0.05

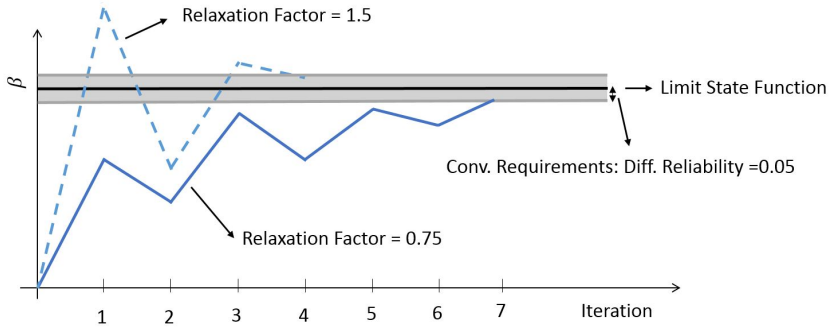

Figure 5.9: Explanation of relaxation factor and conv. requirements

In figure 5.9 a schematisation of the relaxation factor and the convergence requirements are shown. The relaxation factor indicates which percentages of the gradient step size is used in between iterations. A relaxation factor equal to 1 means that the full gradient step size is used. A larger relaxation factor can help to decrease the computation time, however this can also result in divergence. A small relaxation factor can be of use when a finite element method is used. In a limit equilibrium method a safety factor lower than 1.0 does not cause numerical problems and therefore this restriction does not apply on this case.

The convergence requirements for the difference in failure definition is set at 0.05, table 5.4. This means that a bandwidth of 0.05 in failure definition (or safety factor) is allowed within the result, see figure 5.9. This is a rather large uncertainty that could be present in the results. A difference of 0.05 in safety factor could cause a levee to be wrongly classified as safe or unsafe. The other convergence requirements indicate that β should not vary to much from step to step. In appendix C the convergence requirements are tightened to investigate possible unwanted effects. Tightening of the convergence requirements does not influence the results in this thesis.

The Probabilistic Toolkit requires a semi-probabilistic model as input file. Since D-Geo Stability does not provide the correct output files, D-Stability is used. Apart from the user interface, D-Geo Stability and D-Stability should give identical results. However implementation of POP values in D-Geo Stability and the use of s_u values in D-Stability can result in a small offset in safety factor, see Appendix C.

The critical slip surfaces found for the LEM of Spencer are nearly circular. Therefore the LEM of Bishop is used to calculate the stability in the probabilistic analysis. The LEM of Bishop is more convenient and faster in a probabilistic calculation. Moreover the LEM of Spencer can cause convergence problems when the critical slip surface is not predefined. A comparison between the LEM of Bishop, Spencer and Uplift Van is made in appendix C.

5.3.2. Sensitivity Analysis

Prior to the probabilistic analysis a sensitivity analysis is performed. The sensitivity analysis consists of multiple semi-probabilistic stability analyses which can help to interpret and predict the results of a probabilistic calculation. Since probabilistic analysis require a lot of computation time, a sensitivity analysis helps to determine which scenarios are most interesting to model. The effect of difference in s_u and $s_{u,k}$, the difference in MHW and DHW and different layer thickness's on the safety factor are examined. From the sensitivity analysis it can be concluded that:

- Implementing MHW and DHW in the stability analysis led to a difference in safety factor of 0.03 on average, see figure 5.8. Therefore only MHW is considered in the probabilistic analysis, implying that the s_u does not need to be rewritten to POP values.
- Implementing s_u and $s_{u,k}$ in the stability analysis led to a difference in safety factor of approximately 1.5. Although this was expected it underlies the importance of the exact estimation of the s_u and the corresponding variation coefficients.
- There is a relativity strong correlation between the thickness of the peat-KR layer and the safety factor, appendix C.

The more extensive sensitivity analysis is presented in appendix C.

Conditions for probabilistic stability analysis

- Use of MHW since the water level hardly influences the safety factor: s_u remains constant and therefore $s_{u,top}$ and $s_{u,bot}$ are implemented in the Probabilistic Toolkit.
- The LEM of Bishop is used in the probabilistic stability analysis since the critical slip surface is nearly circular.
- The required reliability: $\beta_{req} = 4.03$

5.3.3. Scenarios Probabilistic analysis

The main goal of the probabilistic analysis is to determine the relative influence of both layer thickness and undrained shear strength regarding the probability of failure. The layer thickness differs for each cross sections and therefore fluctuates in longitudinal direction. In the probabilistic analysis these fluctuations together with the fluctuation of the undrained shear strength in longitudinal direction are analysed.

In the probabilistic analysis the fluctuations in cross sectional as well as in longitudinal direction will be analysed, therefore 4 scenarios are composed. In which the influence of the undrained shear strength, the layer thickness and the unit weight are analysed. With figure 5.10 the stochastic parameters for each scenario can easily be distinguished, the red dots indicate the cross sectional location where the undrained shear strength is defined, the yellow dots indicate the location where the layer separation is defined. Furthermore numbers are assigned at each layer separation (separation 1,2 and 3). It has to be emphasized that fluctuations in longitudinal direction are considered in this thesis but they are implemented in a cross sectional model.

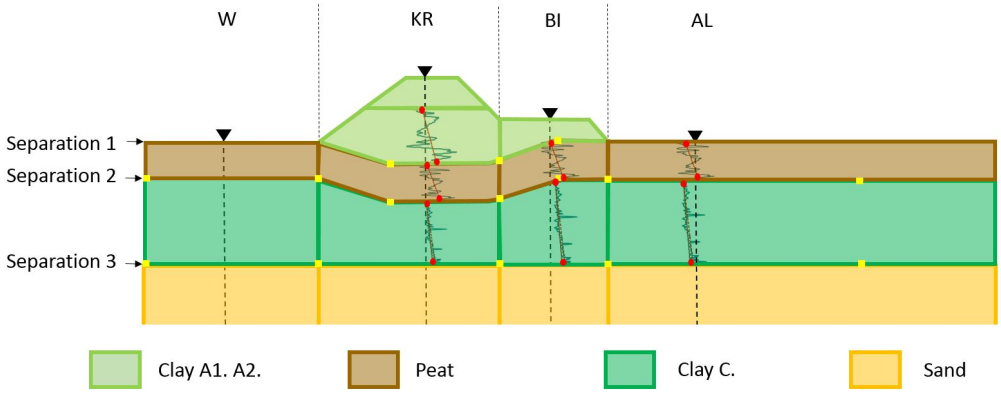

Figure 5.10: Cross section of probabilistic model

Variation in cross sectional direction Scenarios 1 and 4 consider fluctuations in cross sectional direction, see figure 5.11. The distribution of the undrained shear strength in scenario 1 and 4 depend on the variation coefficient determined in chapter 4. Because a probabilistic stability analysis requires significantly more computation time than a semi-probabilistic stability analysis not all 51 cross sections are analysed for scenario 1 and 4. Three cross sections within the research area will be chosen. The weakest link in a levee causes failure, therefore the weakest part of the levee is of greatest interest. In figure 5.7 it can be seen that the lowest

safety factor is found in cross section 80. Besides CS80 two typical/average cross section are chosen as a reference. Cross sections 62 and 83 contain an average layer thickness and undrained shear strength compared to the other cross sections. These therefore give a good representation of the 5 km long levee.

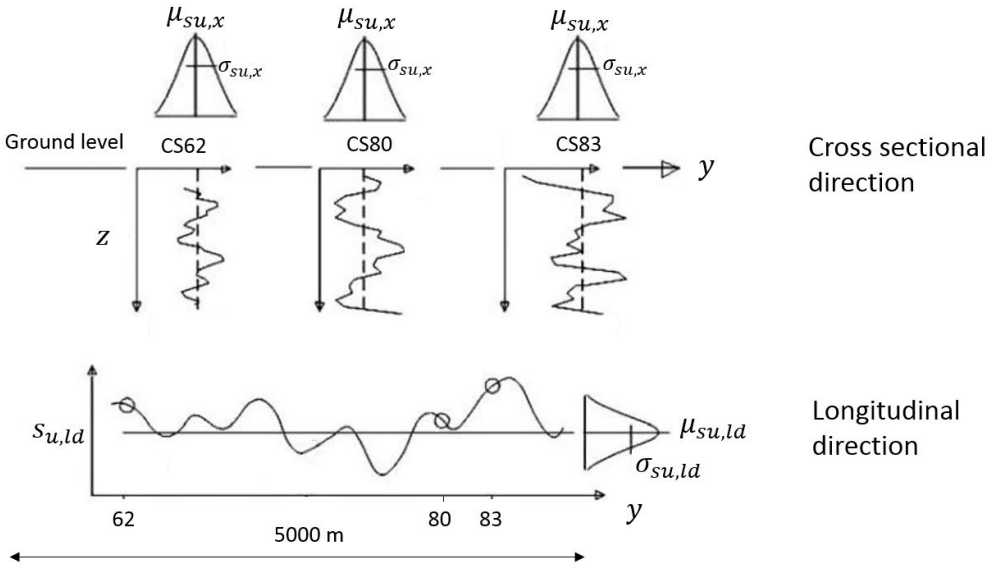

Figure 5.11: Undrained shear strength used in cross sectional scenario and longitudinal

Variation in longitudinal direction Scenario 2 and 3 consider fluctuations in longitudinal directions. Both scenarios use the undrained shear strength in longitudinal direction ($s_{u,ld}$), figure 5.11. The distributions are based on $s_{u,lin}$ found in 51 different cross sections at the top and bottom of each layer. In these scenarios the variation coefficient determined in chapter 4 is not considered. Although scenario 2 makes use of $s_{u,ld}$ the layer thickness still varies per considered cross section. Therefore the layer thickness present in cross sections 62, 80 and 83 are used for scenario 2. In scenario 3 also the fluctuation in layer thickness for 51 cross sections is considered.
In the following enumeration the goal of each scenario, the stochastic parameters, the calculated cross sections and the direction of variation for each scenario is presented.

1.
   - **Direction of variation:** Cross sectional
   - **Calculated cross sections:** 62, 80 and 83
   - **Goal:** Determine the influence of s_u amongst different layers in a cross section to the probability of failure.
   - **Stochastic parameters:** $s_{u,top}$ and $s_{u,bot}$ of the clay A2, peat and clay C. layer in verticals KR, BI and AL are implemented as stochastic values as indicated with the red dots in figure 5.10.
2.
   - **Direction of variation:** Longitudinal direction
   - **Calculated cross sections:** 62, 80 and 83 with $s_{u,ld}$[1]
   - **Goal:** Gain more insight in the relative influence of the linearised undrained shear strength in longitudinal direction ($s_{u,ld}$) with respect to the probability of failure.
   - **Stochastic parameters:** $s_{u,top}$ and $s_{u,bot}$ of the clay A2., peat and clay C. layers in verticals KR, BI and AL combined for 51 cross section. This results in two new PDFs for each layer which are indicated with $s_{u,ld,top}$ and $s_{u,ld,bot}$. These PDFs represent the fluctuation in undrained shear strength in longitudinal direction, see figure 5.11.
3.
   - **Direction of variation:** Longitudinal direction
   - **Calculated cross sections:** All 51 cross sections
   - **Goal:** Determine the influence of layer thickness and $s_{u,ld}$ to the probability of failure.

[1] In scenario 2 the undrained shear strength is determined in longitudinal direction for 51 cross sections. The layer thickness is different for all 51 cross sections. Therefore only 3 cross sections are calculated

- **Stochastic parameters:** $s_{u,ld,top}$ and $s_{u,ld,bot}$ in the clay A2., peat and clay C. layers in verticals KR, BI and AL. Furthermore layer separations 1,2 and 3 indicated with the yellow points in figure 5.10 are implemented stochastically.

4.
- **Direction of variation:** Cross sectional
- **Calculated cross sections:** 62, 80 and 83.
- **Goal:** Determine the relative influence of the unit weight and s_u to the probability of failure.
- **Stochastic parameters:** s_u and the unit weight in the clay A2., peat and clay C. layer in verticals KR, BI and AL. The unit weight is defined over the entire layer segment while s_u is determined at the top and bottom of each layer as indicated with the red dots in figure 5.10.

5.3.4. Distribution of input parameters

Prior to the execution of the probabilistic calculation the mean, standard deviation and distribution type of each stochastic parameter are determined. The mean and standard deviation of the stochastically modelled parameters depend on the scenarios presented in the previous section. Since there are seldom sufficient measurements the best distribution type has to be estimated. Furthermore the correlation matrix will be defined in this section.

Table 5.5: Distributions the undrained shear strength for scenario 1 and 4

		All CS	**CS 80 [kPa]**		**CS 62 [kPa]**		**CS 83 [kPa]**		**Distribution**
		VC	$\mu_{su,x}$	$\sigma_{su,x}$	$\mu_{su,x}$	$\sigma_{su,x}$	$\mu_{su,x}$	$\sigma_{su,x}$	
Clay A2.-KR	Top	0.17	22.0	3.70	25.0	4.21	25.3	4.26	Log-Normal
	Bot	0.17	25.5	4.29	32.8	5.52	29.3	4.94	Log-Normal
Peat-KR	Top	0.24	40.4	9.58	32.8	7.78	17.0	4.03	Log-Normal
	Bot	0.24	48.9	11.59	39.7	9.41	59.7	14.15	Log-Normal
Clay C.-KR	Top	0.17	9.4	1.58	15.0	2.52	13.0	2.19	Log-Normal
	Bot	0.17	18.8	3.16	24.0	4.04	21.0	3.53	Log-Normal
Peat-BI	Top	0.24	16.3	3.86	29.1	6.90	20.2	4.78	Log-Normal
	Bot	0.24	25.7	6.09	36.0	8.54	31.4	7.45	Log-Normal
Clay C.-BI	Top	0.17	12.3	2.07	14.5	2.44	8.4	1.42	Log-Normal
	Bot	0.17	23.0	3.87	28.2	4.75	17.5	2.95	Log-Normal
Peat-AL	Top	0.28	12.5	3.45	14.4	3.97	17.6	4.85	Log-Normal
	Bot	0.28	11.4	3.15	13.1	3.61	11.4	3.14	Log-Normal
Clay C.-AL	Top	0.28	12.5	3.47	12.4	3.44	13.2	3.68	Log-Normal
	Bot	0.28	18.7	5.19	18.6	5.17	15.8	4.40	Log-Normal

Scenario 1 The methodology regarding the determination of the undrianed shear strength and its corresponding variation coefficients is shown in section 4.2. The standard deviation depends on the transformation and regional uncertainty and are shown in table 5.5 together with the mean value of cross section 62, 80 and 83. The exact shape (mean and standard deviation) of this logarithmic distribution depends on the selected cross section, the geological deposit and the depth at which the undrained shear strength is obtained. For this scenario s_u is determined at the top and the bottom of each geological layer indicated with the red dots in 5.10.

Scenario 2 In this scenario the mean and standard deviation of the linearised undrained shear strength in longitudinal direction $s_{u,ld}$ is used (5 km long research area). The distributions are based on $s_{u,lin}$ found in 51 different cross sections at the top and bottom of each layer. These values of the undrained shear strength can be presented in a histogram which on its turn can be transformed into a log-normal distribution. In figure 5.12 an example of a histogram for 51 $s_{u,lin}$'s found at the top of the peat-AL is presented. The mean and standard deviations of $s_{u,ld}$ are presented in table 5.6. This scenario is composed to indicate the influence of longitudinal fluctuations in s_u. Therefore the calculated transformation and regional uncertainty are not taken into account in this scenario, see appendix C.

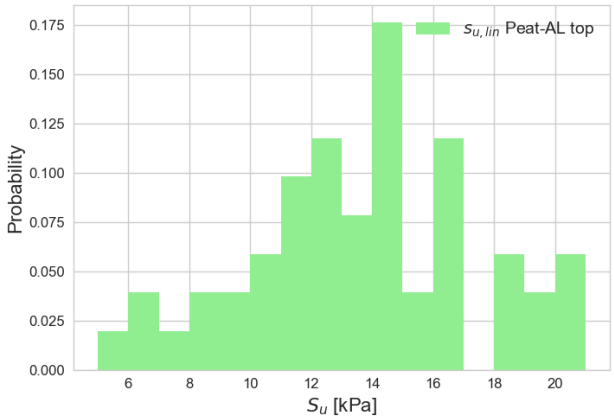

Figure 5.12: Histogram of 51 linearised undrained shear strength values at the top of Peat-AL

Table 5.6: Distributions $s_{u,ld}$ for scenario 2

		$\mu_{su,ld}$ [kPa]	$\sigma_{su,ld}$ [kPa]	**Distribution**
Clay A2.-KR	Top	25.69	5.61	Log-Normal
	Bot	29.32	4.41	Log-Normal
Peat-KR	Top	39.74	9.75	Log-Normal
	Bot	52.25	13.15	Log-Normal
Clay C.-KR	Top	15.87	3.16	Log-Normal
	Bot	24.39	3.96	Log-Normal
Peat-BI	Top	23.60	6.59	Log-Normal
	Bot	32.44	5.74	Log-Normal
Clay C.-BI	Top	11.45	2.20	Log-Normal
	Bot	22.21	3.87	Log-Normal
Peat-AL	Top	13.99	5.58	Log-Normal
	Bot	11.87	4.01	Log-Normal
Clay C.-AL	Top	11.23	1.46	Log-Normal
	Bot	14.83	2.87	Log-Normal

Scenario 3 In this scenario the influence of layer thickness in combination with the $s_{u,ld}$ on the probability of failure is analysed. The distributions for $s_{u,ld}$ as presented in table 5.6 are used in this scenario. A distribution of the layer separation is composed for each yellow dot in figure 5.10. The position in the vertical of a yellow dot differs over all 51 cross sections along the 5 kilometre long research area. The depth of each yellow dot in the cross section is assumed to be normally distributed. The average depth of each layer separation together with the standard deviation is shown in table 5.7. The peat layer is relatively small in comparison to the standard deviation of layer separation 1 and 2 under the crest and inner berm. These large standard deviations can cause layer separation 1 to lie deeper than separation 2. The model is not able to cope with such changes in stratification, moreover it is not the intention to model such a stratification, therefore truncated normal distributions are applied to overcome such problems.

Table 5.7: Assumed distribution of the layer separations within research area used for scenario 3

	μ [m NAP]	σ [m]	Distribution type
Separation 1 KR	-3.24	1.29	Truncated Normal
Separation 1 BI	-2.62	0.39	Truncated Normal
Separation 2 KR	-5.53	0.72	Truncated Normal
Separation 2 BI, AL,W	-4.77	0.57	Truncated Normal
Separation 3 KR,BI,AL,W	-13.00	1.91	Normal

Scenario 4 In this scenario the unit weight is implemented as a stochastic parameter with a normal distribution. The values used for unit weight in the semi probabilistic analysis are used as mean values, see table 5.3. Because the estimation of this parameter is rather accurate the standard deviation is set to 0.5. The unit weight is assumed to have a positive as well as a negative influence on the slope stability and therefore the total influence on the safety factor is expected to be minimal. It is assumed that the absolute minimum unit weight of peat is 9.81 kN/m^3. A truncated normal distribution is used to ensure that no lower value is implemented in the model.

Correlations The correlation between two variables indicates that there is a statistical relationship between the considered variables and can be defined with the correlation coefficient (ρ). When two variables are assumed to be independent ρ is 0, it is 1 when perfect positive dependence is assumed and ρ is -1 when perfect negative dependence is assumed. A perfect positive correlation between the undrained shear strength at the top and bottom is assumed in this thesis. The assumption ensures that the linearisation preserves equal sign, either positive or negative, for all solutions. In appendix C other correlations in vertical and horizontal direction are analysed.

The layer separations are correlated in horizontal direction. A layer separation consist of multiple points, as can be seen in figure 5.10. One layer separation is assumed to be perfect positively correlated. In other words, the layer moves up and down as one. This does not necessarily mean that the separate points in one layer separation have the same mean and standard deviation.

In 'Handreiking Faalkansanalyses Macrostabiliteit' it is stated that in common practice most of the variables are assumed to be independent [50]. This would imply that their correlation coefficient is equal to 0. Incorrect assumption of independent undrained shear strength parameters leads to higher reliability estimations. A good understanding regarding the effect of the correlation matrix is required to perform a probabilistic stability analysis, see appendix C.

5.4. Results probabilistic stability analysis

The results of the probabilistic analysis are presented according to the proposed scenarios in section 5.3.3. The relative influence of each input parameter on the stability of the levee can be determined with a probabilistic stability analysis. In a probabilistic stability analysis the reliability index and the probability of failure are calculated instead of a safety factor. The sensitivity analysis emphasized that the uncertainty in the undrained shear strength has a large influence on the safety factor. The difference in safety factor applying MHW and DHW is not significant and therefore all probabilistic analyses are modelled with MHW, s_u does therefore not have to be rewritten to a POP.

5.4.1. Scenario 1

The goal of scenario 1 is to gain more insight in the relative influence of s_u for each layer with respect to the reliability. For this scenario three cross sections within the research area are chosen: CS62, CS80 and CS80. The mean, standard deviation and distribution type of the undrained shear strength for all three cross sections are presented in table 5.5. The standard deviations are based on the transformation and regional uncertainty, which differ per geological layer but are constant in longitudinal direction in the specified research area.

Table 5.8: Reliability index for scenario 1 in cross section 62, 80 and 83

	β	$\beta_{cs,req}$
CS62	4.12	4.03
CS80	3.62	4.03
CS83	3.88	4.03

The calculated reliability index for cross sections 62, 80 and 83 are shown in table 5.8. This corresponds to the safety factors found in section 5.2, which are 1.18, 1.07 and 1.13 for cross sections 62, 80 and 83 respectively. The required reliability index ($\beta_{cs,req}$) is 4.03 and therefore cross section 62 would be classified as safe, whereas the same cross section was characterised as unsafe in the semi-probabilistic analysis. As expected the safety is higher for the probabilistic analysis in comparison with the semi probabilistic analysis. This can

partly be devoted to the elimination of the schematisation factor for the probabilistic analysis.

In figure 5.13 and 5.14, the influence and alpha factors for each cross section are presented for the LEM of Bishop. Because the shear strength at the top and bottom of each layer are fully positively correlated the alpha factors are only presented per layer. In these scenarios only positive alpha factors are found, this is in agreement with an increasing reliability when s_u increases. As expected only positive alpha factors are found, since the reliability increases with increasing undrained shear strength.

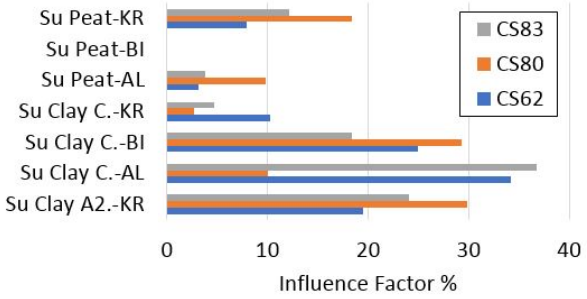

Figure 5.13: Influence factors s_u for scenario 1 in cross section 62, 80 and 83

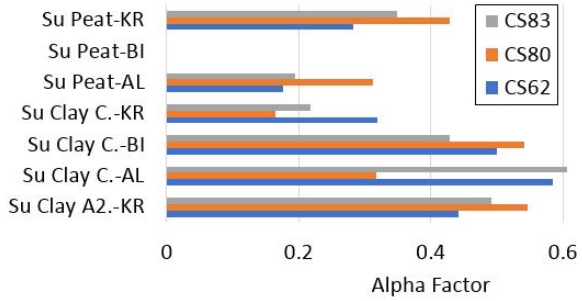

Figure 5.14: Alpha factors s_u for scenario 1 in cross section 62, 80 and 83

The figures show that the undrained shear strength in peat-BI, peat-AL and the clay A2. layers have a large influence on the reliability index for all cross sections. A large alpha factor indicates that a small increase in s_u has relatively large influence on the reliability compared to similar changes in s_u of other layers. The uncertainty and thus the standard deviations of the undrained shear strength determine for a significant part the influence on the reliability index. After all, a deterministic parameter has no influence on the reliability index.

The s_u of the clay C.-BI layer has a relatively small standard deviation, nevertheless it still has a significant influence on the reliability. The large influence can partly be attributed to its bottom position in the slip surface and the relatively low shear strength.

The high influence factors of clay C.-AL can partly be devoted to its position in the slip surface, and the large area of slip surface present in this layer. However the large standard deviation causes it to have a large influence as well. The variation coefficients of the BCPT are adopted from the Markermeerdijken project and are relatively large in comparison with the variation coefficients determined for the layers in the crest and inner berm. The layers in the hinterland therefore have a large effect on the reliability. In cross section 80 clay C.-AL has less influence because only a small part of the critical slip surface crosses this layer, see figure 5.15. Peat-BI has no influence since the critical slip surface is not located in this layer, see figure 5.15.

5.4.2. Scenario 2

In the second scenario the influence of $s_{u,ld}$ is analysed in cross section 62, 80 and 83. The implemented distributions are shown in table 5.6. These values are implemented in the three cross sections presented in scenario 1. Despite the fact that the undrained shear strength is based on the values found in 51 cross sections the stratification is not jet stochastically implemented and therefore 3 different cross sections can be analysed. Doing so, gives a first insight in the influence of layer thickness's with respect to the reliability index.

The reliability indexes calculated for cross section 62, 80 and 83 with $s_{u,ld}$ are shown in table 5.9. These reliability indexes cannot be compared to $\beta_{cs,req}$ because $s_{u,ld}$ is a combination of 51 cross sections. Notable is the fact that cross section 80 is no longer the critical cross section with the lowest reliability. Most of the undrained shear strengths are higher for cross section 80 and 83 compared to scenario 1, whereas they are lower for cross section 62, see table 5.5.

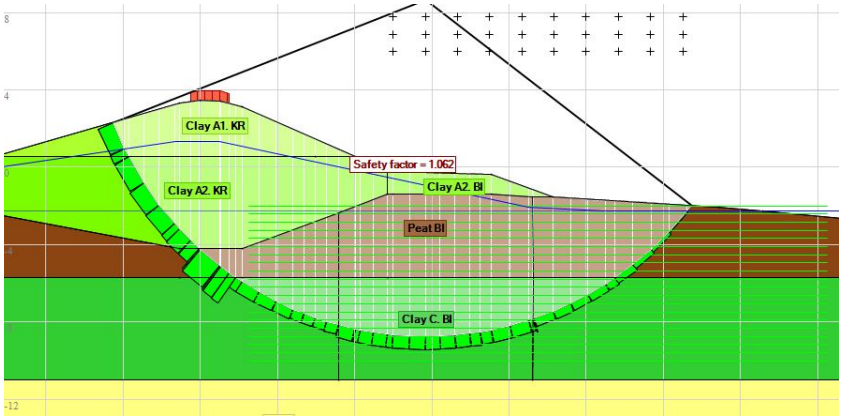

Figure 5.15: Critical slip surface cross section 80 (D-Stability)

Table 5.9: Reliability index with $s_{u,ld}$ for stratification in cross section 62, 80 and 83

	β
CS62	3.67
CS80	4.36
CS83	5.07

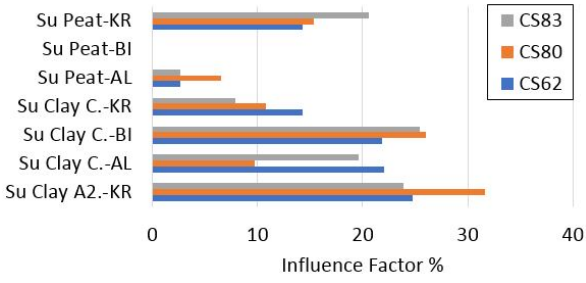

Figure 5.16: Influence factors $s_{u,ld}$ for scenario 2 in cross section 62, 80 and 83

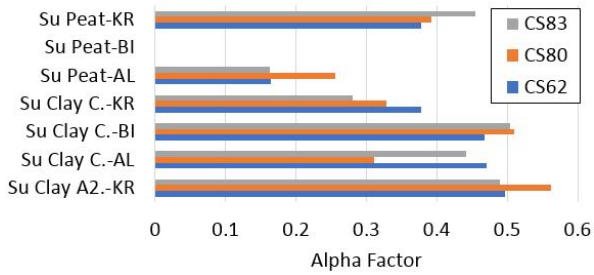

Figure 5.17: Alpha factors $s_{u,ld}$ for scenario 2 in cross section 62, 80 and 83

The standard deviations of most $s_{u,ld}$ are larger in comparison with scenario 1, which is logical considering the regional variability of the data. A larger standard deviation results in a larger influence in the probabilistic analysis. In figure 5.16 and 5.17 the relative influence of all $s_{u,ld}$ on the reliability index is shown. Similar to the results of scenario 1 the influence of the clay C.-BI is high whilst the standard deviation is relatively low in comparison with clay A2.-KR.

The influence of clay C.-AL layer is less in comparison to scenario 1. Where the standard deviation depends on the variation coefficient obtained from the Markermeerdijken project in scenario 1, it depends on uncertainty in $s_{u,ld}$ along the levee for scenario 2. The variation in undrained shear strength in this layer is rather small which results in a small standard deviation, resulting in a decreasing influence.

Although the stochastic input parameters are kept constant there is a difference in alpha factors amongst the analysed cross sections, especially cross section 80 differs from the other two. This difference can be attributed to the difference in layer thickness and thereby emphasizes that layer thickness can have a significant influence as found in the sensitivity analysis.

5.4.3. Scenario 3

In the second scenario it already was underlined that the difference in layer thickness in longitudinal direction of the levee influences the reliability. In this scenario the layer separations are implemented as stochastic parameters, the distributions are shown in table 5.7.

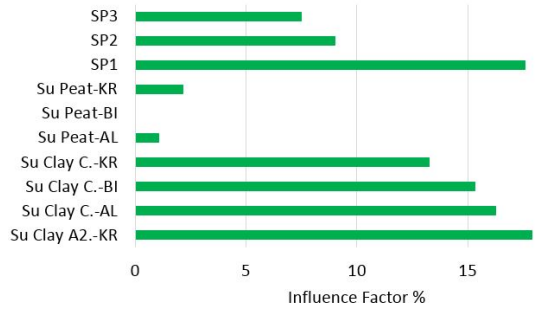

Figure 5.18: Influence factors for scenario 3

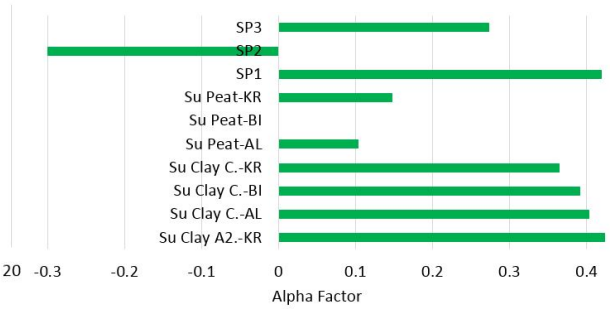

Figure 5.19: Alpha factors for scenario 3

The reliability index for this scenario is equal to 3.45. The influence and alpha factors for scenario 3 are shown in figure 5.18 and figure 5.19. Only three alpha factors are presented for the influence of the layer separations since it is assumed that the points in each layer separation are fully correlated in horizontal direction. Separation 1 is the separation between clay A2. and peat, separation 2 between peat and clay C. and separation 3 is located between clay C. and sand, see figure 5.10.

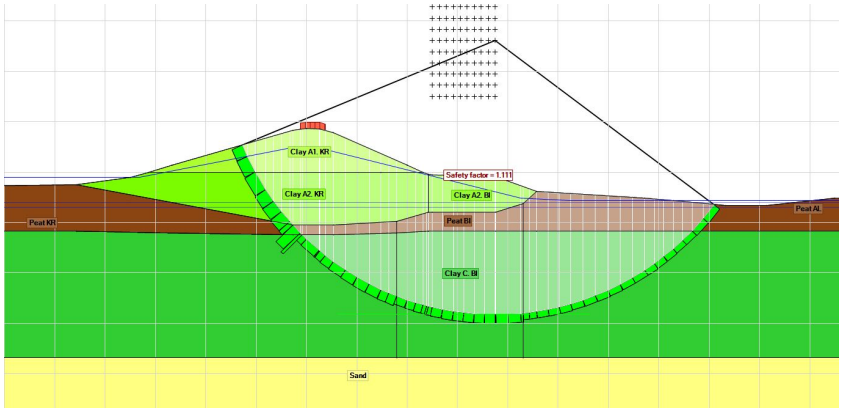

Figure 5.20: Critical slip surface for scenario 3

Although the standard deviations of the layer separation are much smaller than those of the undrained shear strength the influence is comparable. In practice however each cross section is modelled separately and the layer separation is known with a relatively large precision. The influence of layer separation in figure 5.18 can therefore be seen as a maximum, whereas this is not the case for the undrained shear strength.

The critical slip surface is presented in figure 5.20. The physical values of the layer boundaries are -4.21, -4.66 and -14,80 meter for layer 1, 2 and 3 respectively. In figure 5.19 a negative alpha value is present which means that an increase in the corresponding parameter will lead to failure and thereby a lower reliability. The thickness of the peat layer is decreased significantly in comparison to the starting values, table 5.7. As a matter of fact it is 0.25 m thinner than smallest peat layer observed in the research area. As a result the clay C. layer starts at a smaller depth compared to all other scenarios. This explains the negative alpha factor for the first layer separation. If separation 1 is situated at greater depth, the thickness of the peat layer decreases, which will result in a smaller reliability index, because $s_{u,ld}$ for peat is higher in comparison to $s_{u,ld}$ of clay A2..

The fact that scenario 3 results in a 'fictive' [2] layering emphasizes the influence of the $s_{u,ld}$ on the reliability.

5.4.4. Scenario 4

In this scenario the unit weight will be implemented as a stochastic parameter for cross sections 62, 80 and 83. A stochastic unit weight influences the determination of the undrained shear strength in two ways:

- q_{net} depends on the unit weight

[2] The layering in the outcome of scenario 3 is not actually fictive, but is not encountered in the data

- N_{kt} differs, since q_{net} depends on the unit weight

A change in unit weight influences the effective stresses which are required to calculate q_{net}. In report 'POVM Beter benutten actuele sterkte KIJK' a method to stochastically implement the unit weight is given [48]. However the unit weight can be estimated based on CPT data with the method presented in section 4.1.2. With a numerical model the effect of different unit weights in the estimation of s_u can easily be analysed. The most important conclusion are:

- In figure 5.21 the cone factor is determined for 3 different units weights of clay C: 12.87, 14.3 and 15.73 kN/m^3. These values coincide with a 10% increase and decrease in unit weight. The corresponding N_{kt} values are 20.44, 19.62 and 18.78 for 0.9γ, 1.0γ and 1.1γ respectively. The influence on the unit weight on the cone factor can thus be significant, especially when soft or organic soils are analysed.
- Despite the difference in cone factor the difference in s_u is minimal since this is based on q_{net}/N_{kt}. A 10 % increase in unit weight results in a lower q_{net} and a lower N_{kt}, the difference in s_u is therefore minimal.

Based on these findings the unit weight can be implemented as a stochastic parameters without large erroneous estimations of s_u. Since N_{kt} is determined in the same layer, it is assumed that the unit weight determination in the testing field is positively correlated to the unit weight in the field.

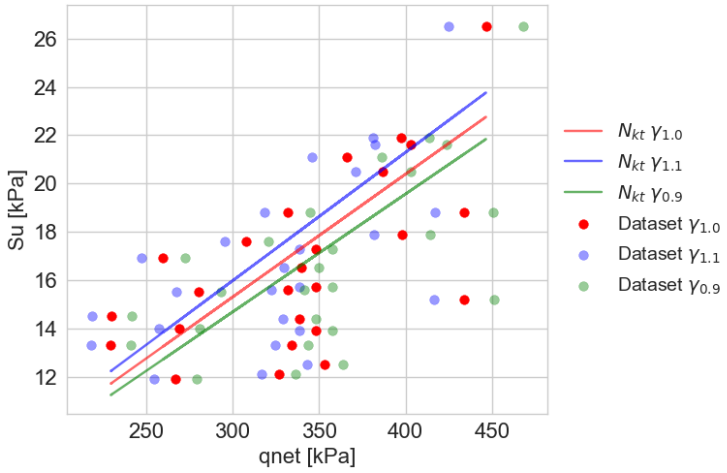

Figure 5.21: N_{kt} for 10% increase and decrease of unit weight

In figure 5.22 and 5.23 the influence and alpha factors of scenario 4 are presented. The calculated reliability indexes for cross section 62, 80 and 83 are shown in table 5.10. The implementation of a stochastic unit weight decreases the reliability of all three cross sections, which indicates that the unit weight can have a significant influence on the reliability.

Table 5.10: Reliability index for scenario 4 in cross section 62, 80 and 83

	β	$\beta_{cs,required}$
CS62	3.91	4.03
CS80	3.49	4.03
CS83	3.73	4.03

As expected an increase in unit weight of the clay A1. and clay A2. layers, that are situated within the levee, result in a lower reliability, which is confirmed by the negative alpha values. An increase in unit weight of peat-AL results in a higher reliability because the resisting moment regarding the inner slope increases. In general it can be concluded that the undrained shear strength has a larger influence on the stability in the considered research compared to the unit weight.

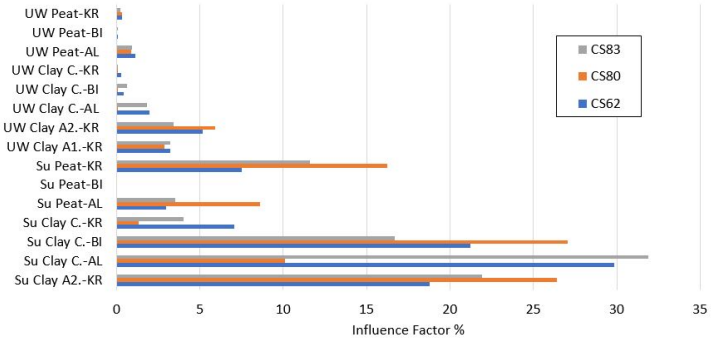

Figure 5.22: Influence factors for scenario 4 in cross section 62, 80 and 83

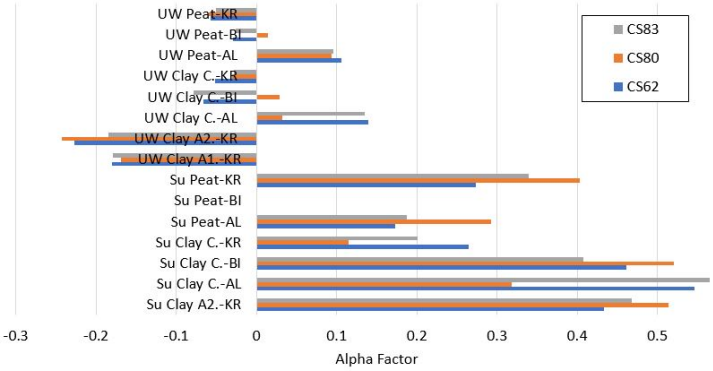

Figure 5.23: Alpha factors for scenario 4 in cross section 62, 80 and 83

5.5. Conclusions and Remarks

The semi-probabilistic and probabilistic analysis showed that the influence of the undrained shear strength on the reliability is large in the considered research area. The relative influence is higher than the layer separations, DHW or unit weights. Moreover the unit weight, DHW and layer thickness can be estimated with a higher accuracy, which enhances the influence of the undrained shear strength on the probability of failure. This underlies that an accurate estimation of s_u and $s_{u,k}$ is of importance to safely design a levee.

Whereas the schematisation factor accounts for the implementation of a particular scenario in the semi-probabilistic analysis, no such factor is applied in the probabilistic analysis. It is assumed that all continuous parameters will be implemented stochastically and all non-continuous parameters have to be modelled with scenarios. The elimination of the schematisation factor suggests that all scenarios are considered and all parameters are stochastically implemented, in practice this is not always the case. The elimination of the schematisation factor can therefore lead to a higher reliability in a probabilistic stability analysis compared to a semi probabilistic stability analysis. Extra caution is required in case the reliability requirements are fulfilled with a probabilistic analysis, whereas they are not met in semi-probabilistic analysis.

A probabilistic stability analysis is a very useful method to determine the reliability in a levee. Probabilistic analysis should however be performed with care and are not necessarily better than semi-probabilistic analysis. Incorrectly assuming independence in between parameters can result in progressive reliability determinations.

A 10% increase or decrease in unit weight can lead to a significant change in q_{net} and therefore in N_{kt}. In the determination of s_u based on the S_u-measured method this difference is almost equalized, since $s_u = q_{net}/N_{kt}$. This assumes that the unit weight determined in the testing field is positively correlated to the unit weight estimated in the field. Nevertheless an accurate estimation of the unit weight is important, since it can have a significant influence on the reliability.

Since the relative influence of the undrained shear strength of a specific layer depends on the size of the slip surface through this layer, the relative influences change when LEMs of Spencer or Uplift Van are used. Spencer and Uplift Van are thought to give a better representation of the actual critical slip surface, it is therefore expected that the use of these LEMs in a probabilistic analysis results in a lower reliability compared to Bishop. However these models allow for lower model factors, as a result the calculated reliability is higher compared to the LEM of Bishop.

6

Effect of different CPT interval sizes

Whereas the focus in chapter 4 lied on the transformation of the cone tip resistance to the undrained shear strength and the accompanied uncertainties, the focus in this chapter will lie on the limited amount of CPTs in the 'field' (not in the testing field) and the accompanied uncertainties in longitudinal direction.

6.1. Introduction

As became clear in chapter 4, a lot of guidelines and equations are available to ensure a proper estimation of the characteristic undrained shear strength ($s_{u,k}$). Such guidelines have to ensure that sufficient safety is incorporated within each cross sectional stability analysis. However there are hardly any guidelines regarding the spatial variability of s_u in longitudinal direction and its accompanied uncertainty. In the considered case study the fluctuation of s_u in longitudinal direction influences the safety factor significantly as indicated in figure 5.7. In addition the probabilistic stability analysis substantiated that s_u has a significant influence on the inner slope stability.

As a matter of fact there are limited (non-compulsory) guidelines regarding the interval size in between CPTs in longitudinal direction [54]. The CPTs are used to estimate s_u but are also required to construct a cross sectional model. Since there are no restriction regarding interval size, in theory one CPT could be conducted per kilometer to set up a cross sectional model and thereby design a levee. In practice an interval size of approximately 100 meter is often conducted in levee projects.

Usually one cross section is selected to represent a few hundred meters of levee in longitudinal direction. The schematisation factor (γ_b) accounts for the fact that only one cross section is calculated within a couple hundred meters, see section 2.5.1. In practice often the most unfavourable cross section is selected as the representative one, since the schematisation factor is lowest in that case. The minimum value for the schematisation factor is 1.0, to incorporate some additional safety a value of 1.1 is often applied in practice. The most unfavourable cross sections and thus the schematisation factor, depends among other things on the phreatic line, stratification, OCR and the slope steepness. The most unfavourable cross section is thought to result in the lowest safety factor. Decreasing the CPT interval size will most certain lead to the discovery of a more unfavourable cross section. As a result additional data does not result in an optimization of the design in terms of costs, which seems counter intuitive. The current design methodology does therefore not encourage requesting additional data due to two reasons: first, it is not mandatory to conduct additional CPTs and second it will most certain result in a more unfavourable schematisation. On the contrary CPT densification results in a safer levee design which is obviously desirable.

The schematisation factor accounts for uncertainty in all parameters with the exception of soil parameters. Hence it does not account for fluctuations in undrained shear strength in longitudinal direction as presented in figure 5.11. In this chapter the effect of different CPT interval sizes on the levee design is therefore analysed. Subsequently an attempt is made to come up with an new partial safety factor to cover the spatial uncertainty present within $s_{u,ld}$.

The influence of different CPT interval sizes is presented in figure 6.1. The orange line shows the safety factors determined in case the CPT interval is 100 m, whereas the blue line indicates the safety factors which are found in case the CPT interval size would be 300 m. In figure 6.1 it can be observed that some (local) minima

are not observed when the interval size would be 300 m. Some of the maxima are also not observed; however these are of minor interest regarding a safe levee design. The figure entails the importance of a dense CPT grid to properly calculate the safety of the levee.

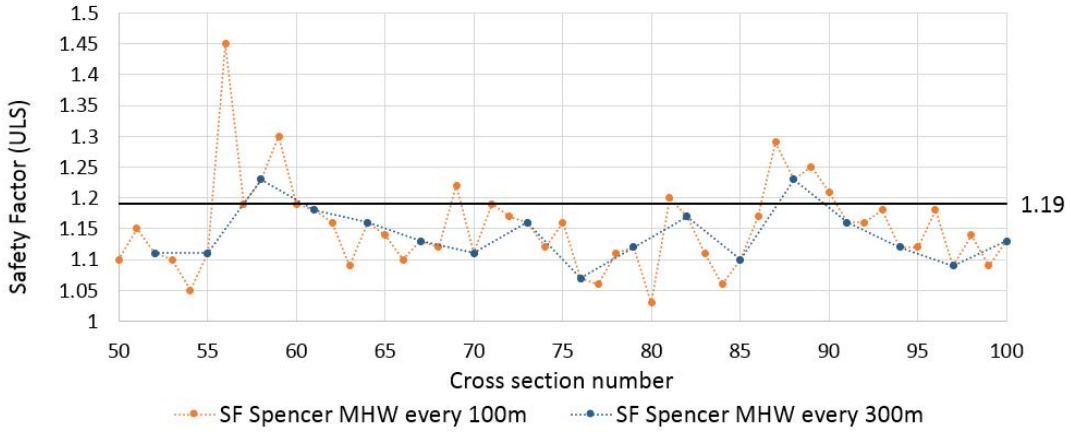

Figure 6.1: Comparison of safety factor found for CPT interval sizes of 100 m and 300 m

The spatial variability and the fact that the number of CPTs and boreholes within a levee to determine geotechnical parameters are limited, means that the estimated parameters always contain uncertainties. Intuitively it seems obvious that data densification results in less uncertainty in $s_{u,ld}$. It is however still hard to quantify the effect of this additional data, specifically additional CPTs. The way a soil investigation is set up is therefore of importance to diminish these uncertainties as much as possible, or in other words to gain as much information as possible.

Uncertainty can generally be divided into aleatory and epistemic uncertainties as presented in section 2.5. The uncertainty in $s_{u,ld}$ can be characterised as an epistemic uncertainty. 'A common misconception is that additional information will reduce the uncertainty; uncertainty can decrease, remain unchanged, or increase with additional data' [37]. A CPT per meter would most definitely improve mapping of fluctuations in $s_{u,ld}$, however this cannot be considered as a practical solution. It is however uncertain which interval size provides sufficient information regarding the spatial variability of $s_{u,ld}$. The theory of entropy is a measure of information/uncertainty and can provide more insight in this case.

6.2. Theory of entropy

The amount of information/uncertainty in a dataset is measured with the theory of information entropy [37] [4]. Entropy originates from the field of thermodynamics and is now used in many different fields of engineering [9]. Shannon derived the formulation for information entropy (H) in 1948, see equation 6.2 [52]. Information entropy is often used in computer science to effectively decrease the amount of bits required to send a particular amount of information. In this thesis entropy is used to determine the amount of information present in multiple discrete datasets containing s_u values, composed with different amounts of CPTs. Comparing these dataset could provide more insight in the effect additional CPTs have towards the design of a levee.

As an introduction to the theory of entropy, an example is presented here. In this example there are 3 buckets: each bucket is filled with 4 balls which can have two different colors, blue or red (see figure 6.2). Bucket 1 contains 4 red balls; bucket 2 contains 3 red balls, and 1 blue ball; bucket 3 contains 2 red balls, and 2 blue balls as in figure 6.2 [51]. How much information do we get regarding the color of the ball when a ball is drawn at random?

- Bucket 1: We are certain that the ball coming out is red. As a result the outcome contains no uncertainty.
- Bucket 2: Since the probability of drawing a red ball is 75% and the probability to draw a blue ball is 25%, it is most likely we will draw a red ball. However, drawing a red ball contains more uncertainty compared to bucket 1.

- Bucket 3: We have equal probability to draw a red or blue ball. Little is known regarding the possible outcome of a random draw, as a result its outcome contains more uncertainty than bucket 2.

The entropy for bucket 1 is equal to 0 while the entropy of box 2 and 3 is 0.81 and 1.0 respectively [1]. A low entropy coincides with low uncertainty and vice versa: a high entropy means a high uncertainty.

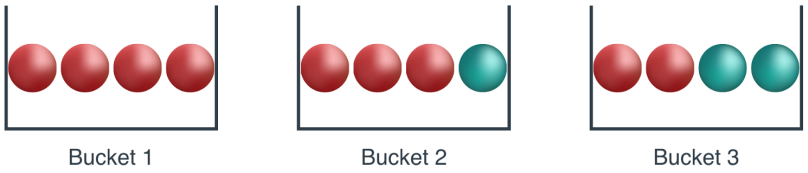

Figure 6.2: Explaination of entropy: The entropy from left to right is 0, 0.81 and 1 [51]

Note: entropy is a measure of uncertainty, choice and information[52]. This threefold definition can be misleading sometimes; in this thesis the focus lies on the determination of the uncertainty in a particular dataset. A distinction can be made between continuous and discrete entropy. In this thesis only the discrete entropy is used.

Discrete entropy The uncertainty or amount of information ($I(p)$) can be defined with equation 6.1. As the probability of an event is certain ($p = 1$), the uncertainty ($I(p)$) is zero. As a matter of fact it also clearly shows that as an event rarely occurs ($p = 0.001$), the uncertainty is large ($I(p) = 6.91$). Combining multiple events results in the formula for discrete entropy ($H(X)$) as shown in equation 6.2.

$$I(p) = ln(\frac{1}{p_i}) = -ln(p_i) \tag{6.1}$$

$$H(X) = \sum p_i ln(\frac{1}{p_i}) = -\sum p_i ln(p_i) \tag{6.2}$$

The discrete entropy can be used as a measure to determine the uncertainty in a dataset with a finite amount of samples. The discrete entropy has the property to always be positive. Entropy does not depend on the actual values within a dataset, but on the probabilities of its outcome. The maximum discrete entropy is present when each event has an equal likely probability to occur, as in bucket 3 in the example. Equal probability of all considered events results in an uniformly distributed PDF[2] [52].

$$H_{max} = ln(n) \tag{6.3}$$

To compare datasets with different amount of samples it can be convenient to use the normalized entropy, also referred to as efficiency, see equation 6.4 [52] [36] . The normalized entropy is defined by the division of the discrete entropy with the maximum entropy and varies between 0 and 1. This is, thereby a measure to determine the ratio between the maximum uncertainty that a dataset could have and the actual uncertainty of a dataset. The normalized entropy is maximum when the discrete entropy is equal to the maximum entropy. In this thesis, equation 6.4 is used to analyse the relative uncertainty within a dataset. **The outcome of the normalized entropy will also be referred to as the relative uncertainty in this thesis.** Not to confuse with relative entropy principles (e.g. Cross entropy, Kullback-Leibler divergence). Relative entropy computes the difference in entropy of datasets containing equal amount of samples and is only briefly discussed in appendix D [32] [26].

$$H_{nor} = \frac{H(x)}{H_{max}} = \frac{H(x)}{ln(n)} \quad , 0 \leq H_{nor} \leq 1 \tag{6.4}$$

[1] The entropy is based on log_2 in this example
[2] Note that the maximum entropy for a discrete variable is not equal to the maximum entropy for a continuous entropy, see appendix D

In which:

$H(X)$	=	Discrete entropy	$[nat]$
H_{max}	=	Maximum discrete entropy	$[nat]$
I_p	=	Measure of information/uncertainty	$[nat]$
p_i	=	Probability of occurrence	[%]
n	=	Number of samples	[−]
H_{nor}	=	Normalized entropy	[−]

The choice of the logarithms base is up to the user, since entropy is translation invariant [52] [3]. In this thesis the base is equal to Euler's number e, which turns the logarithm in a natural logarithm as in equation 6.2. Therefore the units are equal to 'nat'.

6.3. Entropy in case study

This section explains how the theory of entropy is applied on the considered case study, subsequently the results of the calculated entropy and normalized entropy are shown.

6.3.1. Set up

The (normalized) entropy is used to determine the amount of uncertainty present in the estimation of $s_{u,ld}$ and thereby in the CPTs in longitudinal direction. To do so multiple datasets with varying interval sizes are composed out of the available CPT data in the crest and inner berm. In the Markermeerdijken project the minimum interval between successive CPTs is 100 m. To model a 200 m interval size, half of the available CPTs are used, therefore 2 different datasets with an interval of 200 meter can be obtained, for a 300 m interval 3 datasets are obtained and 4 datasets for a 400m interval. These datasets are characterised with a letter A, B, C, and D, as in figure 6.3. Datasets A,B,C and D contain 51, 26/25, 17 and 13/12 CPTs respectively. The CPTs in the crest and the inner berm are used in separate datasets. The selected area size is kept constant at 5 km.

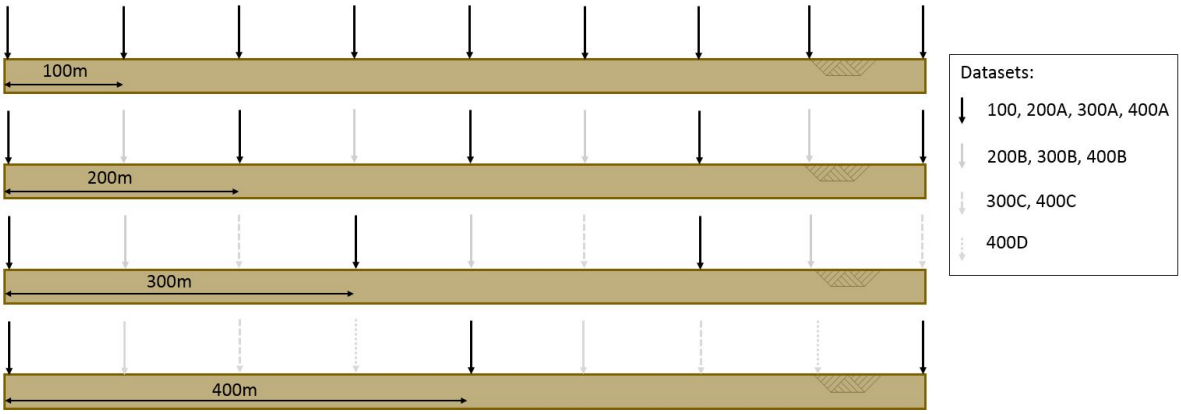

Figure 6.3: Set up to determine (normalized) entropy for different interval sizes.

Practice is not as easy and straightforward as the example shown in figure 6.2, therefore some simplifications and measures have to be implemented in order to apply entropy to the case study. The S_u-measured method results in an s_u every 2 centimetres in a CPT. The cone tip resistance can vary a lot over a small distance in vertical direction and therefore the linearised undrained shear strength of a layer is used. Because the undrained shear strength increases with depth (most of the times) it would be convenient to compare the undrained shear strengths at similar depths. However not all layers are present at equal depth, therefore the linearised undrained shear strength at the top and bottom of each layer are used to define the amount of information in longitudinal direction. This is also convenient because these parameters are required in the (probabilistic) stability analysis. As a result of these simplifications the same $s_{u,ld}$ as used in section 5.3.3 is used in this chapter.

To compare the different undrained shear strengths, the values are first rounded up to zero decimals. This adjustment is required because the datasets are relatively small, 12 to 51 samples respectively. The probability

that s_u is identical at two locations is very small in case these values are not rounded. In case all s_u have different values the entropy is equal to the maximum entropy and H_{nor} is 1.0. The consequences of these adjustments are elaborated in appendix D.

Conditions The main requirements and assumptions for the use of entropy as a measure of uncertainty in $s_{u,ld}$ of the Markermeerdijken case are itemized here:

- The size of the considered research area will remain constant at 5 km.
- The linearised undrained shear strength in 51 cross sections ($s_{u,ld}$) at the top and bottom of each layer as indicated with the red dots in figure 5.10 are used to determine the uncertainty in the undrained shear strength in longitudinal direction.
- The undrained shear strength is rounded to zero decimals in order to determine the entropy in the dataset.
- It is assumed that a 50 meter interval size is the minimum CPT interval size to safely design a levee regarding inner slope stability. However the minimum CPT interval size is 100 m for the considered case study and therefore this interval size is set as benchmark.

6.3.2. Results entropy in case study

In this section the (normalized) entropy is determined for different interval sizes within the Markermeerdijken project and the results are elaborated upon. The assumptions and requirements presented in the summary of section 6.3.1 apply on all results in this section.

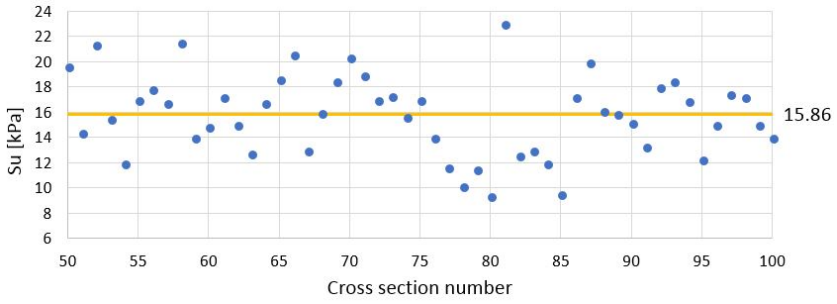

Figure 6.4: $s_{u,ld}$ at the top of clay C.-KR layer

Entropy is used to determine the effect of different CPT intervals for the Markermeerdijken project. $s_{u,ld}$ at the top and bottom of each geological layer is used to determine the (normalized) entropy in longitudinal direction. As an example the variation of $s_{u,ld}$, at the top of the clay C.-KR layer, over the 5 kilometre long research area is presented in figure 6.4, with a mean X_m and a standard deviation σ_x of 15.86 and 3.16 kPa respectively. No strong visual trend in $s_{u,ld}$ along the levee can be identified in figure 6.4. Additionally all other layers do not show any trend in longitudinal direction. Therefore each value of s_u in longitudinal direction can be compared to a random draw, as example in figure 6.2. For convenience $s_{u,ld}$ at the top of clay C.-KR is used as an example throughout this section, the remaining relevant data is presented in Appendix D.

In figure 6.5 the orange dots resemble the entropy of $s_{u,ld}$ at the top of clay C.-KR for different interval sizes and thereby different CPT quantities. More orange dots are present at larger interval sizes since more datasets are available, in figure 6.5 the distinction between dataset 200A and 200B is illustrated. The blue dots represent the average of all datasets with similar interval size, e.g. 200m, 300m and 400m. As the interval size decreases the amount of information increases in most cases, i.e. the entropy increases, see figure 6.5. In case a random sample is drawn from the dataset the uncertainty also increases for decreasing interval size. The figure thereby underlines the common misconception that additional data results in less uncertainty [3]. In figure 6.5 it can also be observed that one of 400m datasets ($H(x) = 2.1$ nat) contains more uncertainty compared to a 300m dataset ($H(x) = 2.08$ nat).

[3] Uncertainty describes the variation within the dataset, but is not similar to the standard deviation

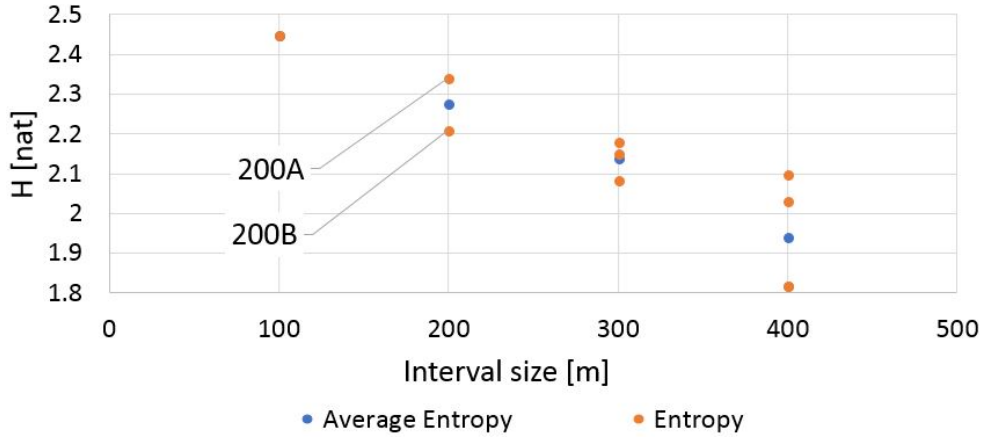

Figure 6.5: Entropy of $s_{u,ld}$ at the top of clay C.-KR for different interval sizes

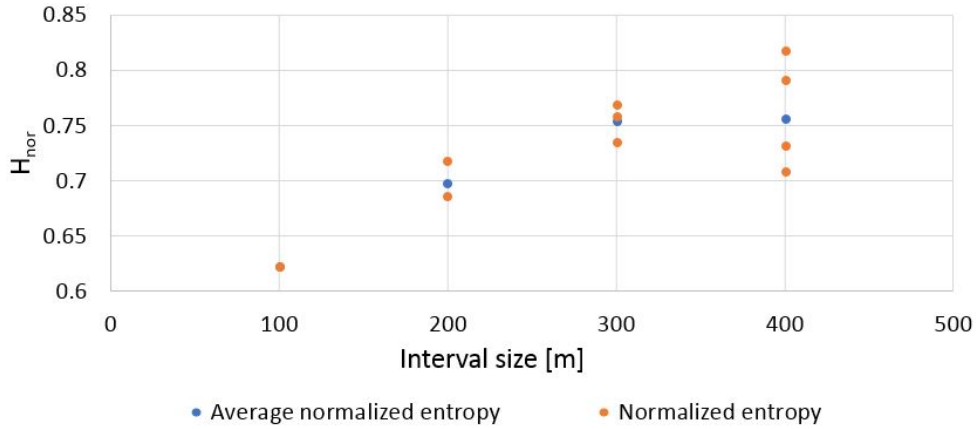

Figure 6.6: Normalized entropy $s_{u,ld}$ at the top of clay C.-KR for different interval sizes

Looking at the example from figure 6.2, it seems logical that the uncertainty in a random draw increase as more various coloured balls are present in the bucket. This also applies to the s_u values within a dataset. After all, the range of s_u values will most likely increase as more measurements are conducted (up to a certain maximum). To account for the number of samples the normalized entropy can be used. In figure 6.6 the normalized entropy of the $s_{u,ld}$ at the top of clay C.-KR is presented. In general a decreasing trend towards smaller interval sizes is found since the number of samples increases with decreasing interval size. This means that the relative uncertainty generally decreases with decreasing interval size. The minimum of zero normalized entropy is only reached when the entropy of the considered dataset is zero, which will not occur in practice as this would imply that all s_u's are the same. This suggests that the minimum normalized entropy is never reached, regardless of sample size.

In figure 6.7 the normalized entropy is determined for all layers in the considered case study. The lines in between two successive intervals, e.g. 100-200 m, are only used to improve visualisation. A large diversity is present in between the calculated normalized entropies of different layers, however a general decreasing trend towards smaller interval sizes is observed.

In figure 6.7 it becomes clear that the $s_{u,ld}$ in most peat layers under the crest and inner berm contain a relatively large uncertainty and therefore a large normalized entropy. This originates from the fact that the fluctuations in cone tip resistance is large for peat-KR and peat-BI compared to clay C.-KR and clay C.-BI, as indicated in figure 6.8. As a result there is more variation in linearisation and therefore the value of the range in s_u value is larger for the peat layers, as is shown in figure 6.9. This results in a relatively large normalized entropy for peat-KR and peat-BI.

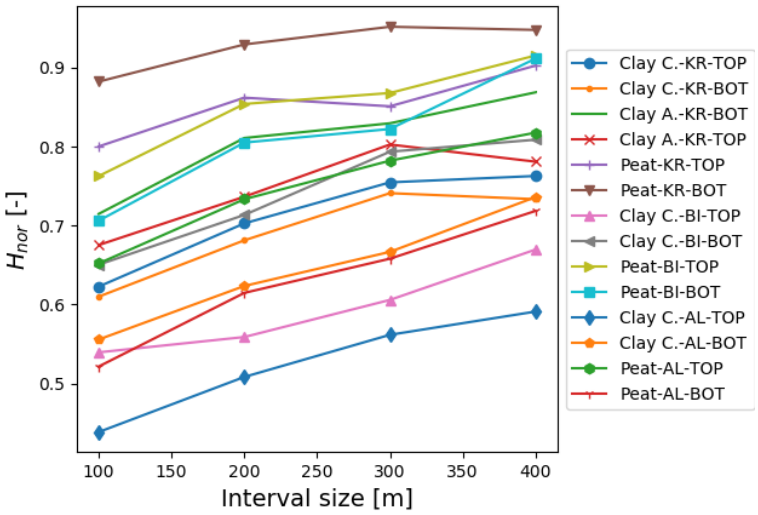

Figure 6.7: Averaged normalized entropy $s_{u,ld}$ at the top and bottom of all layers in research area

To put this into perspective the s_u values of peat-AL and clay C.-AL are compared in figure 6.10. The difference between s_u range for peat-AL and clay C.-AL is much less compared to the peat-KR and clay C.-KR. As a result the uncertainty in the peat-AL is significantly lower compared to the peat-KR. The lower uncertainty can be the result of more accurate measurements with a ball cone in the hinterland. Another reason could be that there are no additional loads due to the presence of the levee, which results in less fluctuation in q_c.

All s_u values have equal probability in the peat-KR layer at a 400 m interval, as a result the normalized entropy is maximized. If additional data could be obtained for one specific dataset, than the information gain would be largest for the $s_{u,ld}$ at the bottom of Peat-KR. As the inclination of the lines in figure 6.7 is small a lot of information is gained in between two successive interval sizes, vice versa a relatively large inclination indicates that relatively little information is gained in between two interval sizes.

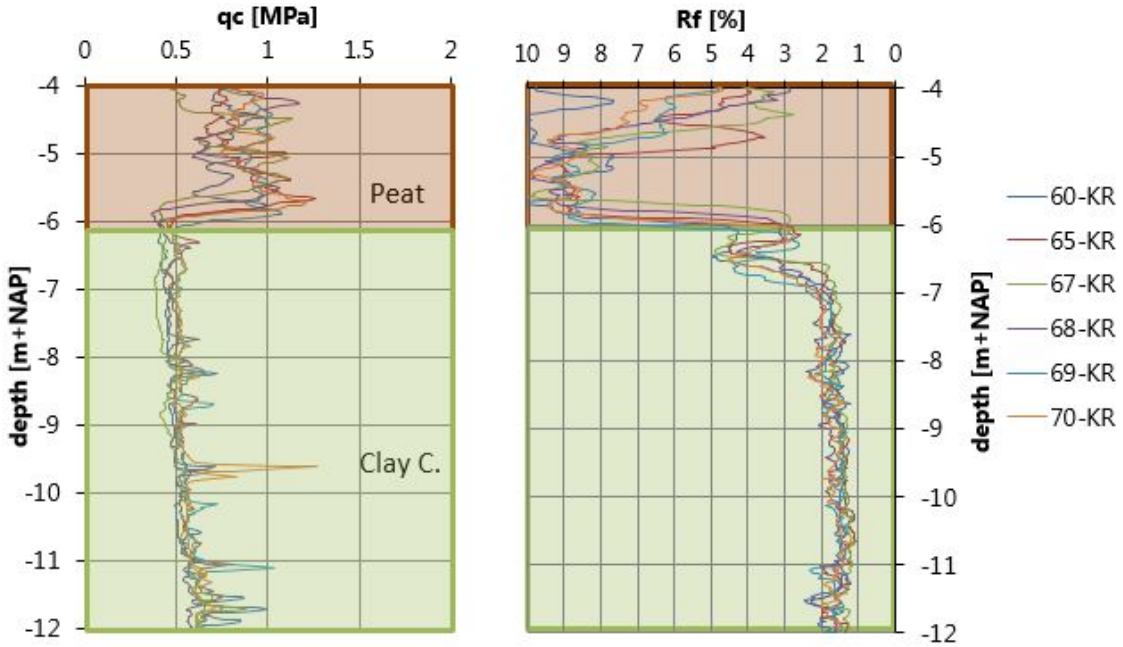

Figure 6.8: Cone tip resistance (q_c) and friction ratio (R_f) of 6 CPTs in crest

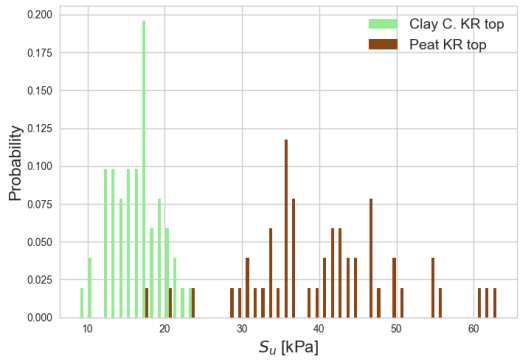

Figure 6.9: Probabilities of s_u at the top of the Clay C.-KR and Peat-KR layer (CPT class I)

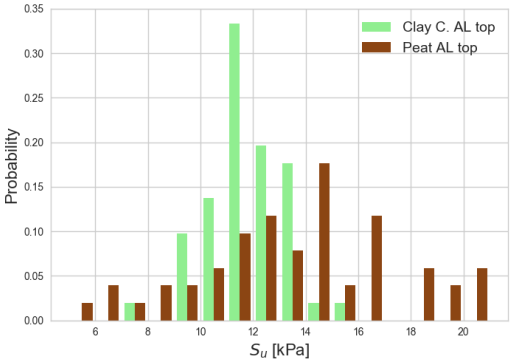

Figure 6.10: Probabilities of s_u at the top of the Clay C.-AL and Peat-AL layer (Ball cone)

6.4. Proposed method to account for changing CPT interval size

In section 6.1 it is concluded that a larger CPT interval size could result in an overestimation of the safety factor. This is partially caused by the fluctuation in undrained shear strength in longitudinal direction. The uncertainty involved with all non-soil parameters, e.g. slope steepness, OCR etc., is covered in the schematisation factor (γ_b). The schematisation factor does not account for soil parameters and therefore does not account for potential risks regarding the overestimation of s_u when CPT interval sizes increase. In this section a method is proposed to assign additional safety when the CPT interval size is larger than 100 m. The conditions in section 6.3.1 indicate that although a 50 m interval size is assumed to be the minimum interval size to safely design a levee, in this thesis a 100 m interval size is used as a benchmark due to limited amount of data in the Markermeerdijken project.

Normalized entropy provided a method to indicate the relative uncertainty in a dataset. From the results of the case study it can be concluded that a larger dataset and thereby a smaller interval size will most likely result in a decrease in normalized entropy. This is under the assumption that the size of the specified area remains constant. Since H_{nor} represents uncertainty it can be used to cover uncertainty in the design in the form of a partial factor. The normalized entropy is used to assign additional safety when the CPT interval size within the case study would exceed 100 m. The proposed method accounts for the spatial variability present in the undrained shear strength in longitudinal direction and indirectly for increasing interval sizes.

Multiple methods and equations were investigated to cover the uncertainty present in the undrained shear strength in longitudinal direction and relatively large CPT interval sizes. Most of these methods were found to contain mathematical/statistical errors or required the entropy for a 50 m interval, which is not present in the Markermeerdijken case. These methods resulted in the method that is presented in this section.

In this thesis a new partial factor is proposed which accounts for the uncertainty in undrained shear strength in longitudinal direction and the CPT interval size. Since the 100 m interval is used as a benchmark the partial factor is equal to 1.0 for this interval size. The normalized entropy found for a 100 m interval size, referred to as H_{nor100}, divided by 10 is used as an angle (α_H) to determine the partial factors for increasing interval size, see equation 6.5 and figure 6.11. The interval size is referred to as x in figure 6.11 and the difference between two interval sizes is referred to as Δx. As 100 m is chosen as the benchmark Δx increases for interval sizes larger than 100 m. The tangent of α_H is multiplied with Δx to determine the new proposed partial factor $\gamma_{su,ld}$, see equation 6.6. In case a relatively large uncertainty is present the angle (α_H) increases, resulting in an increase in $\gamma_{su,ld}$ for the considered layer. The partial factor therefore assigns the highest factor ($\gamma_{su,ld}$) to the layers that contain the most uncertainty in $s_{u,ld}$. To clarify: the partial factor for s_u in peat-KR top is higher compared to s_u at the top of clay C.-KR, see figure 6.9. The maximum of $\gamma_{su,ld}$ is set to 1.3 since it would otherwise result in unrealistic low safety factors for very large interval sizes, i.e. larger than 400 m.

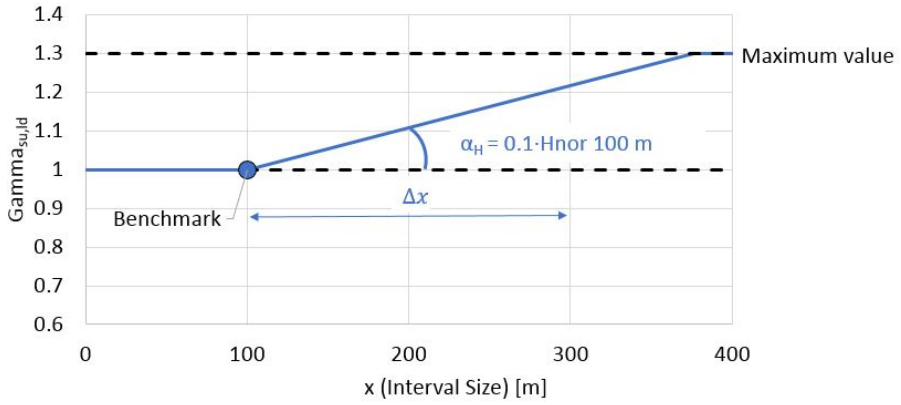

Figure 6.11: Determination of $\gamma_{su,ld}$ based on α_H and Δx

$$\alpha_H = \frac{H_{nor100m}}{10} \tag{6.5}$$

$$\gamma_{su,ld} = \begin{cases} min(1 + (tan(\alpha_H) \cdot \Delta x), 1.3) & \text{if } x > 100m \\ 1 & \text{if } x = 100m \end{cases} \tag{6.6}$$

Whereas the schematisation factor is part of the required safety factor (load), this partial factor is related to the resistance. The partial factor is therefore multiplied to the total variation coefficient (VC_{tot}) of the undrained shear strength as determined in chapter 4, see equation 6.7. The uncertainty found in $s_{u,ld}$ in longitudinal direction is thereby assigned to s_u in cross sectional direction. As a result $s_{u,k}$ and thereby the safety factor decreases. **Equation 6.6 is referred to as the 'spatial factor' in the rest of the thesis.**

$$VC_{su,ent} = \gamma_{su,ld} \cdot VC_{tot} \tag{6.7}$$

In which:

$VC_{su,ent}$	The variation coefficient for the s_u based on the spatial factor	[−]
H_{nor100}	Normalized entropy for 100 m CPT interval size	[−]
$\gamma_{su,ld}$	Spatial factor: Partial safety factor that accounts for uncertainty in $s_{u,ld}$	[−]
α_H	Angle based on H_{nor100} to determine $\gamma_{su,ld}$	[deg]
x	Interval size	[m]
Δx	Difference in interval sizes	[m]

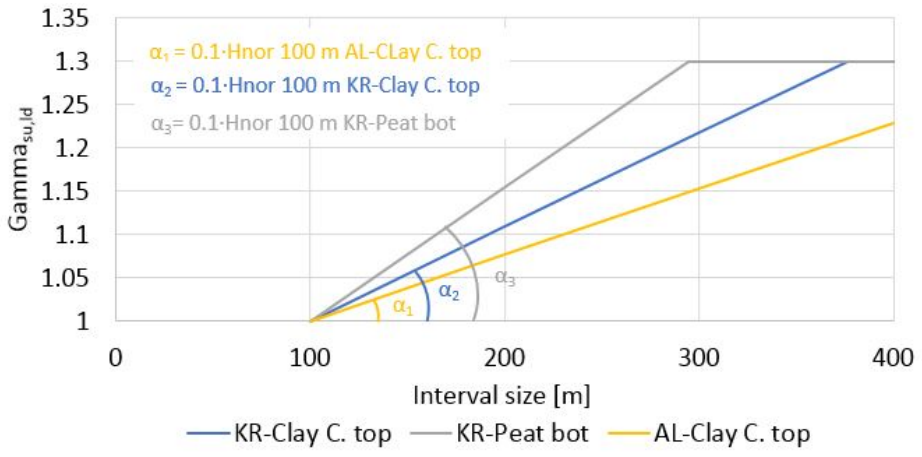

Figure 6.12: Spatial factor ($\gamma_{su,ld}$) with respect to the interval size for different layers

This method accounts for the uncertainty and the risk that is taken in case relatively large CPT interval sizes are conducted. Applying this equation assumes that the stratification in between two CPTs is linearly interpolated and that therefore no other soils are present in between the CPTs.

The implementation of normalized entropy means that the variation of the undrained shear strength in longitudinal direction is accounted for in two ways. In the regional variability and by means of equation 6.7. The regional variability focusses on the error made within the linearisation of q_{net} for each CPT in the testing field. The spatial factor as presented in this section only makes use of $s_{u,ld}$ to determine the variation in longitudinal direction and depends on the quantity and the domain of available data. Because these two uncertainties are fundamentally different it cannot simply be assumed that the one replaces the other. Moreover the regional variability is determined in the testing field and the normalized entropy is only based on CPTs in the field.

6.4.1. Results proposed method case study

In case a CPT interval larger than 100 m was implemented local minima in the calculated safety factor could be overseen, as is shown in section 6.1. A spatial factor ($\gamma_{su,ld}$) is proposed in equation 6.6 to account for sufficient safety for interval sizes larger than 100 meter. This additional partial factor results in a lower characteristic value for s_u, which on its turn will result in a lower safety factor.

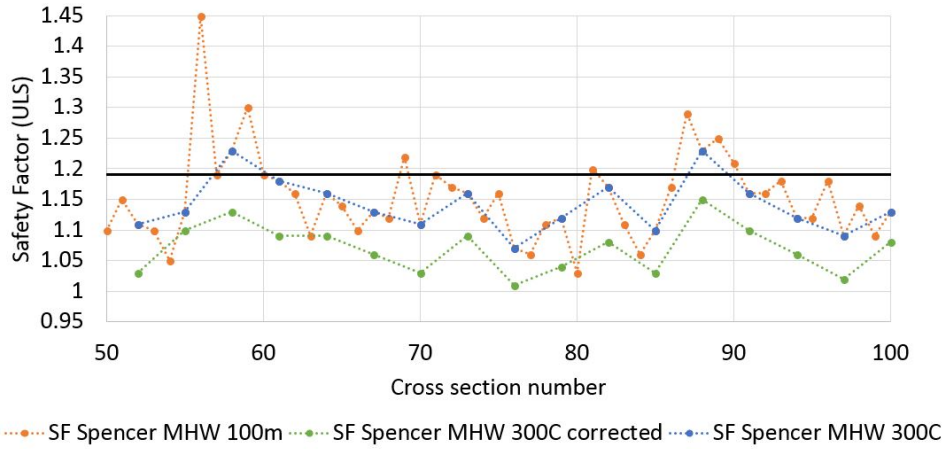

Figure 6.13: Recalculated safety factor for an interval of 300C m based on adjusted undrained shear strength

The safety factors determined in a semi-probabilistic analysis are recalculated with the new characteristic values for the undrained shear strength, see figure 6.13. While in figure 6.1 some of the minima were overseen, most of the minima are covered in case the spatial factor is multiplied with VC_{tot} as can be seen by the green line in figure 6.13. For instance cross section 52 covers the minimum located at cross section 54. Cross sections 61 and 64 cover the minimum safety factor in cross section 63, which otherwise would be overseen. The safety factors in cross section 76 and 85 cover the minimum safety factor (CS 80) present in the research area.

On the counter side this method could result in conservative estimations of the safety factor. The safety factor found in cross section 90 till 100 does not cover a minima and can therefore be seen as a conservative estimation. Nevertheless the lowest safety factors in longitudinal direction are of most interest, since the levee will fail at the weakest spot.

In figure 6.14 an example of the spatial factor for an interval size of 200 m is shown. In this example most of the local minima are covered with the application of the spatial factor. Cross section 83 and 85 cover the minimum found in cross section 84, whereas cross section 53 covers the minimum in cross section 54.

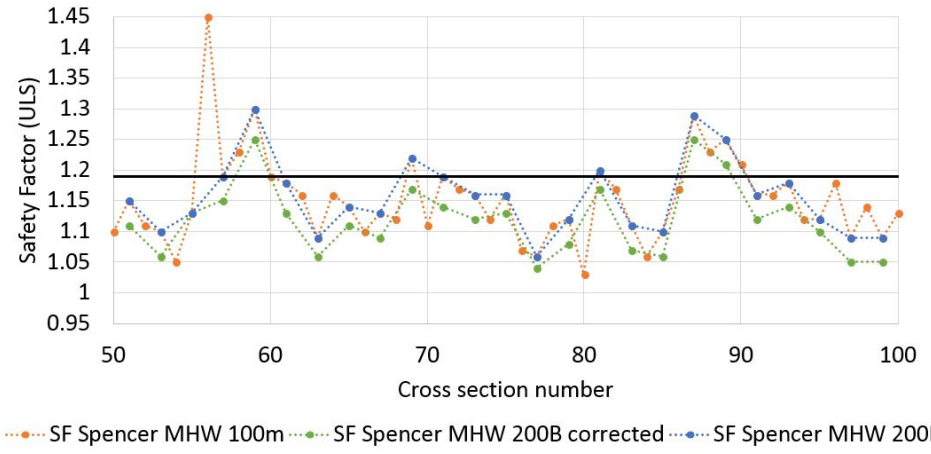

Figure 6.14: Recalculated safety factor for an interval of 200B m based on adjusted undrained shear strength

In figure 6.15 another example of the spatial factor for an interval size of 400 m is presented. In this example at some locations the minimum are properly covered, for instance in between CS 75 till 86. Nevertheless the safety factors in the area between CS 63 and CS 72 are conservative estimations.

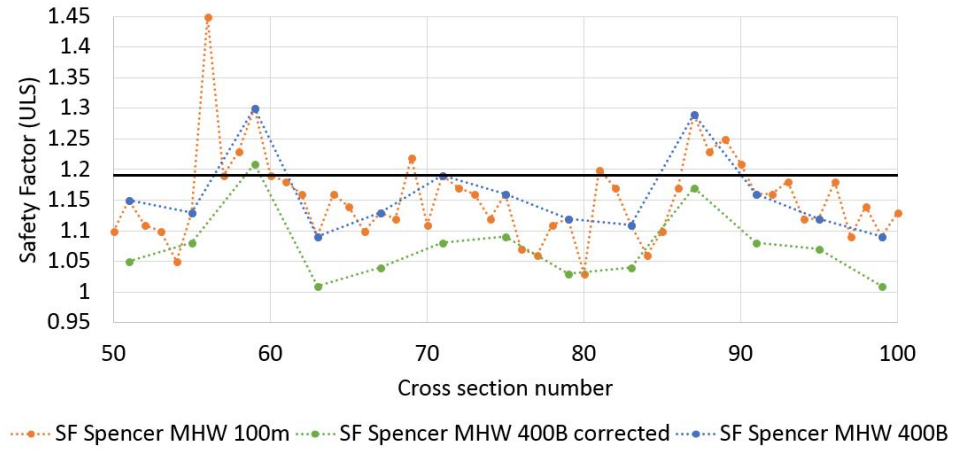

Figure 6.15: Recalculated safety factor for an interval of 400B m based on adjusted undrained shear strength

The corrected safety factors are calculated for all datasets considered (interval sizes 200, 300 and 400 m) in appendix D. These figure show that for other interval sizes also most of the minima in safety factor are covered with the proposed method. It can thereby be concluded that this method properly indicates the minimum safety factor in case the CPT interval size increases within the specified research area. It thereby accounts for the uncertainty present in s_u in longitudinal direction.

For the Markermeerdijken project most of the cross sections did not fulfil the required safety factor ($SF_{req,spencer}$ =1.19, equation 3.1). As the safety factor decreases in case the CPT interval size increases, the cross sections remain unsafe. The proposed spatial factor would therefore not influence the design within the considered research area.

6.4.2. Application proposed method in practice

In practice often a relatively large CPT interval size is conducted at first, densification of the CPT interval size is done in a later stadium. In the proposed method the normalized entropy for a 100 m interval size is used, it would be useful if the spatial factor could be estimated in case relatively large CPT intervals are present, 300 m or more. In this section therefore a more generic method is proposed which can provide such an estimation of the spatial factor.

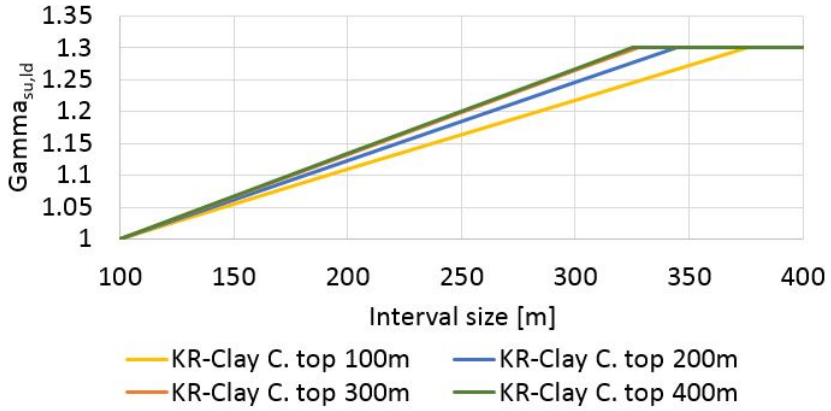

Figure 6.16: Spatial factor ($\gamma_{su,ld}$) determined with H_{nor100}, H_{nor200}, H_{nor300} and H_{nor400} for clay C.-KR top

Table 6.1: Spatial factor ($\gamma_{su,ld}$) determined with H_{nor100}, H_{nor200}, H_{nor300} and H_{nor400} for clay C.-KR top

Dataset	H_{nor}	α_H	$\gamma_{su,ld}$ 100 m	$\gamma_{su,ld}$ 200 m	$\gamma_{su,ld}$ 300 m	$\gamma_{su,ld}$ 400 m
100	0.62	0.011	1.00	1.11	1.22	1.30
200 averaged	0.70	0.012	1.00	1.12	1.25	1.30
300 averaged	0.75	0.013	1.00	1.13	1.26	1.30
400 averaged	0.76	0.013	1.00	1.13	1.27	1.30

The spatial factor depends on three things as indicated in figure 6.11:

- The chosen maximum value of $\gamma_{su,ld}$: for case study 1.3
- The determination of α_H: for case study based on H_{nor100}
- The chosen benchmark where $\gamma_{su,ld}$ is 1.0: for case study 100 m interval

Choice of maximum value An upper limit for $\gamma_{su,ld}$ is set equal to 1.3 in the previous section. For the considered case study this resulted in acceptable result regarding the estimation of the safety factor. In case no upper limit is determined this could lead to unrealistic low safety factor when the interval size becomes larger than approximately 400 m for the specified research area. Therefore the upper limit is kept equal to 1.3 for the application of the proposed method in practice.

Choice of α_H As the uncertainty in undrained shear strength increases for a particular soil the angle (α_H) increases. For the case study α_H depends on H_{nor100}; the normalized entropy found at a 100 m interval size. However this angle can also be based on the normalized entropy found at any other interval size, it not necessarily have to coincide with the interval size at which the benchmark is determined. Generally the normalized entropy increases for increasing interval size, as a result α_H increases.

To illustrate this methodology an example for s_u at the top of the clay C.-KR layer is presented in table 6.1 and figure 6.16. In table 6.1 $\gamma_{su,ld}$ is determined for different interval sizes and different α_H values. The α_H are based on normalized entropies for an interval of 100, 200, 300 and 400 meter (H_{nor100}, H_{nor200}, H_{nor300}, H_{nor400}). In table 6.1 it can be seen that α_H increases when the normalized entropy of larger interval sizes is used. In table 6.1 the benchmark is equal to an interval size of 100 m, $\gamma_{su,ld}$ is therefore always 1.0 at an interval size of 100 m.

In an early stage of the design it could occur that a large interval size is conducted to get an indication of the expected soil profile and properties. The adaptation of α_H as described in this section can help to give an indication of the spatial factor even in case only large CPT interval sizes are present. As in general the normalized entropy decreases with decreasing interval sizes, implementing the normalized entropy of larger interval sizes result in more conservative results compared to the use of smaller interval sizes.

Choice of benchmark A 100 meter interval size is chosen as a benchmark, since it is the minimum CPT interval size present in the Markermeerdijken project. Moreover it helps to validate the proposed spatial factor.

In this thesis it is stated that a 50 m interval can be seen as the minimum interval size, since it covers most of the uncertainties required to calculate the inner slope stability. Therefore some local minima could still be overseen when using the 100 m interval. For the application of the proposed method in practice the benchmark could therefore be set to a 50 m interval size. As the benchmark is chosen at lower interval sizes the spatial factor becomes more conservative compared to higher interval sizes, it is however uncertain what the actual benchmark should be. Additional research could point out what the best position of the benchmark is, note that this could differ per project.

6.5. Reflection proposed method

In this section the proposed spatial factor is reflected upon. The pros and cons of the proposed method are discussed and its actual use in practice will be elaborated.

Since a levee only fails at its weakest point the lowest s_u is often most interesting. This is not necessarily equal to the smallest safety factor, however small undrained shear strengths often result in a low safety factor. Nevertheless the theory of entropy uses the probability of occurrence of s_u instead of the actual value of s_u. This means that outliers, very low or very high values of s_u are not explicitly taken into account.

Two different datasets containing 51 points each are compared in figure 6.17 as an example. In figure 6.17 the range in s_u values is larger for example 2 in comparison with example 1. Although the distribution of s_u values differ significantly, the calculated entropy is the same for both datasets. Concluding that entropy does not consider the actual value of s_u, in appendix D this issue is discussed to a further extend.

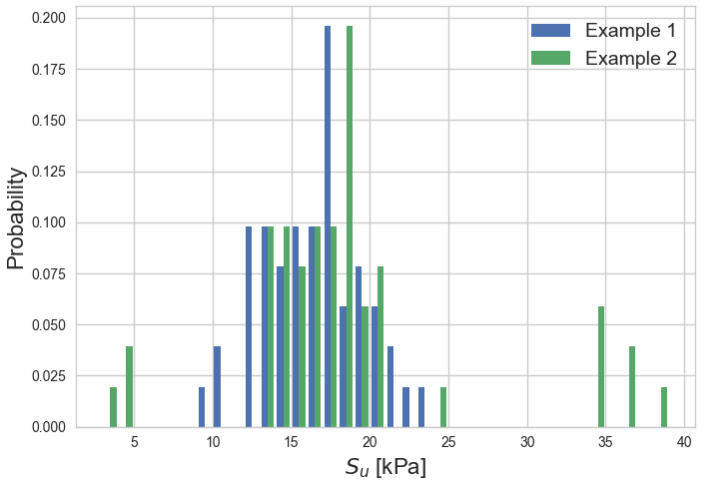

Figure 6.17: Example of two datasets with equal entropy and a different range of s_u

The proposed spatial factor can only be applied to assess the safety of an existing levee. Because the spatial factor is based on s_u, changes in effective stress due to rising water levels are not accounted for, therefore only uncertainties in N_{kt} are considered. In practice the water level is most certainly relevant and therefore uncertainties in S and m should be considered as well. In addition, the determination of s_u based on N_{kt} becomes less relevant in case the critical strength is exceeded within a new design, i.e. a raising of the levee or inner berm. In that case S and m are more relevant. The undrained shear strength that are used to estimate the spatial factor are then no longer present. This is also elaborated in section 4.3.

When the spatial factor would be applied in practice, additional CPTs could result in a lower $\gamma_{su,ld}$ and thereby in a higher safety factor. Data densification is only of interest in case the calculated safety factor is just below the required safety factor ($SF_{req,Spencer}$). The proposed spatial factor thereby encourages to obtain additional

data, which is thought to be the basic starting point for any partial factor that is assigned to cover epistemic uncertainties. If the calculated safety factor is higher than the required safety factor, additional data would be less useful. For the Markermeerdijken project most of the cross sections did not fulfil the required safety factor at a 100 m interval($SF_{req,spencer}$ =1.19). The cross sections therefore remain classified as unsafe for larger interval sizes, the proposed factor would therefore not influence the design.

The proposed method requires a continuous layer in longitudinal direction. In the considered case study it is assumed that a continuous peat and clay layer are present. In practice it could be unknown if the examined layer is continuous when a large CPT interval size is present. The spatial factor depends on H_{nor} which on its turn depends on the number of samples (CPTs). As the continuous layer increases, and the interval size remains constant, the spatial factor decreases. Large continuous layers in longitudinal direction are thereby beneficial in terms of the spatial factor compared to more heterogeneous soil profiles.

In case the undrained shear strength of different soils are used to quantify uncertainty in longitudinal direction it will most likely result in high spatial factors. In such a case the uncertainty in $s_{u,ld}$ as well as other soil parameters is high, a dense CPT interval size (50 to 100 m) is therefore required to minimalize these uncertainties.

The major goal of the proposed method is to ensure a safe levee design, to create awareness of uncertainties in s_u in longitudinal direction and to ensure that additional data is beneficial. The proposed method encourages additional data, in terms of decreasing partial factors. In practice generally already an interval size of 100 or 200 m is conducted, the proposed method would hardly influence the design in that case (depends on the location of the benchmark).

Limitations In this paragraph the limitations of the proposed method are listed:

- The spatial factor assumes that the indicated layers are continuous in longitudinal direction: Application of the proposed method has to be done with care, since the stratification is often unknown with large CPT interval sizes.
- The theory of entropy only considers probabilities and not actual s_u values.
- The safety factors estimated with the spatial factor can be conservative, depending on the maximum value of $\gamma_{su,ld}$.
- The spatial factor does not account for difference in effective stress. Therefore does not account for difference in water level, a raising and uncertainties in S and m.
- A larger area results in lower spatial factors for similar CPT interval sizes, since the number of samples increases.
- The exact position of the benchmark is unknown and can differ for each location.

6.6. Conclusions and Remarks

In the current guidelines for levee design, spatial uncertainty in longitudinal direction is only partly accounted for in the schematisation factor. The proposed spatial factor, which makes use of normalized entropy, provides a useful tool to assign additional reliability when the CPT interval size is larger than 100 meters for the considered research area. This method therefore accounts for spatial uncertainty in the estimation of $s_{u,ld}$. Moreover this methodology promotes the collection of additional data, which is thought to be the basic starting point for any partial factor that is assigned to cover epistemic uncertainties. It is advised to validate the application of the spatial factor in other projects as well.

The spatial factor is based on s_u, changes in effective stress due to rising water levels are not accounted for, therefore only uncertainties in N_{kt} are considered. The determination of s_u based on N_{kt} becomes less relevant in case the critical strength is exceeded within a new design, i.e. a raising of the levee or inner berm. In that case S and m are more relevant. The proposed spatial factor is therefore only useful to assess the safety of an existing levee.

In case a CPT interval size larger than 100 m would be applied in the Markermeerdijken case the safety could locally be overestimated. It has to be emphasized that in this thesis the minimum interval, to safely design a levee on inner slope stability, is assumed to be 50 meter. In the case study the minimal interval size is 100 m. The actual minimum safety could therefore still be overseen with a 100 meter CPT interval size.

The theory of entropy uses the probability of occurrence of s_u instead of the actual value of s_u. This means that outliers, very low or very high values of s_u are not explicitly taken into account in the spatial factor. The estimated spatial factor depends on the chosen benchmark which is set to 100 m for the considered case study. It is thought that a 50 m CPT interval size always results safe levee design regarding inner slope stability, additional research has to point out if this is the case.

In principle the spatial factor can be applied to any levee project. As α_H can be based on the normalized entropy found at any interval size, a conservative estimation of the spatial factor can even be made in case only a 300 or 400 m interval is present within a project. It is advised to use at least 10 CPTs in order conclude on the uncertainty in the available data. The probability that two or more identical s_u values are found is very unlikely in case less than 10 CPTs are used.

The advantage of using the discrete entropy is that it can be used on all possible soil types, which perhaps could have different continuous distributions, since it only depends on its discrete measurements. The anthropogenic clay can therefore be analysed in the same manner as any geological layer. If in fact antropogenic clay would consist out of multiple different soil types it would simply result in a higher entropy/uncertainty.

In this thesis entropy is used to quantify the amount of information/uncertainty in a set of CPTs, because it focusses on the probability of occurrence of a value and not the value on itself. However there are many other methods that could potentially be used to analyse the uncertainty within a dataset, e.g. Maximum Likelihood [37].

7
Conclusions

The main research question of this thesis is: **How does the quantity of CPTs in longitudinal direction affect the estimation of the undrained shear strength, and how is that related to the probability of failure considering inner slope stability?** This question can be answered by answering the following sub-questions:

- *What is the current way to deal with the uncertainty regarding inner slope stability and how does this relate to engineering practice?* Implementation of design values of s_u provides safety on the resistance and partial factors have to ensure that sufficient safety is assigned in the design loads. The variation coefficient of s_u is based on uncertainty in cone factor determination and the linearisation of q_{net} for the S_u measured method. Whereas in practice the focus lies on proper estimation of $s_{u,k}$, uncertainties in longitudinal direction are seldom addressed, apart from the schematisation factor which is often set to 1.1 in practice. As a result the frequently applied 100 m CPT interval size is based on the identification of different soil types and not related to s_u estimation.
- *How does the quantity of CPTs and laboratory tests influence the uncertainties within the estimation of the cone factor (N_{kt})?* The quantity of CPTs nor laboratory tests influences the uncertainties within the estimation of N_{kt} directly, since the statistical coefficient is always equal to 1.645. Since N_{kt} is determined in the testing field, CPTs in the field do not influence N_{kt}. Application of a dataset with laboratory test containing inaccuracies due to sample disturbance, inaccurate measurements or wrongly classified soil types can lead to large uncertainties within the estimation of the cone factor. Composition of a clean dataset is therefore required prior to any statistical analysis. Although a larger quantity of CPTs results in a better estimation of N_{kt}, it also leads to an increase of $VC_{av,reg}$.
- *How does the amount of soil investigation (CPTs) influence the calculated inner slope stability?* Fluctuations in undrained shear strength in longitudinal direction are not considered in the design, hence the quantity of CPTs does not influence the estimation of s_u in current design practice. Apart from the choice of stratigraphy and the schematisation factor the quantity of the CPTs does not affect the calculated inner slope stability. As a levee fails at its weakest point, the lowest reliability is of most interest. In case a 200, 300 or 400 m CPT interval size would be applied in the specified research area along the Markermeer the reliability is locally overestimated. Concluding that the amount of CPTs only partly affect the estimated stability, nevertheless a limited CPT interval size is of importance to ensure the minimum safety factor along a levee is not overseen.

The probabilistic stability analyses emphasizes that s_u has the largest influence on the reliability for the considered research area. As a result the relative influence of s_u is higher than the influence of the outside water level, the layer thickness or the unit weights of the considered soils. Additionally, the estimation of these parameters is generally significantly more accurate causing an amplification of the relative influence of s_u on the reliability.

This research underlines that the fluctuations in s_u in longitudinal direction affect the calculated probability of failure and therefore require adequate attention in the levee design. CPT densification in longitudinal direction helps to identify these fluctuations. As the CPT interval size increases, the probability of over- or underestimating the actual safety factor increases as well. It is shown that the amount of information of the estimated s_u in longitudinal direction generally increases as the interval size decreases.

As the influence of s_u on the probability of failure is large and an increasing interval size can lead to overestimations of the actual reliability, a new partial factor (spatial factor) is proposed based on the principle of normalized entropy. The proposed spatial factor accounts for spatial uncertainty in the undrained shear strength and assigns additional safety when the CPT interval size is larger than 100 m for the considered research area. This methodology promotes the collection of additional data, which is thought to be the basic starting point for any partial factor that is assigned to cover epistemic uncertainties.

8

Discussion and Recommendations

This chapter discusses the results, conclusions and the assumptions made within the calculations as presented in the previous chapters. Additionally this results in a list of recommendations.

8.1. Discussion

This thesis is based on one specific case of a primary flood defence at the Markermeer. All data used in this thesis is obtained from the Markermeerdijken project, within which a 5 km long research area is chosen. As a result, most of the conclusions are only valid for this specific research area. Additionally the parameter determination and formulas presented in this thesis are based on 'Dijken op Veen II, DOV werkwijze voor bepaling macrostabiliteit Markermeerdijk' [64]. The applied formulas to determine the variation coefficients of the cone factor are slightly alternated in more recent reports [59] [65]. As a result some equations, results or conclusions within this thesis may no longer be relevant.

In this thesis the laboratory test that are used to determine the cone factor were chosen based on multiple criteria. These criteria are necessary to compose a purified dataset which in turn is required to perform a reliable statistical analysis. A purified dataset is not polluted by inaccuracies due to sample disturbance, inaccurate measurements or wrongly classified soil types. These requirements have to be fulfilled prior to any statistical analysis to prevent subjectivity towards the determined parameters. The variation coefficient of the cone factor (VC_{Nkt}) increases significantly without these criteria.

Multiple methods are available to determine the cone factor. In this thesis the 'DOV method' is applied since it accounts for a larger uncertainty when the cone tip resistance and the undrained shear strength increase, which is in line with practice. Although the DOV method is thought to be the best method for linear regression, a quadratic regression could provide a better representation of the data. For the data used within this thesis hardly any difference is found in between the DOV method and a quadratic regression.

The unit weight can have a large influence on q_{net}, especially for soft and organic soils. In this thesis the effect of a deviating unit weight, due to inaccurate measurements, on the cone factor is specified. A 10% increase or decrease in unit weight can lead to a significant change in q_{net} and therefore in N_{kt}. However in the determination of s_u based on the S_u-measured method this difference is almost equalized, since $s_u = q_{net}/N_{kt}$. A systematic error in the estimation of the unit weight will therefore hardly influence the estimation of s_u. A non-systematic error present in the estimation of unit weight could lead to erroneous s_u estimations, since the estimation of unit weight in the testing field could differ from the estimation in the field within the same layer.

Although objectivity is strived upon in this thesis, the parameter determination involves reasoning and therefore subjectivity. Subjectivity is present in the linearisation of the undrained shear strength. The undrained shear strength is linearised, thereafter this linearisation is adapted (if needed) to create the best representation for the considered cone tip resistance. The 'best representation' is a linearisation in which the major part of the undrained shear strength coincides with the linearisation. Large local peaks in s_u can affect the angle or translate the linearisation, which results in different estimations of $s_{u,top}$ and $s_{u,bottom}$. Adjustment for large peaks can lead to a conservative or optimistic linearisation. In chapter 5 and 6 the linearised undrained shear strength ($s_{u,ld}$) is used to quantify effects of the fluctuation of s_u in longitudinal direction. The linearisation

involves subjectivity which can influence the results of the probabilistic stability analysis and the outcomes regarding the effect of different CPT interval sizes. The regional uncertainty already accounts for the error made within the linearisation, however VC_{reg} is only based on CPTs within a testing field, whereas the error within the linearisation process in the field can be different.

The regional variation coefficient (VC_{reg}) is a combination of all local variation coefficients (VC_{loc}) determined per CPT in each layer. The thickness of the considered layer can vary. As a result a different layer thickness can be found in each CPT. The vertical reduction factor γ_v depends on this layer thickness and can therefore vary for each CPT. Nevertheless γ_v is multiplied with VC_{reg} in equation 4.9. Therefore one layer thickness has to be assumed over all CPTs used in the estimation of VC_{reg}. This can to lead to misunderstanding and inaccurate estimation of $VC_{av,reg}$.

To provide a clear insight regarding the influence of s_u in the levee stability, some simplifications are made. The ground level, the unit weight, S and m, the water level, phreatic and headlines and the stratification are assumed to be constant along the 5 kilometre long levee. These simplifications influence the estimated reliability of each cross section, which therefore deviates from reality. The fluctuation in safety factors along the 5 kilometre long research area could either decrease or increase as a results of these simplifications.

The critical slip surface found in the stability analysis resembles a near circular shape and therefore all probabilistic analyses are performed with the LEM of Bishop. In practice often the LEM of Spencer or Uplift Van are used since these methods give a more accurate description of the slip surface. In this case the critical slip surfaces determined with Uplift Van and Spencer are also near circular, justifying the use of the LEM of Bishop. For the LEM of Uplift Van and Spencer a lower model factor can be applied in the probabilistic analysis resulting in a higher reliability compared to Bishop. The estimated reliability therefore depends on the chosen model. It is striking that the reliability in a probabilistic analysis for LEM of Spencer is higher compared to the LEM of Bishop, whereas it is always lower in a semi-probabilistic stability analysis. Furthermore it has be emphasized that the use of a LEM assumes that no deformations are present within the soil body, which is certainly not the case during the failure of the inner slope.

Scenario 2 and 3, as presented in chapter 5, are used to study the relative influence between the layer thickness and the fluctuation of s_u in longitudinal direction. These two analyses are not comparable to a regular 2D probabilistic analysis performed with the Probabilistic Toolkit, since it analyses longitudinal fluctuations in a cross sectional model. In practice the layer separation is known with more precision and therefore will be implemented either deterministically or with a lower standard deviation. The influence factors therefore indicate the maximum influence of the layer separation within the considered research area. Furthermore no transformation and regional uncertainties are considered within the probability density function of $s_{u,ld}$ which is not realistic, but necessary to analyse the longitudinal fluctuations in s_u.

Whereas the schematisation factor accounts for the implementation of a particular scenario in the semi-probabilistic analysis, no such factor is applied in the probabilistic analysis. The elimination of the schematisation factor suggests that all scenarios are considered and all parameters are stochastically implemented, this is not always the case in practice. The elimination of the schematisation factor can therefore lead to a higher reliability in a probabilistic stability analysis compared to a semi probabilistic stability analysis. Extra caution is required in case the reliability requirements are fulfilled with a probabilistic analysis, while they are not met in a semi-probabilistic analysis.

Incorrectly assuming independence between parameters can results in optimistic reliability estimations in a probabilistic stability analysis. On the other hand it is hard to audit the correctness of the correlation matrix. In this thesis the undrained shear strength at the top and bottom of each layer is assumed to be fully positively correlated, because they had to bear the same loads over time. This assumption ensures that the linearisation preserves equal sign, either positive or negative. Nevertheless the layers are assumed to be independent in horizontal direction which means if you would specify twice the number of layers in your model, reliability would increase. The embankment/slip circle does not know its divided into vertical segments: crest(KR), inner berm(BI) and hinterland(AL). Since each geological deposit has similar origin they are correlated in some manner, a fully positive correlation results in unrealistically low reliability estimations. Since the exact correlation is unknown, the undrained shear strength is only correlated based on loads in a specific layer (vertical

direction) and not origin (horizontal direction).

In case a 200, 300 or 400 m CPT interval size would be applied in the Markermeerdijken case the reliability could locally be overestimated. Decreasing the CPT interval size from 200, 300 or 400 to 100 meter helps to identify local minima in reliability, which could be overseen otherwise. It has to be emphasized that in this thesis the minimum interval size, to safely design a levee on inner slope stability, is assumed to be 50 meters, whereas the minimal interval size is 100 m in the specified research area. The actual minimum safety could therefore still be overseen with a 100 meter CPT interval size. In depth research regarding the fluctuation of s_u in longitudinal direction can give more insight in the required minimal CPT interval size. Such a research could also point out if the calculated safety factor contains sufficient safety.

The spatial safety factor assigns additional safety in case a interval size larger than 100 meter is conducted. In this thesis the spatial factor is assigned to an area where the stratification is known with relatively high accuracy. Applying the spatial factor in practice in case a CPT interval of 200 m or more would be present increases the risk of overseeing potentially weak layers. Applying the spatial factor should therefore always be done with care.

The spatial factor is based on s_u, changes in effective stress due to rising water levels are not accounted for, therefore only uncertainties in N_{kt} are considered. In practice the water level is most certainly relevant and therefore uncertainties in S and m should be considered as well. In addition, the determination of s_u based on N_{kt} becomes less relevant in case the critical strength is exceeded within a new design, i.e. a raising of the levee or inner berm. The proposed spatial factor is therefore only useful to assess the safety of an existing levee. It would be of interest to come up with a spatial factor that can be applied in either testing or design.

To compare different undrained shear strengths in longitudinal direction ($s_{u,ld}$), the values are first rounded up to zero decimals. This measure is required because the datasets that are available only contain a minimum of 12 to a maximum of 51 samples. The probability that two identical s_u's are found is very small in case these values are not rounded. Without this assumption the discrete entropy would be equal to the maximum value for most datasets. This simplification influences the required spatial factor significantly.

The anthropogenic clay layer within the levee is assumed to have constant properties in longitudinal direction. Since the levee is a man-made structure it can contain different soil types, moreover the soil parameters can differ. The anthropogenic clay layer could therefore show different fluctuation patterns of undrained shear strength in longitudinal direction compared to geological deposits. The use of discrete entropy makes the exact fluctuation less relevant since entropy depends on the probability of occurrence of s_u within discrete measurements. Nevertheless difference in soil behaviour can still influence the reliability.

Statistics are not necessarily a method that yield automatic correct results. The calculated entropy therefore should only be applied with good understanding of the problem, in the end 'statistics are only an objective tool to support sound reasoning' [5].

8.2. Recommendations

- It is recommended to account for the uncertainty in undrained shear strength in longitudinal direction and CPT interval sizes larger than 100 m in the design of all primary flood defences. It is thereby advised to further investigate the effect of the proposed spatial factor on the levee design. Validation of the spatial factor in other projects is recommended.
- The proposed spatial factor is useless in case the critical strength is exceeded, a spatial factor that includes S and m and their corresponding uncertainties would therefore be useful. Thereby it is of interest to analyse the state parameters (POP and σ'_{vy}), since these are generally used in stability analysis.
- It is recommended to analyse a set of CPTs with a 50 m interval to more accurately determine the fluctuation in undrained shear strength in longitudinal direction. This can also help to verify the assumption that a 50 m CPT interval size is required to safely design a levee.
- Experience thought that probabilistic stability analyses should be performed with care and are not necessarily better than a semi-probabilistic analyses. Since the schematisation factor is eliminated in a

probabilistic analysis, overseeing a potentially hazardous scenario results in an overestimation of the reliability. Additionally, caution is required in the determination of the correlation matrix. Extra care is required in case the reliability requirements are fulfilled with a probabilistic analysis, while they are not met in a semi-probabilistic analysis.

- In this thesis the semi probabilistic model is simplified to determine the influence of the undrained shear strength. It is advised to investigate the effect of the spatial factor in a case without a simplified stratification, constant ground level, water level and phreatic lines.
- The spatial factor as presented in this thesis has to be used with care when only large CPT interval sizes are present, since the stratification is unknown. A better prediction of the expected soil profile would therefore be interesting. It would therefore be interesting to combine the WBI-SOS or similar models that predict the probability of a certain stratification with the proposed partial factor.
- Since the normalized entropy in this thesis only uses the linearised s_u at the top and bottom of a layer it is prone to subjectivity. It is recommended to seek for a method that includes less subjectivity and can include the large numbers of measurements in vertical direction in a CPT.

Bibliography

[1] Probabilistic toolkit - Manual. Technical report, Deltares, Delft, 2015.

[2] M.L. Aalberts. Ontwerpbasis Dijken DO. Technical report, Alliantie Markermeerdijken, 2017.

[3] Razan Al-nakhli. *On Upper Bounding Discrete Entropy.* PhD thesis, Queen's University Kingston, 2011.

[4] G.B. Baecher and J.T. Christian. *Reliability and Statistics in Geotechnical Engineering*, volume 47. John Wiley & Sons Ltd, Chichester, 2003.

[5] Christophe Bauduin. Determination of characteristic values, 2002.

[6] Ertan Bol. The influence of pore pressure gradients in soil classification during piezocone penetration test. *Engineering Geology*, 157(157):69–78, 2013.

[7] A. Bond and A. Harris. *Decoding Eurocode 7.* CRC Press, 2008.

[8] Ed Calle, Ton Vrouwenvelder, Jaap Lindenberg, Geerhard Hannink, and Edward Bruijn. Representatieve waarden voor grondparameters in de Geotechniek. *Geotechniek*, (april):24–29, 2008.

[9] Rudolf Julius Emmanuel Clausius. IoHT :: Clausius' Mechanical Theory of Heat [1850-1865], 1865.

[10] Muawia A. Dafalla. Effects of Clay and Moisture Content on Direct Shear Tests for Clay-Sand Mixtures. *Advances in Materials Science and Engineering*, 2013:8, 2012.

[11] H.T.J. de Bruijn, M.A.T. Visschedijk, and G. A. van den Ham. Dijken op Veen II - Eindrapport Heterogeniteit. Technical report, Deltares, 2014.

[12] R. de Jager and J. van der Meer. Geotechnische Ontwerpbasis DO - Werkwijze en rekenparameters geotechnische stabiliteit. Technical report, Alliantie Markermeerdijken, 2017.

[13] Deltares. *D-Geo Stability - User Manual.* Deltares, Delft, 16.2 edition, 2016.

[14] A. Van Duinen. Handreiking voor het bepalen van schuifsterkte parameters. Technical report, Deltares, Delft, 2014.

[15] ENW - Expertise Netwerk Waterveiligheid. Addendum bij het technisch rapport waterkerende grondconstructies. Technical report, ENW, Den Haag, 2007.

[16] ENW - Expertise Netwerk Waterveiligheid. Technisch Rapport - Grondmechanisch Schematiseren bij Dijken. Technical report, ENW, 2012.

[17] Fugro GeoServices B.V. AANVULLEND GRONDONDERZOEK PROJECT DIJKEN OP VEEN (DOV) – FASE 2. Technical report, Fugro, 2016.

[18] Fugro GeoServices B.V. Aanvullend onderzoek bepaling N-waarden in klei. Technical report, Fugro GeoServices B.V., 2017.

[19] G. Greeuw, H.M. van Essen, and T.A. van Duinen. Protocol laboratoriumproeven voor grondonderzoek aan waterkeringen. Technical report, Deltares, Delft, 2016.

[20] B. Hardeman and M.P. Hijma. Stochastische Ondergrond Schematisatie (SOS), 2016.

[21] M.P. Hijma and K.S. Lam. Globale stochastische ondergrondschematisatie (WTI-SOS) voor de primaire waterkeringen. Technical report, Deltares, Delft, 2015.

[22] M.P. Hijma, K.S. Lam, and J.M. van der Hammen. Scenario ' s van de ondergrond voor WBI 2017 : kansen en toepassing. *Geotechniek*, Oktober:16–21, 2016.

[23] R.B. Jongejan. Kalibratie van semi-probabilistische toetsvoorschriften. Technical report, Deltares, Delft, 2013.

[24] S. N. Jonkman, A. C. W. M. Vrouwenvelder, R. D. J. M. Steenbergen, O. Morales-nápoles, and J. K. Vrijling. *Probabilistic Design : Risk and Reliability Analysis in Civil Engineering*, volume 3th. TU Delft, Delft, 3th edition, 2016.

[25] H. Keijer. *1-2-3 Geologie voor Ingenieurs*. KIVI, afdeling Geotechniek, 2015.

[26] S. Kullback. *Information Theory and Statistics*. Dover Publications Inc., 1959.

[27] C.C. Ladd and R. Foott. New design procedure for stability of soft clays. *Journal of the geotechnical engineering division*, 100(GT7):24, 1974.

[28] H J Lengkeek, J De Greef, and S Joosten. CPT based unit weight estimation extended to soft organic soils and peat. page 6, 2018.

[29] M. Lloret-Cabot, M. A. Hicks, and A. P. van den Eijnden. Investigation of the reduction in uncertainty due to soil variability when conditioning a random field using Kriging. *Géotechnique Letters*, 2(3):123–127, 2012.

[30] M Long and N. Boylan. In situ testing of peat – a review and update on recent developments. *Geotechnical Engineering Journal of the SEAGS & AGSSEA*, 43(4):15, 2012.

[31] T. Lunne, P. K. Robertson, and J.J.M. Powell. *Cone penetration testing in geotechnical practice*. Taylor & Francis, New York, 1997.

[32] Charles Marsh. Introduction to Continuous Entropy, 2013.

[33] P.W. Mayne, J. Peuchen, and D. Bouwmeester. Soil unit weight estimation from CPTs. In *2nd International Symposium on Cone Penetration Testing*, volume 2, page 8, Huntington Beach, 2010. 2nd International Symposium on Cone Penetration Testing.

[34] NEN. National Annex to NEN-EN 1997-1 Eurocode 7: Geotechnical design - Part 1: General rules, 2016.

[35] W.A. Nohl and A.J. van Seters. Nieuwe sondeernorm NEN-EN-ISO 22476-1 'Elektrisch sonderen'. *Geotechniek*, juli:3, 2013.

[36] Daniel Pele, Emese Lazar, and Alfonso Dufour. Information Entropy and Measures of Market Risk. *Entropy*, 19(5):226, 2017.

[37] K. K. Phoon and J. Ching. *Risk and reliability in geotechnical engineering*. CRC Press, Boca Raton, 2015.

[38] Rijkswaterstaat. Achtergrondrapport Ontwerpinstrumentarium 2014v4. Technical Report 4, Rijkswaterstaat, 2016.

[39] Rijkswaterstaat. Schematiseringshandleiding Macrostabiliteit. Technical Report 2.1, Rijkswaterstaat, 2016.

[40] Rijkswaterstaat. Handreiking ontwerpen met overstromingskansen. Technical report, Rijkswaterstaat, 2017.

[41] Rijkswaterstaat. Waterveiligheid | Deltaprogramma | Deltacommissaris, 2018.

[42] P. K. Robertson. Interpretation of cone penetration tests — a unified approach. *Canadian Geotechnical Journal*, 46(11):1337–1355, 2009.

[43] P. K. Robertson and K. L. Cabal. *Guide to Cone Penetration Testing for Geotechnical Engineering*. Gregg Drilling & Testing, Signal Hill, 6th edition, 2014.

[44] Peter K. Robertson. Soil behaviour type from the CPT: an update. In *2nd International Symposium on Cone Penetration Testing*, page 8, Signal Hill, 2010. Gregg Drilling & Testing.

[45] Peter K. Robertson and K. L. Cabal. Estimating soil unit weight from CPT. In *2nd International Symposium on Cone Penetration Testing*, page 8, Huntington Beach, 2010. 2nd International Symposium on Cone Penetration Testing.

[46] P.K. Robertson. Comparing CPT and Vs Liquefaction Triggering Methods. *Journal of Geotechnical and Geoenvironmental Engineering*, 141(9):1–10, 2015.

[47] A. Rozing, F. Van den Berg, H. Schelfhout, and E. Calle. Dijken op Veen II - Veiligheidsfilosofie. Technical report, Deltares, 2014.

[48] A. Rozing and T. Schweckendiek. POVM Beter benutten actuele sterkte KIJK. Technical Report 2, POVM, Delft, 2017.

[49] T. Schweckendiek. *Structural Reliability applied to deep excavations: Coupling reliability methods with finite elements*. Msc thesis, Delft Universtity of Technology, 2006.

[50] T. Schweckendiek, M. van der Krogt, B. Rijneveld, and A. Martins Teixeira. Handreiking Faalkansanalyses Macrostabiliteit. Technical report, Deltares, Delft, 2017.

[51] L Serrano. Shannon Entropy, Information Gain, and Picking Balls from Buckets, 2017.

[52] C.E. Shannon. A Mathematical Theory of Communication. *The Bell system Technical Journal*, 27(April 1924):379–423, 623–656, 1948.

[53] J. Stafleu, D. Maljers, F.S. Busschers, J.L. Gunnink, J. Schokker, R.M. Dambrink, H.J. Hummelman, and M.L. Schijf. GeoTop modellering. Technical report, TNO, Utrecht, 2013.

[54] Ruud Stoevelaar and A van Duinen. Protocol sonderen voor Su-bepaling. Technical report, Deltares, Delft, 2016.

[55] R. 't Hart, H. de Bruijn, and G. de Vries. Fenomenologische beschrijving. Technical report, Deltares, Delft, 2016.

[56] TAW. Technisch Rapport Waterspanningen bij dijken. Technical report, TAW, 2004.

[57] Jurjen van Deen and Alexander van Duinen. Schematiseringshandleiding Macrostabiliteit. Technical Report december 2016, Deltares, Delft, 2015.

[58] A. Verruijt. *Soil Mechanics*. TU Delft, Delft, 2001.

[59] M. Visschedijk. POVM Rekentechnieken - Basisrapport Eindige-elementenmethode. Technical report, POVM, 2018.

[60] J. K. Vrijling, Timo Schweckendiek, and Wim Kanning. Safety standards of flood defences. In N. Vogt, editor, *Proceedings of the 3rd International Symposium on Geotechnical Safety and Risk, ISGSR 2011, Munich, Germany*, number June, pages 67–84, Munich, 2011. ISGSR2011.

[61] Yu Wang, Kai Huang, and Zijun Cao. Probabilistic identification of underground soil stratification using cone penetration tests. *Canadian Geotechnical Journal*, 50(7):766–776, 2013.

[62] D.J. Wheeler. What They Forgot to Tell You About the Normal Distribution | Quality Digest, 2012.

[63] Sompote Youwai and Dennes T Bergado. Strength and deformation characteristics of shredded rubber tire - sand mixtures. *Canadian Geotechnical Journal*, 40(2):254–264, 2003.

[64] C Zwanenburg. Dijken op Veen II - DoV werkwijze voor bepaling macrostabiliteit Markermeerdijken. Technical report, Deltares, 2014.

[65] Cor Zwanenburg. Werkwijze parameterbepaling BEEM, 2018.

A

Additional information CPT

Several in-situ soil measurement equipment is available nowadays of which the cone penetration test (CPT) is most used in the Netherlands. A CPT consist of a cone connected to a number of rods. The cone is pushed into the ground at a constant rate which results in a nearly continuous measured profile of the resistance , see figure A.6. This profile gives a detailed overview of the stratigraphic profile and can be used in the estimation of geotechical parameters. The advantages of a CPT test are [43]:

- Fast and nearly continuous profiling
- Repeatable and reliable data
- Economical and productive
- Strong theoretical basis for interpretation

Some disadvantages are:

- No soil sample
- Requires skill operators
- Relatively high capital investment
- Penetration can be restricted in gravel

A CPT is one of the most valuable in-situ tests considering soil mechanics [42]. The CPT shows promising results and with great accuracy in comparison with other in-situ measurements. The CPT is widely used and it is therefore of importance to further optimize its use in geotechnical parameter estimations. Researchers tried to estimate a lot of parameters from raw CPT data. The following list contains some of these parameters: soil unit weight, undrained strain shear, soil sensitivity, overconsolidation ratio, in-situ stress ratio, relative density, state parameter, friction angle, stiffness and modulus, shear wave velocity and its modulus, hydraulic conductivity, consolidation characteristics, constrained modulus. The complexity of soil causes these parameters to be obtained with the help of empirical formulas. Although a lot of parameters can be estimated, depending on the size and risk of a project soil samples are required to test in the laboratory.

A.1. Soil Behaviour Type

During a CPT both the cone tip resistance (q_c) and the sleeve resistance (f_s) are measured every 2, 5 or 10 cm, depending on CPT class. To correct for the pore water pressure which acts on the cone the corrected cone resistance q_t is often used. The factor a is determined from laboratory calibration and defines the net area ratio, typical values lie between 0.7 and 0.85.

$$q_t = q_c + u_2(1-a) \tag{A.1}$$

Besides the estimation of geotechnical soil parameters, the CPT is also very useful to determine the soil type and the soil profile. Each soil type has some specific behaviour which causes it to be different from other types. The soil type is often indicated with a Soil Behaviour Type (SBT). SBT chart can be separated into the

non-normalized SBT charts and the normalized SBT charts. The first one was developed by Robertson in 1986. It displayed the direct relation between the cone tip resistance (q_t) and the friction Ratio (R_f) [46]. The advantage of the non-normalized SBT is that it can directly be presented after the cone test. It is important to notice that the friction Ratio depends on both cone tip resistance as well as sleeve friction, see equation A.2.

$$R_f = \frac{f_s}{q_t} \tag{A.2}$$

Both the tip resistance as well as the sleeve resistance increase with depth. Therefore the non-normalized SBT chart can only be used up to depths of approximately 20 m. This limitation resulted in the normalized SBT chart, where both the sleeve and the tip resistance are normalized for overburden stress.

$$Q_t = \frac{q_t - \sigma_{vo}}{\sigma'_{vo}} \tag{A.3}$$

$$F_r = \frac{f_s}{q_t - \sigma_{vo}} 100 \tag{A.4}$$

In figure A.1 two different SBT charts are presented. The normalized Robertson chart is a popular graph for soil characterisation (left in figure A.1). However little difference between the non-normalized SBT chart is present when the in-situ vertical effective stress is between 50 kPa to 150 kPa [44]. This chart displays the normalized cone tip resistance (Q_t) on the vertical axis and the normalized sleeve friction(F_r) on the horizontal axis. The chart is divided into 9 different zones, which represent different soil type behaviours. The left chart changes from sand to clay to organic soil from the top left to the bottom right. Besides that age, sensitivity and over consolidation(OCR) are indicated. The right chart in figure A.1 makes use of the normalized excess pore pressure (B_q) as shown equation A.5 and is used to better identify soft soils.

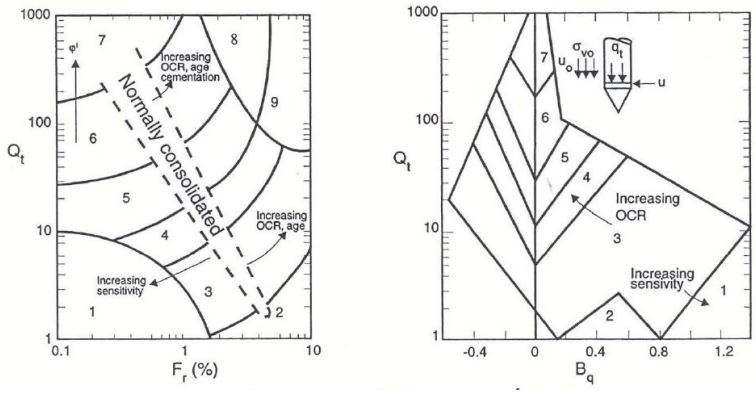

Figure A.1: Normalized SBTn charts [46]

$$B_q = \frac{u_2 - u_0}{q_t - \sigma_v} \tag{A.5}$$

The Soil Behaviour Type Index (I_c) is often used to classify different soil types, see equation A.6. Throughout the last decades several Soil Behaviour Type indexes are composed by different researchers. All of them are set up in some kind of similar way, with a square root and several empirical parameters. The first few did not make use of the normalized cone tip and sleeve resistance but often made use of the normalized excess pore pressure parameter (B_q). Every formula has a list of I_c values which belong to a specific soil type. The I_c value can also be shown in the normalized Robertson chart with the help of concentric circles, of which the origin is situated outside the SBT chart itself.

$$I_c = ((3.47 - logQ)^2 + (logF + 1.22)^2)^{0.5} \tag{A.6}$$

Besides the SBT charts that were developed also methods that interpert the CPT data in different manners where developed, for instance soil layer classification with the help of bayesian approaches [61] or with pore

pressure gradients [6]. TNO uses Neural Networks (NN) to determine the probability of a certain soil type from CPT data.

The Robertson SBT chart as illustrated in figure A.1 often lacks accuracy when indicating soft and organic soil types, which are often present in the Netherlands. These soils are often not well represented in the Robertson chart and therefore an adjustment is made regarding Dutch soil behaviour, as can be seen in figure A.2. Often this chart is complemented with the following boundary condition: For $q_c < 1.5$ MPa and $R_f > 5$ % the soil is classified as peat. This boundary conditions helps to better indicate the Holocene peat layers. An example of the adjusted Dutch SBT chart along a CPT profile is given in figure A.6 [18].

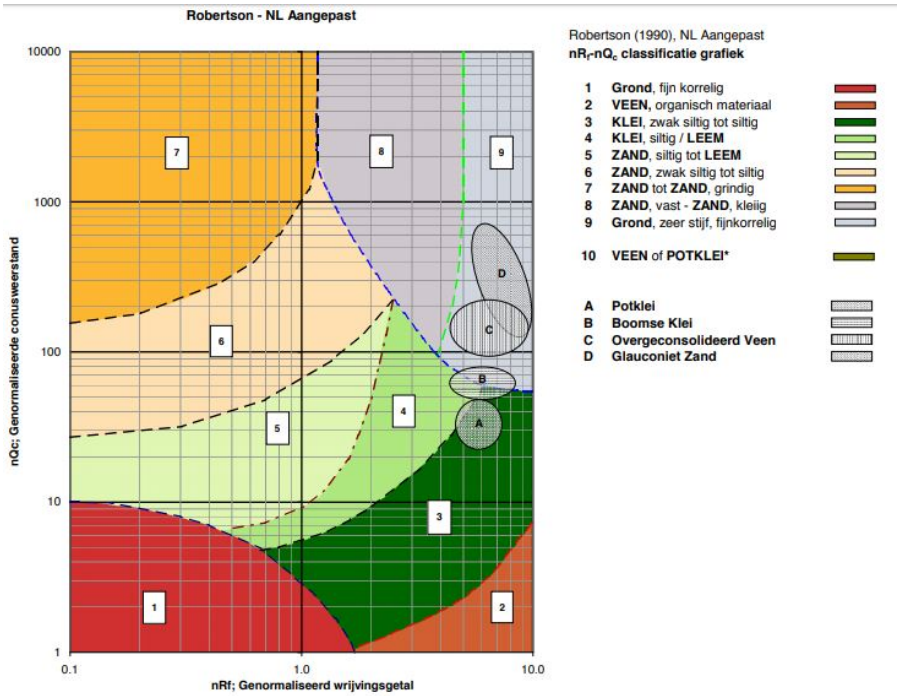

Figure A.2: Normalized SBT chart Robertson adapted for Dutch soil conditions [18]

A.2. Cone design

The cone is used to measure the cone tip resistance and friction ratio. The tip of the cone has a angle of approximately 60 degrees. The most common used cones have an area of 10 cm^2 or 15 cm^2 and a diameter of 35,7 and 43,7 mm respectively. Smaller cones (2 cm^2) are often used for shallow investigation, whereas relatively large cones (40 cm^2) are used to improve accuracy in case soft soils are present. With a some CPT types it is possible to measure pore pressures. There are 3 possible positions to measure the pore pressure. The most common, u_2, is behind the cone as can be seen in figure **??**.

A.2.1. CPT classes

A distinction between four CPT classes can be made according to their accuracy, type and distance between the measurements. The NEN determined the boundary conditions for every class, these are distinguished in table A.1 [35]. Class 1 CPTs are preferred when high accuracy is required, for example in soft soils.

A.2.2. Special cone types

The cone tip resistance in soft soils is very small, it was therefore concluded by Landva "that CPT is 'of little use' in determining the engineering properties of peat soils" [30]. A larger cone results in more accurate measurements of the tip resistance. In order to better identify these soft soils and to measure there differences special cone types are developed, the Ball probe and T-Bar as shown in figure A.4. Although the results are promising there is no standardisation in the design [30]. Besides that the cones are often too 'big' to use in

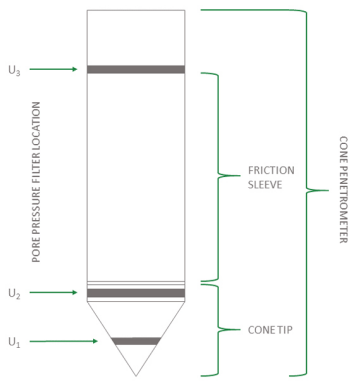

Figure A.3: Terminology for cone penetrometers [31]

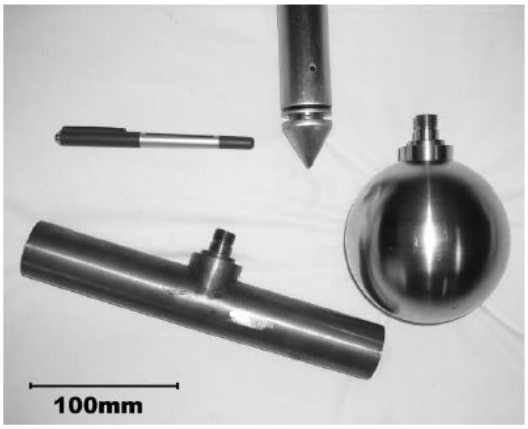

Figure A.4: Special cones for soft soil [30]

Table A.1: Different CPT classes [35]

CPT Class	Test Type	Measured Parameter	Allowed maximum accuracy	Maximum length between measurements
1	TE 2	Cone tip resistance Sleeve friction Pore pressure Inclination CPT depth	35 kPa or 5 % 5 kPa or 10 % 10 kPa or 2% 2 degrees 0.1 m or 1%	20 mm
2	TE1 TE2	Cone tip resistance Sleeve friction Pore pressure Inclination CPT depth	100 kPa or 5 % 15 kPa or 15 % 25 kPa or 3% 2 degrees 0.1 m or 1%	20 mm
3	TE1 TE2	Cone tip resistance Sleeve friction Pore pressure Inclination CPT depth	200 kPa or 5 % 25 kPa or 15 % 50 kPa or 5% 5 degrees 0.2 m or 2%	50 mm
4	TE1	Cone tip resistance Sleeve friction CPT depth	500 kPa or 5 % 50 kPa or 20 % 0.2 m or 1%	50 mm

dense sandy soils. Such cones are therefore not applicable when a combination of soft and dense soils are present, which often is the case in the Dutch subsoil. Moreover often the sleeve friction is not measured, which can cause complications in soil classification.

A.3. Estimation of volumetric weight of soil from CPT data

Robertson estimated the unit weight based on CPT data with equation A.7 [45]. The unit weight of soil divided by the unit weight of water (γ/γ_w) is plotted as diagonal lines on the non normalized SBT chart. In figure A.5 it can be seen that the lower limit of the lines reach till a minimum volumetric weight of 14 kN/m^2. Equation A.7 indicates volumetric weights which coincide with soft organic soils cannot be computed, as the minimum lies at approximately 12 to 13 kN/m^2. The unit weight of soft or organic soils is often overestimated with this formula or chart.

$$\gamma/\gamma_w = 0.27log(R_f) + 0.36log(q_t/p_a) + 1.236 \tag{A.7}$$

Besides Robertson, Mayne estimated the volumetric weight based on CPT data, see equation A.8 [33]. The main disadvantage is the iteration that has to be performed with this formula, due to the presence of the

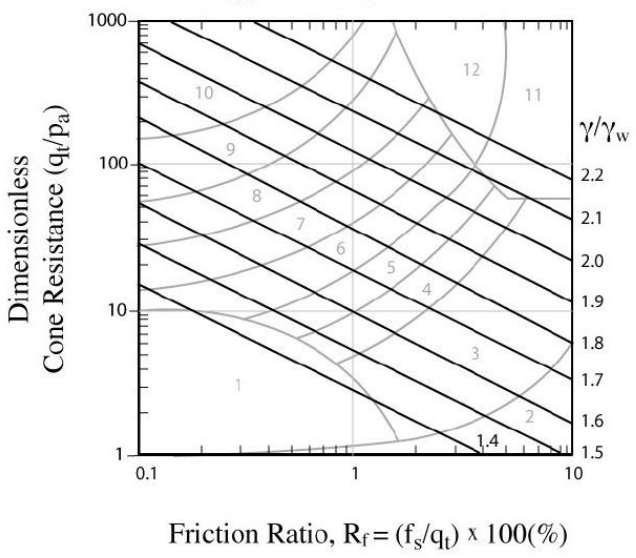

Figure A.5: Unit weight determined by Robertson [46]

effective stress σ'_{vo}. Similar to Robertson the formula of Mayne lacks accuracy in case the unit weight of soft soils has to be estimated.

$$\gamma = 1.95 \cdot \gamma_w (\frac{\sigma'_{vo}}{P_a})^{0.06} (\frac{f_s}{P_a})^{0.06} \tag{A.8}$$

A.4. Example CPT and BCPT

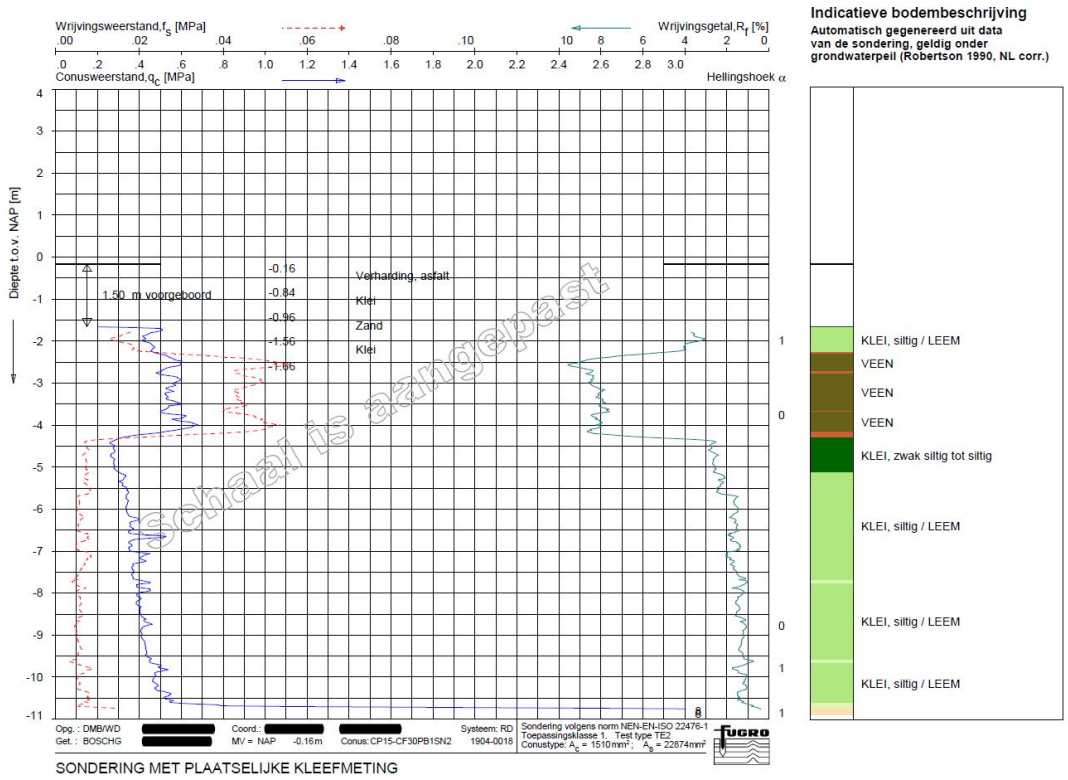

Figure A.6: Example of CPT profile with SBT Dutch corrected obtained in MMD project [17]

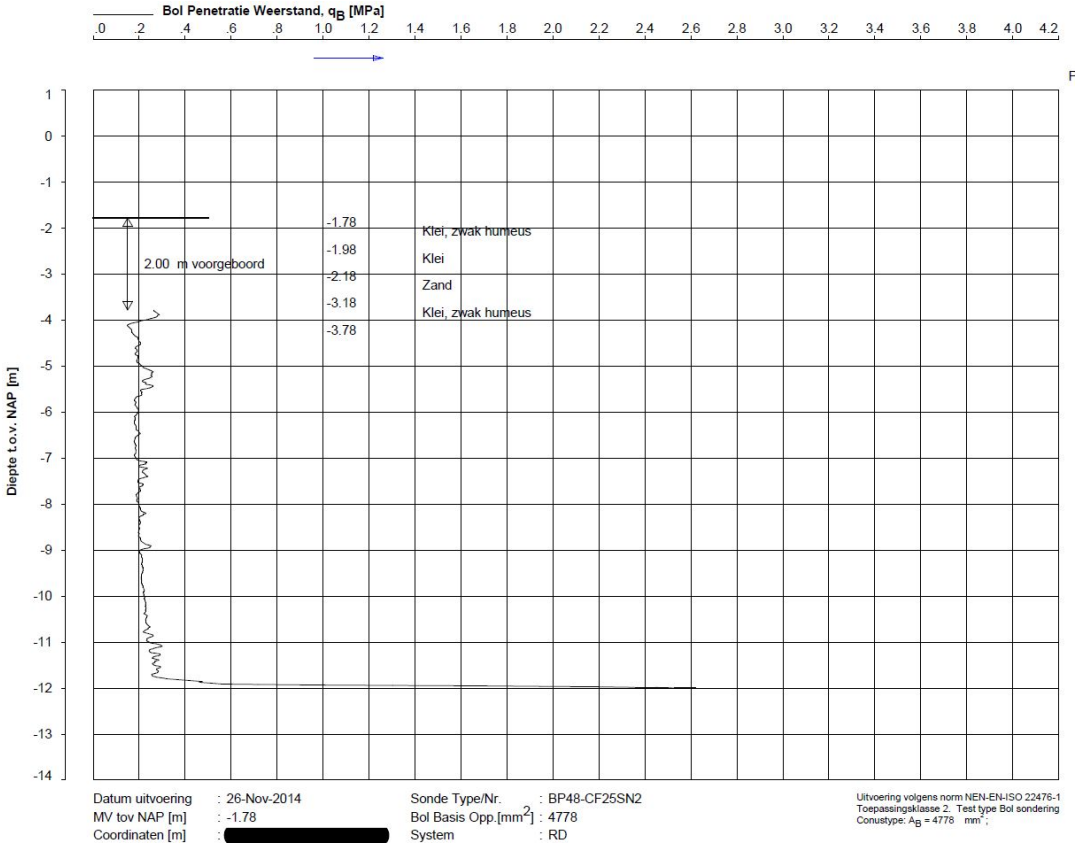

Figure A.7: Example of BCPT profile obtained in MMD project [17]

B

Parameters for determination s_u

In this appendix additional information regarding the quantification of the cone factor and the corresponding transformation and regional uncertainty is given. The requirements regarding the laboratory test which are used to determine N_{kt} are reviewed. Furthermore the adjustment in linearisation for local peaks in q_{net} and thereby the involved subjectivity is discussed.

B.1. Reflection requirements laboratory test

In this section the results of all DSS test in combination with the normalized cone tip resistance are shown. Furthermore the reason to reject the other laboratory test is evaluated.

B.1.1. Laboratory test used to determine Cone Factor

In tables B.1 and B.2 all the results obtained from DSS test which are used to determine the cone factor are presented. The borehole and depth at which the sample is obtained is indicated together with the cross sectional location. The s_u is determined 25% and 40% strain for clay and peat respectively. Some DSS test in clay C. failed before reaching the 25% strain. In such a case a deviation shear strength is used to determine the cone factor, these values are shown in column $s_{u,failure}$. Additionally the corresponding normalized cone tip resistance (q_{net}) is shown in tables B.1 and B.2.

Table B.1: DSS test used in cone factor determination of peat

Borehole	**Depth [m NAP]**	**Location**	$s_{u,40\%}$ **[kPa]**	q_{net} **[kPa]**
B25-1+90	-1.91	BI	28.7	463.4
B25-1+90	-2.46	BI	24.4	430.7
B25-1+90	-4.50	BI	17.5	382.0
B25-1+90	-4.88	BI	19.0	396.2
B25-1+90	-3.65	KR	42.0	583.1
B25-1+90	-4.15	KR	46.0	758.8
B25-2+90	-3.22	BI	19.7	292.1
B25-2+90	-3.95	BI	17.3	271.1
B25-2+90	-3.94	KR	35.2	719.4
B25-4+90	-3.62	BI	20.1	309.2
B25-4+90	-4.77	BI	21.4	441.8
B25-4+90	-5.05	BI	20.0	489.9
B25-4+90	-3.98	KR	40.4	779.7
B25-4+90	-5.19	KR	44.5	779.2
B28-130	-6.59	KR	25.0	526.6
B28-130	-5.36	KR	25.5	547.1
B28-131+90	-7.32	BI	27.9	367.6
B28-132+90	-3.07	BI	41.0	469.1
B28-132+90	-6.82	BI	35.0	509.2
B28-132+90	-7.47	BI	35.5	428.9

Table B.2: DSS test used in cone factor determination of clay C.

Borehole	Depth [m NAP]	Location	$s_{u,25\%}$ [kPa]	$s_{u,failure}$ [kPa]	q_{net} [kPa]
B3	-5.37	BI	14.0	13.9	348.1
B3	-5.57	BI	12.2	12.1	326.8
B3	-5.82	BI	15.4	16.5	340.0
B3	-5.97	BI	12.5	12.5	353.3
B3	-9.37	BI	17.4	17.9	398.0
B3	-9.77	BI	18.8	18.8	433.8
B3	-9.97	BI	14.5	15.2	433.6
B3	-5.36	BI	17.3	17.3	348.1
B3	-5.36	BI	15.7	15.7	348.1
B3	-5.41	BI	14.6	14.4	338.7
B3	-5.46	BI	12.8	13.3	334.1
B3	-5.52	BI	15.7	15.6	331.8
B3	-9.32	BI	20.3	20.5	387.0
B3	-9.47	BI	21.8	21.9	397.3
B4	-5.26	KR	16.0	16.9	259.9
B4	-5.41	KR	17.8	17.6	308.0
B4	-5.56	KR	14.9	15.5	280.5
B4	-5.71	KR	18.8	18.8	331.7
B4	-10.01	KR	21.2	21.1	365.9
B4	-10.26	KR	20.4	21.6	403.1
B4	-10.71	KR	25.7	26.5	446.4
B10	-7.52	BI	13.2	14.0	269.3
B10	-8.02	BI	11.4	11.9	266.9
B10	-7.36	BI	12.7	13.3	229.7
B10	-7.38	BI	14.3	14.5	230.2

B.1.2. Triaxial Test

Figure B.1 shows the 'accepted'[1] triaxial test conducted in the Markermeerdijken. Because triaxial test can not simply be compared with DSS test and due to the limited amount of test for each geological deposit it is determined that the triaxial test are not used in the determination of the cone factor.

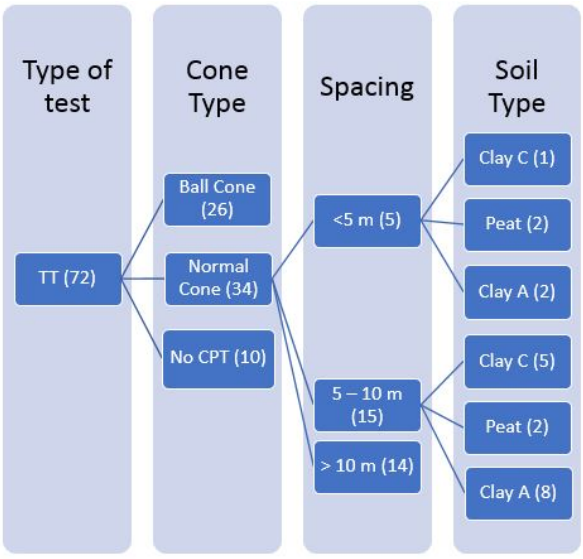

Figure B.1: Flow chart representing the requirements regarding laboratory test

[1] Based on the requirements in section 4.1

B.1.3. Rejected DSS test

In this section the cone factor (N_{kt}) is determined based on all available DSS test, implying that the requirements regarding sample disturbance etc. are not taken into account. The cone factors for peat and clay C. are shown in figure B.3 and B.2 respectively. The number of test for the cone factor determination are roughly doubled for both peat and clay C..

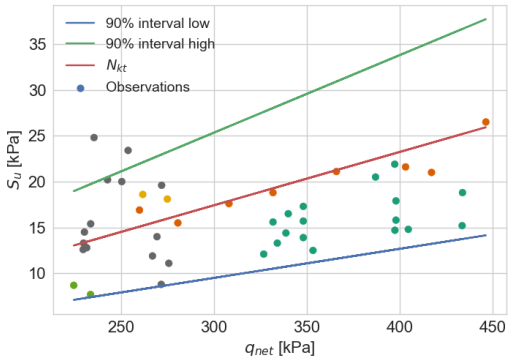

Figure B.2: N_{kt} for all DSS test on clay C.

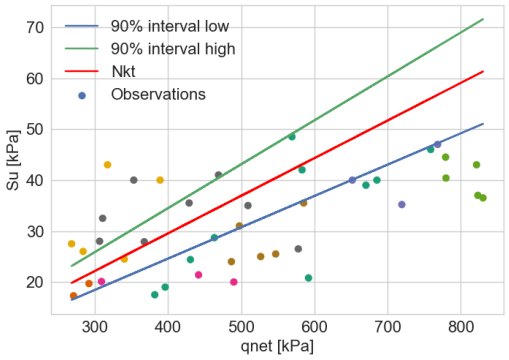

Figure B.3: N_{kt} for all DSS test on peat

The cone factor for ball cones, as presented in figure 4.6, has to be determined separately and therefore these DSS test are not taken into consideration.The test that are rejected due to large spacing between the borehole and CPT are also not taken into consideration, since a small spacing is required according to the guidelines [39].

The cone factors are 13.54 and 17.22 and the total variation coefficients (VC_{tot}) are 0.31 and 0.31 for peat and clay C. respectively, as can be seen in table B.3. Although the cone factor is smaller, the total variation coefficient is significantly larger. This indicates that a larger uncertainty in the determination of the cone factor is present. This uncertainty can partly be devoted to inaccurate laboratory test (rejected laboratory test). As a matter of fact this uncertainty can be excluded when laboratory test results are carefully analysed, as is done in this thesis.

Table B.3: Cone factors and variation coefficient based on accepted and rejected test

	Parameter	**Accepted test**	**Rejected and accepted test**
Clay	Number of test	25	43
	N_{kt}	19.62	17.22
	$VC_{av,reg}$	0.08	0.19
	VC_{trans}	0.15	0.25
	VC_{tot}	0.17	0.31
Peat	Number of test	20	46
	N_{kt}	15.98	13.54
	$VC_{av,reg}$	0.15	0.14
	VC_{trans}	0.19	0.28
	VC_{tot}	0.24	0.31

B.2. Determination design values undrained shear strength

In this section the determination of the cone factor, the transformation and regional uncertainty are elaborated. Different methods to determine the cone factor are presented and all equations and constants to determine the regional uncertainty are elaborated on.

B.2.1. Cone Factor

The determination of the cone factor in this thesis is based on the DOV method. Several other methods are available to determine the cone factor of which the following are briefly discussed in this appendix:

- DOV method
- Linear regression
- Linear regression through zero
- Mean N_{kt}
- Quadratic regression
- Quadratic regression through zero

At first is stated that calculation of the mean value of all $q_{net,i}/s_{u,i}$; the division of each normalized cone tip resistance by its corresponding undrained shear strength obtained from DSS or TT test is wrong. Applying this 'method' does not incorporate the random deviations towards an underlying relationship (the linearisation), the use of this 'method' can therefore introduce enormous errors in the cone factor estimation.

Because the undrained shear strength in the field is determined based on $s_u = q_{net}/N_{kt}$, the presented methods that cross the origin are preferred. The cone tip resistance divided by the cone factor will be zero in that case. Additionally the undrained shear strength cannot become negative.

In the linear regression it is assumed that variation along the presented line does not increase or decrease for the considered range q_{net} values. In the DOV method the variation along the presented line may increase with increasing q_{net} values. In practice the q_{net} increase with increasing s_u and therefore the DOV method conforms the trend found in practice [65].

Besides the linear regression methods also quadratic regression can be used to describe the cone factor. The maximum undrained shear strength found in the laboratory test is often limited. The undrained shear strength does not increase linearally with the normalized cone tip resistance at some point. In figure B.4 it can be observed that hardly any samples are present in the top right part of the graph. The figure shows that a quadratic regression results in a better fit for the available data. In practice often linear models are used and, therefore the quadratic method is not applied in the Dijken op Veen methodology [47].

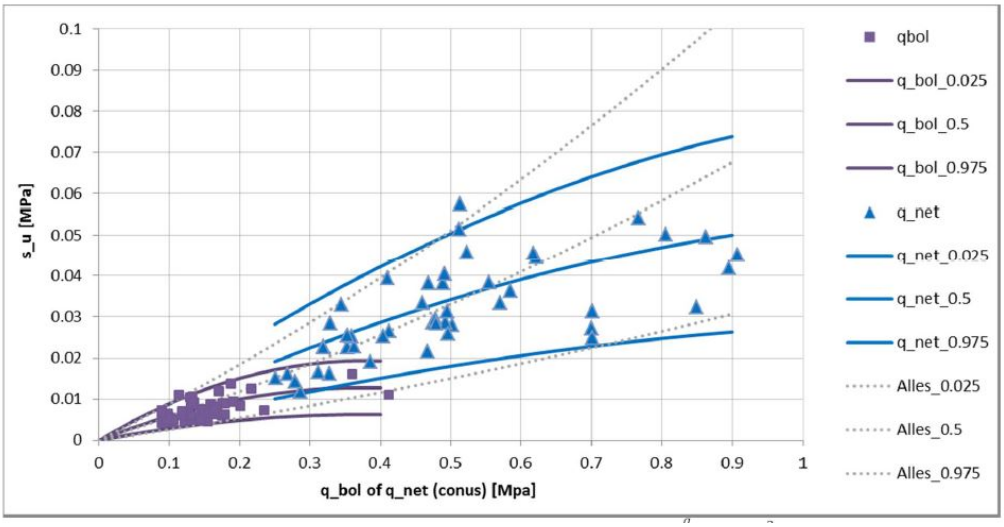

Figure B.4: Example of a quadratic regression in cone factor and VC_{Nkt} determination [47]

All methods are used to determine the best fit for the samples obtained in peat, this is presented in figure B.5. The figure shows no good distinction between the different method, additional data could result in more difference in between the methods. As shown in figure B.4 the quadratic method result in good estimations and it is therefore of interest to further investigate this regression type. The main disadvantage is the complexity compared to linear regression.

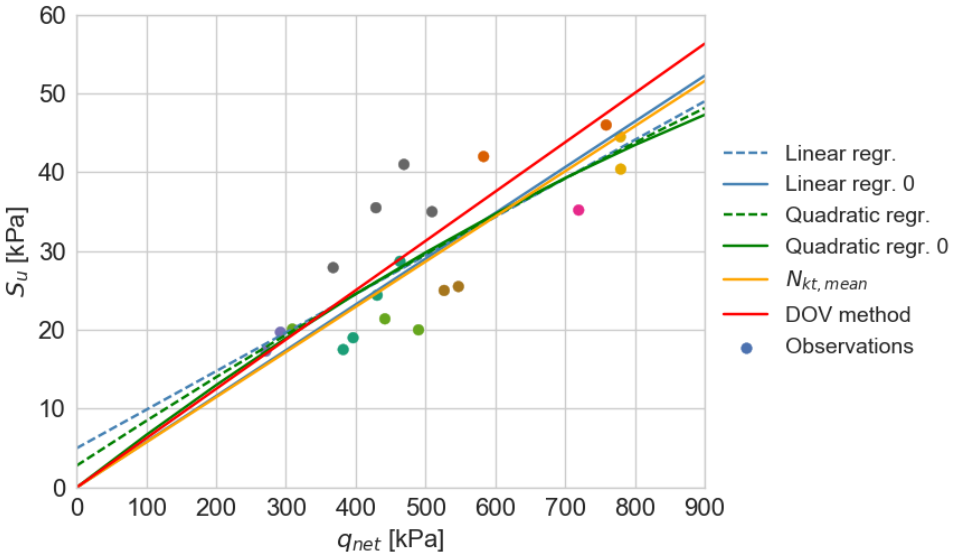

Figure B.5: All considered methods to determine the cone factor for peat in the MMD

B.2.2. Transformation uncertainty

In the 'Schematisatie Handleiding Macrostabiliteit' it is stated that at least 10 CPT-Borehole combination are required with at least 50 laboratory tests [57]. The requirements are not met in this thesis, since in both cone factor determinations fewer test are used. Sufficient test are performed in the field, however only 25 and 20 DSS test fulfilled the requirements stated in section 4.1.3. The 90% confidence interval used in this thesis for VC_{Nkt} is based on $k_n = 1.645$, this resembles an infinite amount of samples. k_n is equal to 1.725 and 1.708 for peat and clay C. when applying a student-t factor. The difference for peat is graphically represented in figure B.6. The difference in k_n is hardly noticable and it can therefore does not seem to influence the outcome significantly. Nevertheless the student-t factor is correctly applied in the new method [65] [59].

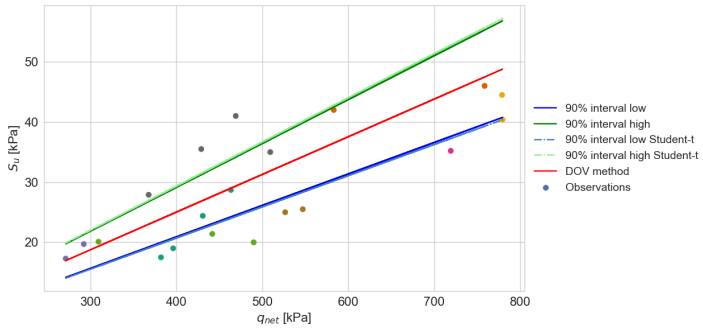

Figure B.6: Cone factor with statistical coefficient (k_n) based on infinite vs actual number or samples

B.2.3. Regional uncertainty

The estimation of all parameters considered the regional uncertainty determination are discussed within this section. bThe parameters and equations that are required to determine the regional uncertainty but are not described in chapter 4 are elaborated in this appendix.

$$VC_{loc,i} = \sqrt{\frac{\sum_{j=1}^{n_{meas,j}} \left(\frac{q_{net}}{N_{kt} \cdot s_{u,lin,i}} - 1\right)^2}{n_{m,loc}}} \tag{B.1}$$

Equation B.1 shows the local uncertainty, which resembles the error made in the linearisation of a single CPT. Combining VC_{loc} of multiple CPTs results in VC_{reg}. To determine the average regional uncertainty ($VC_{av,reg}$), factors that account for layer thickness and the ratio between local and regional uncertainty are taken into account as shown in equation B.2.

$$VC_{av,reg} = \sqrt{\frac{1}{n_{m,regional}} + \Gamma^2 + \gamma_v \cdot (1-\Gamma^2)} \cdot VC_{reg} \tag{B.2}$$

Equation B.3 describes the ratio between the local and regional uncertainty. The outcome of this equation is used to determine the variation reduction factor of the local average (Γ^2) which is used in $VC_{av,reg}$.

Furthermore a correction is applied for the presence of thin layers with equation B.5. In this equation t_{layer} represents the layer thickness found in a CPT. However VC_{reg} is determined for one geological layer with multiple CPTs. The vertical reduction factor γ_v depends on the layer thickness and can therefore vary for each CPT. Nevertheless γ_v is multiplied with VC_{reg} in equation 4.9. The layer thickness is therefore assumed to be a fixed value, it is uncertain if this is the mean, the lowest or the maximum value of t_{layer}. This can lead to misunderstanding and inaccurate estimations of $VC_{av,reg}$. To ensure sufficient conservatism the maximum value, equal to 1 in equation B.5, could be chosen. In this thesis the minimum value of t_{layer} is chosen to ensure sufficient safety. The vertical correlation length D_v is obtained from the DOV report and is equal to 0.3 for peat [11]. A similar value for clay C. is used in this thesis, it is however unknown if this is justified.

$$\alpha_v = \frac{\sum_{i=1}^{n_{cpt}} VC_{loc,i}^2}{n_{cpt} \cdot VC_{reg}} \tag{B.3}$$

$$\Gamma^2 \approx 1 - \alpha_v \tag{B.4}$$

$$\gamma_v \approx min(1, \frac{\sqrt{\pi} D_v}{t_{layer}}) \tag{B.5}$$

In which:

$s_{u,lin,i}$	=	Linearised undrained shear strength	$[kPa]$
$n_{m,loc}$	=	Number of measurements in one CPT	$[-]$
Γ^2	=	Variation reduction factor of local average	$[-]$
α_v	=	The ratio between local and regional uncertainty	$[-]$
γ_v	=	Vertical variation reduction factor	$[-]$
$VC_{loc,i}$	=	Local variation coefficient (per CPT)	$[-]$
t_{layer}	=	Layer thickness	$[m]$
D_v	=	Vertical correlation length (≈ 0.3)	$[-]$

Table B.4: Regional variation coefficients and associated parameters

	Clay C	**Peat**
α_v	0.07	0.13
Γ^2	0.93	0.87
γ_v	0.17	0.10
D_v	0.30	0.30
VC_{reg}	0.08	0.16
$VC_{av,reg}$	0.08	0.15

The input parameters to determine the regional uncertainty are presented in table B.4. These α and Γ^2 deviate significantly in comparison to the values presented in the DOV method. Due to: $\Gamma^2 + \gamma_v \cdot (1-\Gamma^2)$ in $VC_{av,reg}$, this difference hardly influences the regional uncertainty. A considerably large effort is required to understand these equations and to determine their outcome, whereas the influence of these input parameters is minimal. In new method the regional uncertainty is taken into account [65] [59].

B.3. Linearisation undrained shear strength

The undrained shear strength is linearised, thereafter this linearisation is adapted (where needed) to create the best representation for the considered undrained shear strength. The 'best representation' is a linearisation in which the major part of the undrained shear strength coincides with the linearisation. The linearisation of the undrained shear strength is therefore not simply an equation but involves proper judgement.

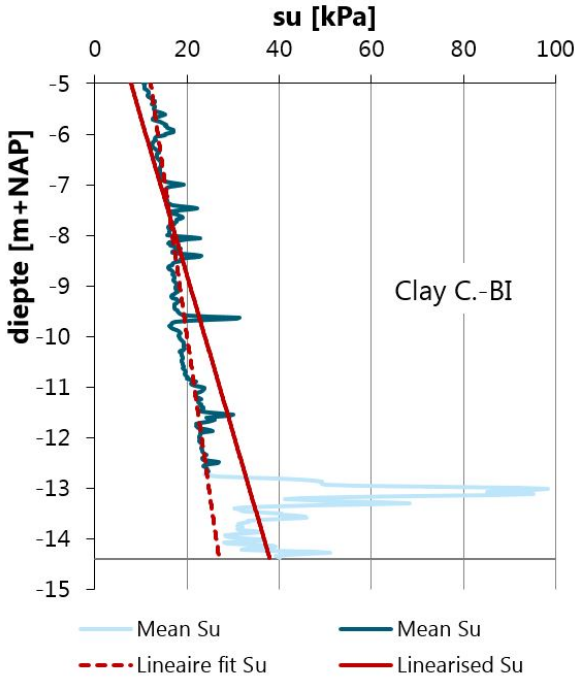

Figure B.7: Adapted linearisation results in rotation of the linearised s_u

Large local peaks in undrained shear strength can affect the angle or translate the linearisation, which results in incorrect estimations of $s_{u,top}$ and $s_{u,bottom}$. A translation occurs when the peak cone tip resistances are situated within the middle of the layer whereas a rotation occurs when the peaks are at the bottom or top part of the considered layer. In figure B.7 an example is given of the adapted linearisation. In figure B.7 part of the peak cone tip resistance at the bottom is not considered which results in a rotation of the linearisation. From equation 4.7 $s_{u,top}$ and $s_{u,bottom}$ are 7.5 and 38 kPa respectively. Due to the adjustment $s_{u,top}$ and $s_{u,bottom}$ are 12 and 27 kPa, mainly the undrained shear strength at top will have a major effect on the calculated stability.

Adjustment for large peaks can thus lead to a conservative or progressive linearisation and involves subjectivity. The error made within the linearisation is accounted for in VC_{reg}. However VC_{reg} is only based on CPTs within a testing field, whereas the error within the linearisation process originates from CPTs in the field. The error made within the linearisation in the testing field can differ from the one made in the field. The distance from the testing field up to the considered research area can be as large as 15 kilometre and therefore the soil structure can differ significantly. As an example the linearisation of a CPT in the testing field is shown. Based on the cone tip resistance and the friction ratio the clay C. layer in this CPT was thought to be situated from -4.5 m up to -11 m. During the linearisation process it became clear that peaks were present at depth of -6.1 m up to -9.2 m, this led to a overestimation of the linearisation at the top and bottom. Therefore the layer was divided into three separate layers as can be seen in figure B.8. The second layer consist of a different soil type and therefore must not be taken into account when the undrained shear strength is linearised. This thereby is a more realistic representation of the actual clay C. layer, additionally leads to a decrease in VC_{reg}, since the error in linearisation decreases.

Because the best linearisation is strived upon, in some cases one geological layer is split into two separate layers to provide a better linearisation. Although this yields the best represenation of the actual cone tip re-

sistance or undrained shear strength, it can cause a optimistic result when a probabilistic stability analysis is performed and the layers are assumed to be independent. As the number of independent layers increases in a probabilistic analysis the reliability increases. Therefore the consequences of a layer division regarding the probability of failure have to be kept in mind.

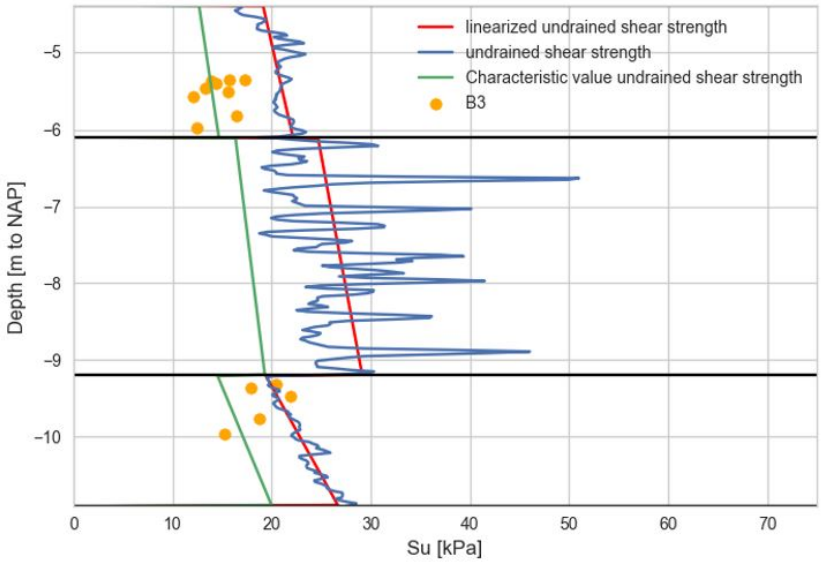

Figure B.8: Layer division to improve linearisation

In figure B.8 the obtained samples from the nearby borehole (B3) are presented with orange dots. It is noticeable that all obtained samples have a lower undrained shear strength in comparison to the estimated s_u from the CPT, some are even lower than the characteristic value ($s_{u,k}$) presented by the green line. It already became clear in figure 4.9 that all samples obtained from borehole B3 lie below the estimated cone factor. It is therefore desirable to use more CPT-Borehole combinations.

C

Sensitivity analysis and validation probabilistic stability analysis

In this appendix the effect of some assumptions and simplifications within the (semi) probabilitistic stability analysis are discussed. Furthermore the sensitivity analysis which is performed prior to the probabilistic stability analysis is presented.

C.1. Simplifications in semi Probabilistic analysis

C.1.1. Effect different ground levels

The influence of the ground level on the safety factor can be significant and therefore the effect of the simplified profile needs to be examined. The safety factor is determined for 9 cross section with the original ground level obtained from AHN data and the simplified ground level, see table C.1. The safety factors are determined with the LEM of Spencer for MHW conditions. The influence of the different ground level profiles can cause the safety factor to be higher or lower, with a maximum difference of 0.07. Although 0.07 is a relatively large difference in safety factor, the simplification in ground level does not affect half of the examined cross section.

Table C.1: Comparison effect safety factor of original and simplified ground level for 9 cross section for Spencer with MHW

Cross section	**Safety Factor original ground level profile (AHN)**	**Safety Factor representative ground level profile (CS 91 simplified)**
CS 51	1.15	1.15
CS 53	1.10	1.15
CS 66	1.10	1.10
CS 68	1.12	1.07
CS 71	1.19	1.18
CS 78	1.12	1.17
CS 85	1.10	1.10
CS 91	1.16	1.16
CS 95	1.12	1.19

C.1.2. Different Phreatic levels

In this section the effect of the simplification regarding the phreatic level are discussed. The phreatic lines in the Markemeerdijken are based on measurements performed in 3 monitoring wells along the research area and are schematised as indicated in the Technical Report 'Waterspanning bij dijken' [56]. The PL-lines differ along the 5 kilometre long research area and can be divided into three areas: CS 50-84, CS 85-92 and CS 93-100 as shown in table C.2. Since cross section 50-84 covers most of the 5 km long area and the calculated phreatic lines and hydraulic heads are the highest these are governing. The phreatic lines for CS 50-84 are used over the entire research area (CS 50-100). The assumption causes cross sections 85-100 to be modelled in a slightly conservative manner as is indicated in figure C.1. The safety factor is 0.03 lower on average for the simplified phreatic line for cross sections 85-100.

Table C.2: Level of the phreatic lines along the considered research area

	CS 50-84 [m to NAP]	**CS 85-92 [m to NAP]**	**CS 93-100 [m to NAP]**
MHW	-0.40	-0.40	-0.40
DHW	1.00	1.00	1.00
Polder level	-2.26	-2.26	-2.26
Water level KR MHW	1.35	0.55	0.55
Water level KR DHW	1.50	0.70	1.35
Hydraulic head in sand MHW	-2.40	-2.80	-2.80
Hydraulic head in sand DHW	-1.81	-2.14	-2.14

Figure C.1: Difference in safety factor between chosen PL-line and PL-line used in Markermeerdijken project for CS 85-100

C.2. Sensitivity analysis

A sensitivity analysis is performed prior to the probabilistic stability analysis. It provides insight in the relative influence of each parameter on the estimated safety factor. In this thesis the sensitivity analysis is used to indicate which parameters have the largest influence on the safety factor and thereby are of most interest to implement as stochastic variables in the probabilistic stability analysis. Since probabilistic stability analysis require a lot of computation time, a sensitivity analysis helps to determine which scenarios are most interesting to model.

The sensitivity analysis consist of multiple semi-probabilistic stability analysis which can help in the interpretation results of a probabilistic calculation. At first, the effect of MHW and DHW are investigated. Then difference in mean and characteristic s_u values are examined. Furthermore the effect of different schematisations on the safety factor are analysed.

C.2.1. Water level

As the water level increases, the phreatic level increases, which causes the effective stresses in the soil to decrease. As a result the undrained shear stresses decrease, which reduces the ability of the soil body to withstand the weight of the levee, and thereby increasing the probability of the inner slope to become unstable. In figure C.2 the difference in safety factor along the selected area during MHW and DHW are shown. Although the difference in water level is 1.4 m, the difference in safety factor is only 0.03 on average. The small difference in safety factor between MHW and DHW can be devoted to the relatively small change in PL-line (20 cm) within the levee.

Implementing MHW and DHW conditions results in a small change in safety factor and therefore the water level is kept constant at MHW in the probabilistic analysis. MHW conditions are chosen since this does not require the undrained shear strength to be rewritten into *POP* values.

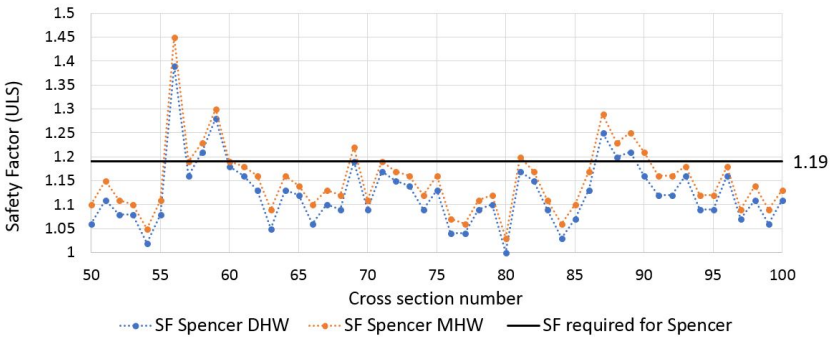

Figure C.2: Difference in safety factor between MHW and DHW calculated with Spencer

The Markermeer is a lake, the duration of high water level is therefore not comparable to a river. The water level within the lake depends on the discharge of the river IJssel and the water level in the IJsselmeer and can partly be controlled. The relatively long duration of height water could influence the phreatic level and thereby the stability. The effect of long lasting high water levels is not explicitly taken into consideration within this thesis.

C.2.2. Undrained shear strength

In practice often a calculation is performed based on design values to ensure sufficient safety is taken into account. The design value for the undrained shear strength is equal to the 5% quantile and depends on the regional and transformational variability, as explained in section 4.2. To determine the sensitivity of the undrained shear strength, multiple stability analysis with mean s_u values are performed. The difference between the mean and the 5% quantile can be significant. A calculation performed with mean s_u values can provide a good insight in the safety that is implemented by applying design values within the calculation.

The safety factor found for mean and design values of s_u is shown in figure C.3. Mean values for s_u result in a safety factor which is 1.5 times higher compared to the safety factor found for design values of s_u. This means that the use of the 5% quantile includes a significant amount of safety within the calculation. Obviously this difference in safety factor is the analogy regarding the use of design values.

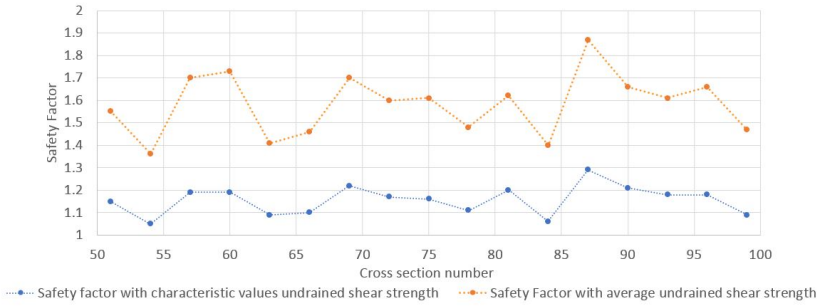

Figure C.3: Safety factor with average values for the undrained shear strength

As design values of s_u result in significantly lower safety factors in comparison to mean values, it is interesting to investigate the possibilities to reduce the uncertainty in the s_u and thereby increase the design value of s_u.

C.2.3. Schematisation

Although the stratification is assumed to be constant along the levee, the layer thickness differs in longitudinal direction. The influence of the layer thickness on the safety factor can not be examined as objective as the water level and the undrained shear strength. The R Pearson coefficient is used to conclude if there is a relation between the layer thickness and the safety factor. The layer thickness differs in cross sectional direction for each vertical (KR, BI and AL). The R Pearson coefficients are presented in table C.3.

Table C.3: Correlation between layer thickness and safety factor

	R pearson correlation coefficient [-]
Thickness Clay A2-KR	-0.56
Thickness Peat-KR	0.68
Thickness Clay C.-KR	0.00
Thickness Peat-BI	-0.39
Thickness Clay C.-BI	0.16
Thickness Peat-AL	-0.50
Thickness Clay C.-AL	0.17

The thickness of the peat-KR layer has a relatively high correlation coefficient of 0.68, table C.3. This seems logical since peat is the strongest layer within the cross section and therefore an increasing thickness results in a higher safety factor. In figure C.4, the layer thickness of peat and the safety factor are plotted; a thick peat layer under the crest often seems to coincide with a high safety factor.

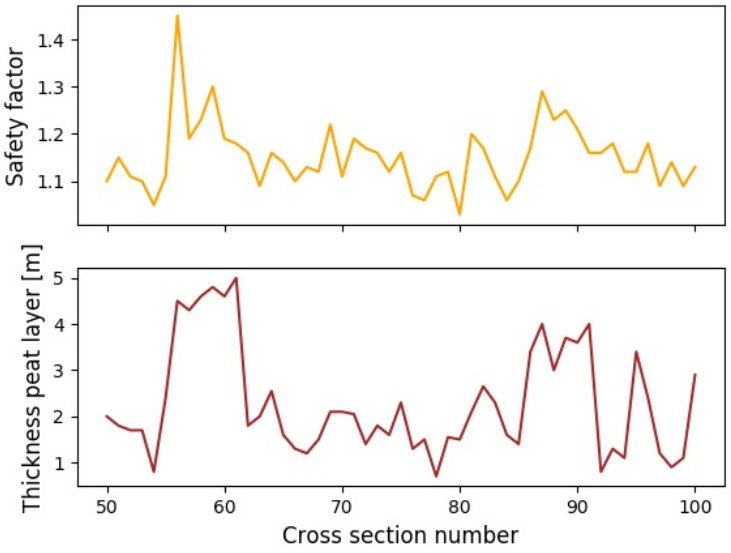

Figure C.4: Safety factor with average values for the undrained shear strength

The maximum safety factor, found in cross section 56, is most likely caused by the lack of a peat layer in the hinterland. The soil in the hinterland functions as a resisting force against the momentum of the soil weight of the levee. In cross section 56 the clay C. layer start at ground level due to absence of the peat layer. The clay layer is heavier in comparison to the peat layer and therefore results in a higher resisting force. In table C.3 the layer thickness of peat-AL shows a relatively strong negative correlation with the safety factor which means that a higher safety coefficient is present in case the layer thickness decreases.

Furthermore the clay A2. layer seems to have a strong negative correlation with the safety factor as well. As the layer becomes thinner the weight and thereby the driving force for levee instability decreases, as a result the safety factor decreases. Additionally, a thicker clay A2. layer will result in a thinner peat layer. The peat has a higher strength and it weights less, which both have a positive influence on the safety factor.

The correlation between the safety factor and the layer thickness as determined in this section is very useful. Besides that, it is also useful to determine the relation between the depth of the layer separation and the safety factor. In the probabilistic stability analysis the position of the layer separations are stochastically implemented and not the layer thickness itself. Secondly the depth of the top of the clay C. layer is more interesting in comparison with its layer thickness, because in most cases the lowest undrained shear strength

is present in the top of this layer. Therefore the correlation coefficient of the depth of the layer separation is also determined, see table C.4.

Table C.4: Correlation between depth layer separations and safety factor

Position layer separation	Pearson correlation coefficient
Depth Peat-KR top	0.56
Depth Clay C.-KR top	-0.11
Depth Peat-BI top	0.15
Depth Clay C.-BI top	0.50
Depth Clay C.-AL top	0.50

Table C.4 shows that the position of the top of the peat-KR layer is of importance with respect to the safety factor. A layer separation positioned closer to the ground level seems to coincide with a higher safety factor. This seems logical because the undrained shear strength is higher in the peat layer and its weight is lower. Layer separations between peat and clay C.-BI and clay C.-AL are equally correlated to the safety factor because they are assumed to be at equal depth, see section 5.1. In this analysis it is emphasized that this layer separation can have some influence on the safety factor. In addition, this sensitivity analysis shows that a thick peat-KR layer and a thin peat-AL layer will probably improve the stability of the levee.

C.3. Assumptions for the probabilistic stability analysis

In this section the results of the LEMs of Uplift Van and Spencer in a probabilistic stability analysis are compared to the results of the LEM of Bishop. The effect of different correlation matrices is examined and the difference between D-Geo Stability and D-Stability is discussed.

C.3.1. Different limit equilibrium methods

In this thesis the LEM of Bishop is used in the probabilistic stability analysis. It is assumed that this method provides an adequate assumption of the reliability since the critical slip surface is almost circular. In figure C.5 and C.6 the critical slip surface in cross section 62 calculated with the LEM of Uplift Van and Spencer are shown. It can be observed that both slip surfaces have near circular shape, which underlines that the application of Bishop is reasonable. In this section analyses are performed with the LEM of Uplift Van and Spencer to indicate the difference in the influence of each parameter and to quantify the difference in reliability.

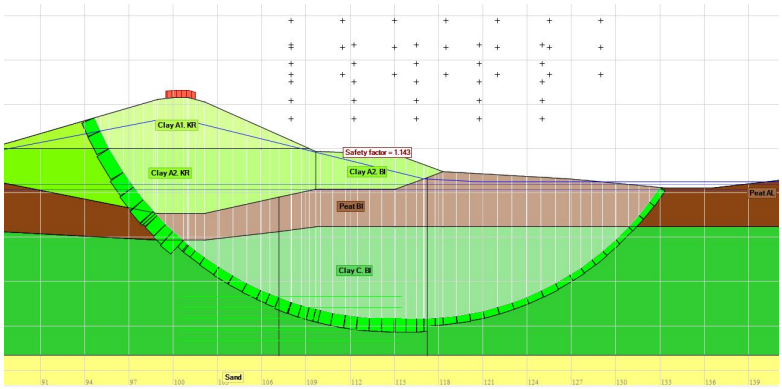

Figure C.5: Critical slip surface for the LEM of Uplift Van for cross section 62

Table C.5: Reliability index for cross section calculated with different LEMs

	β	$\beta_{cs,required}$
Bishop CS62	4.12	4.03
Uplift Van CS62	4.58	4.03
Spencer CS62	4.34	4.03

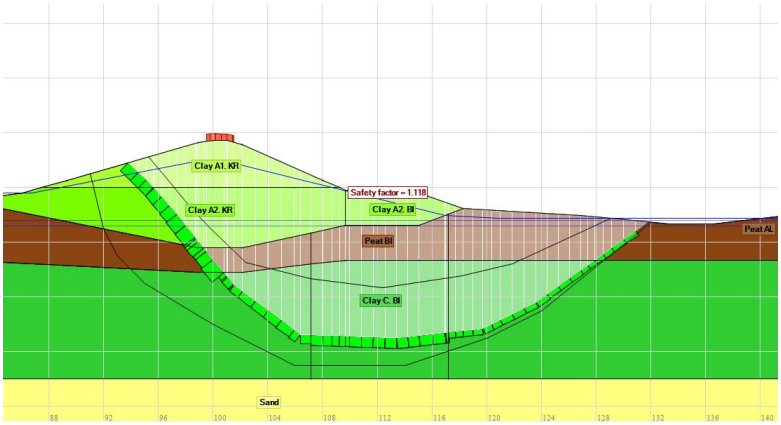

Figure C.6: Critical slip surface for the LEM of Spencer for cross section 62

In figure C.7 the difference in safety factor determined with the LEM of Bishop and Spencer for MHW is shown. The safety factor determined with the LEM of Spencer is lower since this method results in a more realistic schematisation of the actual slip surface. The required safety factor is therefore lower for the LEM of Spencer in comparison with the LEM of Bishop, see equation 3.1 and figure C.7. The difference in safety factor for the two LEMs is less than 0.02 on average.

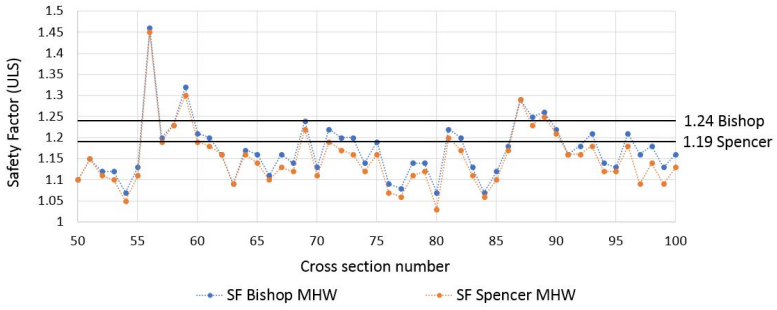

Figure C.7: Safety factor determined with the LEM of Bishop and Spencer for MHW

While for the semi probabilistic stability analysis the LEM of Spencer always results in lower/equal safety factors compared to the LEM of Bishop, this is not necessarily the case for a probabilistic analysis. The calculated reliability indexes are shown in table C.5. The LEMs of Uplift Van and Spencer are assumed to give a better representation of the actual critical slip surface and therefore the model factors are lower, see table 2.1. The lower model factors result in a higher reliability for the LEMs of Uplift Van and Spencer in comparison to the method of Bishop in this particular case. The estimated reliability is therefore dependent on the chosen model type. It can therefore be concluded that the assumption to use the LEM of Bishop results in a rather conservative approach compared to the other LEMs.

In figure C.8 and C.9 the influence and alpha factors for all LEMs are compared. The fact that the influence factors are more or less similar indicates that the critical slip surface is almost similar amongst the different LEMs.

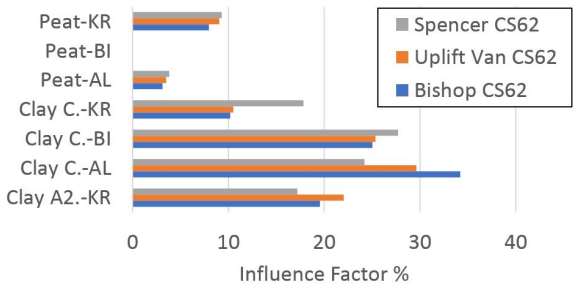

Figure C.8: Influence factors for different LEMs in cross section 62

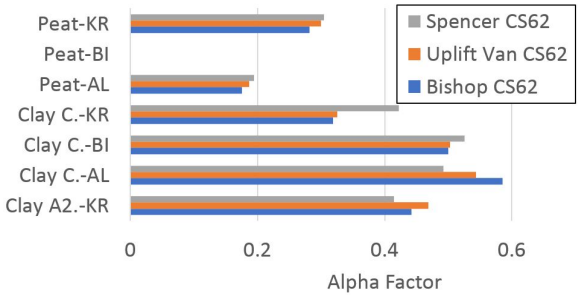

Figure C.9: Alpha factors for different LEMs in cross section 62

C.3.2. Effect correlations

In this section the assumed correlations within the probabilistic analysis are discussed. Incorrectly assuming independence in between parameters can results in optimistic reliability estimations in a probabilistic stability analysis. In the probabilistic stability analysis s_u at the top and bottom of each layer are correlated. In this section the correlation in horizontal and vertical direction is analysed. Although correlation in vertical direction in between layers is presented as an option here it is would not be logical since this indirectly means that S and m of different layers are correlated. Correlation is horizontal direction seems logical since peat-AL, peat-BI and peat-KR all have similar origin. Besides origin, the undrained shear strength mainly depends on load history which strongly differs in horizontal direction.

Five different scenarios are analysed. For all five scenarios the correlation between the top and bottom undrained shear strength value within the same layer remains equal to 1.0, this is referred to as the base case.

- Base case (similar as in chapter 5)
- Horizontal correlation within the same layer: $\rho = 0.3$
- Horizontal correlation within the same layer: $\rho = 0.7$
- Vertical correlation with different layers: $\rho = 0.3$
- Vertical correlation with different layers: $\rho = 0.7$

In table C.6 the reliability index determined for each scenario in cross section 83 is presented. It is hard to audit the correctness of the correlation matrix. An attempt is made by comparing the reliability to the estimated safety factor found for the considered cross section. The safety factor in cross section 83 for the LEM of Spencer is equal to 1.11, the required safety factor is 1.19. The required reliability ($\beta_{cs,req}$) is 4.03. Knowing that the probabilistic analysis results in slightly more optimistic reliability estimations compared to the semi-probabilistic analysis, the base case seems to give the best comparison with the semi-probabilistic analysis. The results obtained from the horizontal and vertical correlations are rather conservative. Since the exact correlation is unknown, the undrained shear strength is only correlated as in the base case and not based on origin (horizontal direction). The alpha and influence factors are shown in figures C.10 and C.11.

Table C.6: Reliability index for different correlations in between s_u in a probabilistic calculation

Scenario	β
Base case	3.88
Horizontal 0.3	3.36
Horizontal 0.7	2.93
Vertical 0.3	3.44
Vertical 0.7	3.06

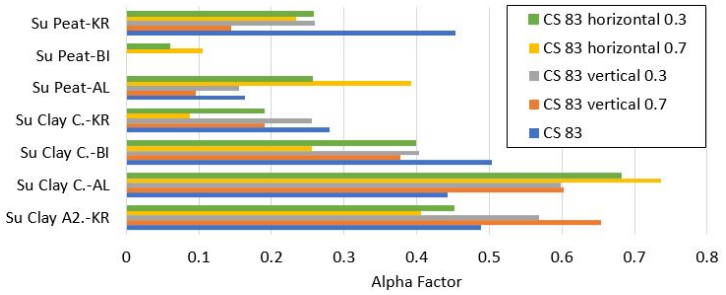

Figure C.10: Alpha factors s_u for different correlations in either horizontal and vertical direction for cross section 83

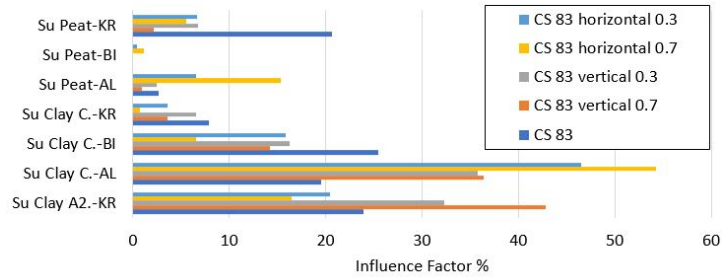

Figure C.11: Influence factors s_u for different correlations in either horizontal and vertical direction for cross section 83

C.3.3. Difference D-Stability and D-Geo Stability

A semi probabilistic model is used as input in the Probabilistic Toolkit. D-Stability provides the input for the Probabilistic Toolkit, while the semi probabilistic analysis in chapter 5.1 and 5.2 are performed with D-Geo Stability. D-Geo Stability does not generate the correct output files to use in the Probabilistic Toolkit, therefore D-Stability (provided by Deltares) is used.

In general both software packages should provide similar results when the input parameters are the same. In the semi-probabilistic analysis the POP_{top} and POP_{bottom} are used as input values whereas in the D-Stability $s_{u,top}$ and $s_{u,bot}$ are implemented. The s_u values are implemented since it was concluded that changes in outside water levels and phreatic levels hardly effect the estimated safety factor. The probabilistic stability analysis are only based on MHW, which makes rewriting s_u's to POP values superfluous. The different implementation results in a slight change in safety factors as shown in table C.7. The small difference in safety factor is not considered in the elaboration of the results.

Table C.7: Differences in safety factor for D-Geo Stability and D-Stability

Cross section	Safety factor D-Geo Stability	Safety factor D-stability
62	1.16	1.15
80	1.07	1.06
83	1.13	1.12

D

Additional information entropy

In this appendix some of the assumptions regarding (normalized) entropy are elaborated on. The corrected safety factors for all interval sizes within the considered research area are presented.

D.1. Discrete and continuous entropy

In this thesis only the discrete entropy is used to determine the uncertainty in s_u of a specified layer. In this section the difference between continuous and discrete entropy is explained. The continuous entropy in equation D.1 depends on the mean, standard deviation, and distribution type.

$$h(X) = -\int_X f(x) ln f(x) dx \tag{D.1}$$

As an example the continuous entropy of a normal distribution is shown in this section. The normal distribution is known as the distribution with the maximum entropy compared to all other continuous distribution with the same variance [62] [3]. The probability density function of a normal distribution is shown in equation D.2, resulting in entropy in equation D.3. Equation D.3 shows that only the standard deviation (σ_x) influences the entropy/uncertainty, which is logical since there is no uncertainty when the standard deviation is zero (i.e. a deterministic value). The continuous entropy has the undesirable property that it can be negative; implying negative uncertainty/information.

$$f(x) = \frac{1}{\sqrt{2\pi\sigma_x^2}} e^{-\frac{(x)-\mu_x)^2}{2\sigma_x^2}} \tag{D.2}$$

$$H_{max,gaus} = \frac{1}{2} ln(2\pi e\sigma_x^2) \tag{D.3}$$

Generally a continuous formula can be derived by taking the limit to zero for the discrete counterpart. Taking the limit of the continuous entropy leads to an infinite offset in the limit! The continuous entropy simply replaces the sum sign in the discrete entropy with a integral. The continuous entropy and discrete entropy are two different things; as a matter of fact, the "continiuous entropy is not a derivation of anything" [32]. The discrete entropy can therefore not be compared to the continuous entropy.

D.2. Effect of rounding entropy

Prior to the determination of the (normalized) entropy the values for s_u are rounded up to zero decimals. This adjustment is required because the datasets are relatively small, 12 to 51 samples respectively. The probability that s_u is identical at two locations is very small in case these values are not rounded.

The rounding to zero decimals has a significant influence on the determined entropy, but is necessary to analyse $s_{u,ld}$ with limited amount of samples. The s_u in the top of clay C.-KR layer for a 100 m interval size is used as an example in table D.1. The entropy is analysed for four different accuracy levels: 2 decimals, 1 decimals, rounded up to 0.5 and, zero decimals. As a result of rounding the difference between 2 and 0 decimals results in a difference of 1.36 nat. Although the difference is large, the adjustment is still necessary. If the maximum entropy is already reached for a 100 m interval size, all other interval sizes would also be equal to the maximum entropy. Rounded s_u values are used to cope with relatively small datasets.

Table D.1: Effect of rounding s_u to determine entropy (top of clay C.-KR layer for a 100 m interval size)

Accuracy in decimals	H(X) [nat]	$H_{max,dis}$ [nat]
0.01	3.81	3.93
0.1	3.57	3.93
0.5	2.91	3.93
1	2.45	3.93

D.3. Other methods to analyse the undrained shear strength in longitudinal direction

It could be discussed if the use of entropy for this problem is the best suitable method. Entropy only considers probability of occurrence of s_u and does not consider the actual value. Therefore, entropy does not focus on the minimum or maximum values whereas in levee design the lowest s_u value is of most interest, since this often coincides with low values for the safety factor. In chapter 6 it is briefly addressed that other statistically methods perhaps could also bring relieve regarding the uncertainty in $s_{u,ld}$. In this section three different methods are discussed: the Student-t method, maximum likelihood estimation and the relative entropy.

The Student-t distribution accounts for small sample sizes and is often applied in engineering practice. The Student-t distribution is not suitable for this problem since the difference in statistical coefficient (k_n) becomes nearly constant after 10 samples. The difference between a 100 and 400 m interval would therefore be very limited; as they contain 51 and 12 samples respectively.

The maximum likelihood estimation helps to indicate which mean and standard deviation given a distribution type are most likely to coincide with the available data. A given dataset, containing undrained shear strength values can be described by infinitely many different distributions. The maximum likelood estimation gives the mean and standard deviation which are most likely to describe the given dataset. The main difference with entropy is that prior to the estimation a distribution type is required. In practice the undrained shear strength is most often assumed to be log-normal distributed, since it is impossible to obtain negative strength. This method could therefore estimate the mean and standard deviation for a given dataset. As the number of CPTs increases the mean and standard deviation of s_u tend to become constant, under the assumption that the research area remains constant. Although the standard deviation is indirectly a measure of information it is less convenient to compare with other standard deviations. Obviously the actual values of s_u are considered in the case the maximum likelihood estimation is used.

In the case more s_u measurement within the same CPT (in vertical direction) are used the problem regarding small datasets (12 to 51 data points) could be overcome. It is thought to be useful to apply KL-divergence or cross entropy on the cone tip resistance in between two successive CPTs within the same layer to analyse their relative entropy [26]. This could be an alternative method to compare CPT results which could be more reliable, since it uses the entire q_c profile instead of a value at the top and bottom. Prior to the use of relative entropy the q_c profile should be normalized to delete any trend in the data. However the comparison does not only consider fluctuations in horizontal direction but also considers fluctuations in vertical direction.

D.4. Corrected safety factors

In table D.2 and figure D.1 the spatial factor at the top and bottom of each layer for different interval sizes is presented. Because the uncertainty in the peat layers is larger in comparison to clay C., $\gamma_{su,ld}$ is generally slightly larger.
In the figures D.2 till D.10 the corrected safety factor is determined for the interval sizes 200, 300 and 400 meter. As can be seen from these figures some of the results do properly account for larger interval sizes, whereas others are rather conservative. Conservative estimations could be overcome by decreasing the maximum value of $\gamma_{su,ld}$.

Table D.2: Average $\gamma_{su,ld}$ at interval 100m, 200m, 300m and 400m for all layers at the top and bottom

	Interval	100 m	200 m	300 m	400 m
KR	$\gamma_{su,ld}$ clay C.-top	1.00	1.11	1.22	1.30
	$\gamma_{su,ld}$ clay C.-bot	1.00	1.11	1.21	1.30
	$\gamma_{su,ld}$ clay A2.-top	1.00	1.12	1.25	1.30
	$\gamma_{su,ld}$ clay A2.-bot	1.00	1.12	1.24	1.30
	$\gamma_{su,ld}$ Peat-top	1.00	1.14	1.28	1.30
	$\gamma_{su,ld}$ Peat-bot	1.00	1.15	1.30	1.30
BI	$\gamma_{su,ld}$ clay C.-top	1.00	1.09	1.19	1.28
	$\gamma_{su,ld}$ clay C.-bot	1.00	1.11	1.23	1.30
	$\gamma_{su,ld}$ Peat-top	1.00	1.13	1.27	1.30
	$\gamma_{su,ld}$ Peat-bot	1.00	1.12	1.25	1.30
AL	$\gamma_{su,ld}$ clay C.-top	1.00	1.08	1.15	1.23
	$\gamma_{su,ld}$ clay C.-bot	1.00	1.10	1.19	1.29
	$\gamma_{su,ld}$ Peat-top	1.00	1.11	1.23	1.30
	$\gamma_{su,ld}$ Peat-bot	1.00	1.09	1.18	1.27

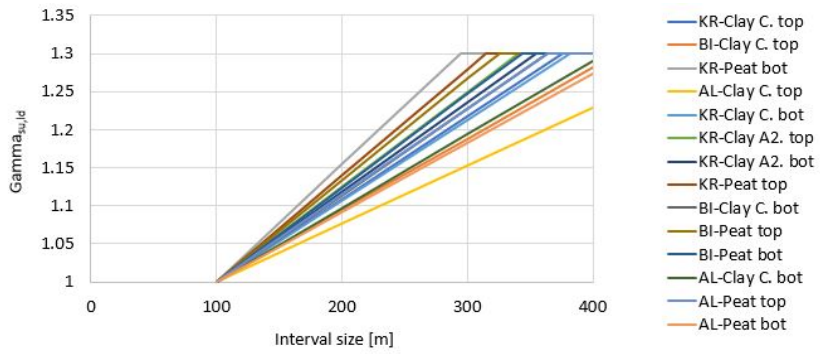

Figure D.1: Average $\gamma_{su,ld}$ at interval 100m, 200m, 300m and 400m for all layers at the top and bottom

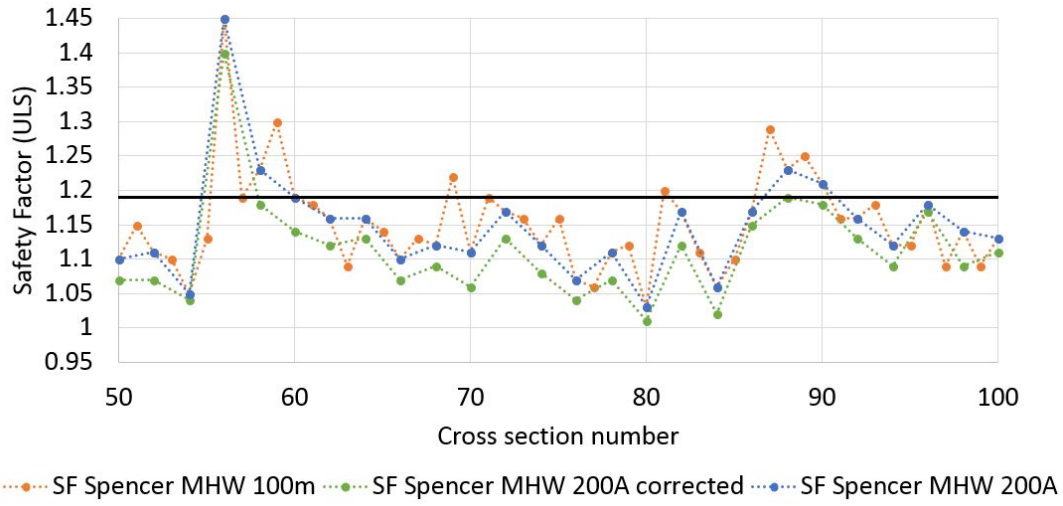

Figure D.2: Recalculated safety factor for an interval of 200A m based on adjusted undrained shear strength

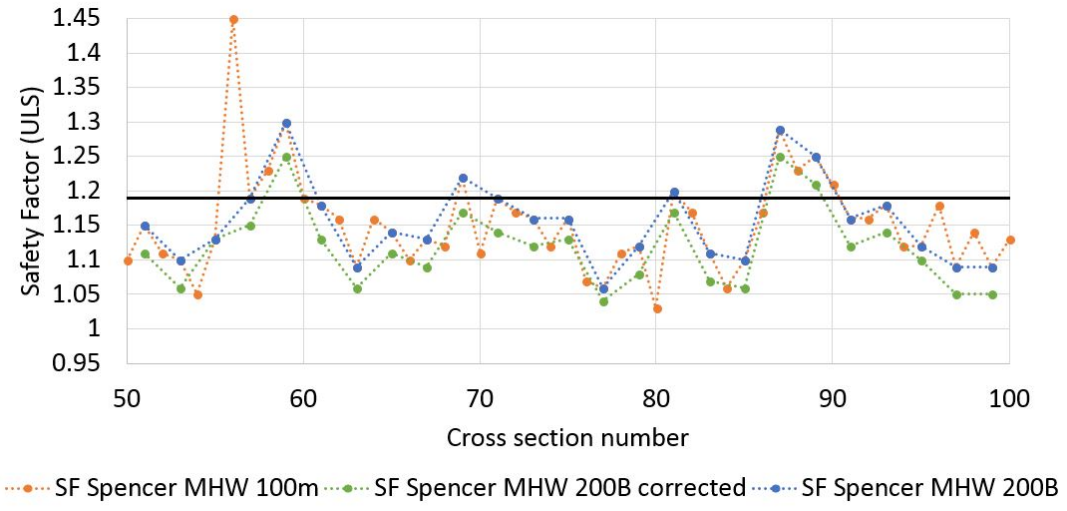

Figure D.3: Recalculated safety factor for an interval of 200B m based on adjusted undrained shear strength

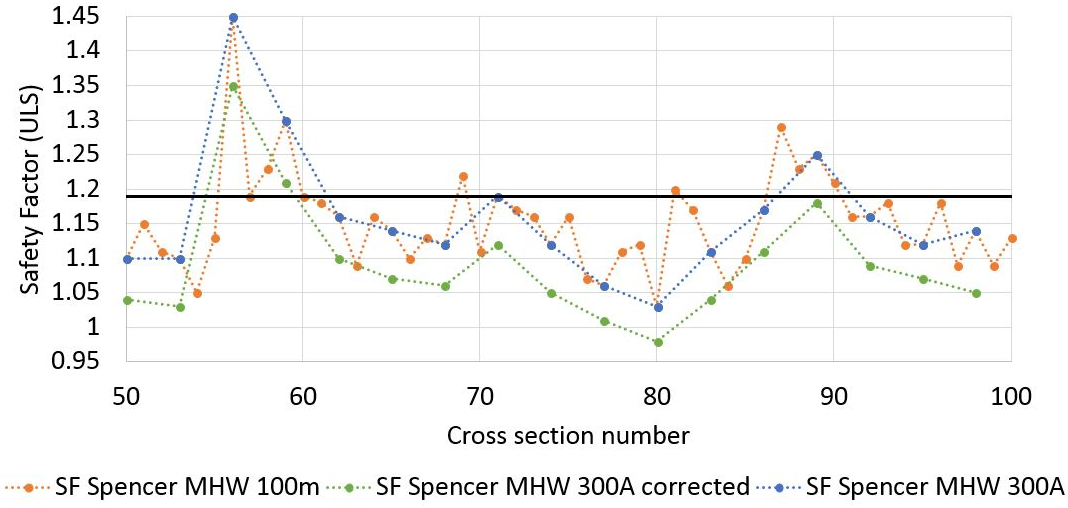

Figure D.4: Recalculated safety factor for an interval of 300A m based on adjusted undrained shear strength

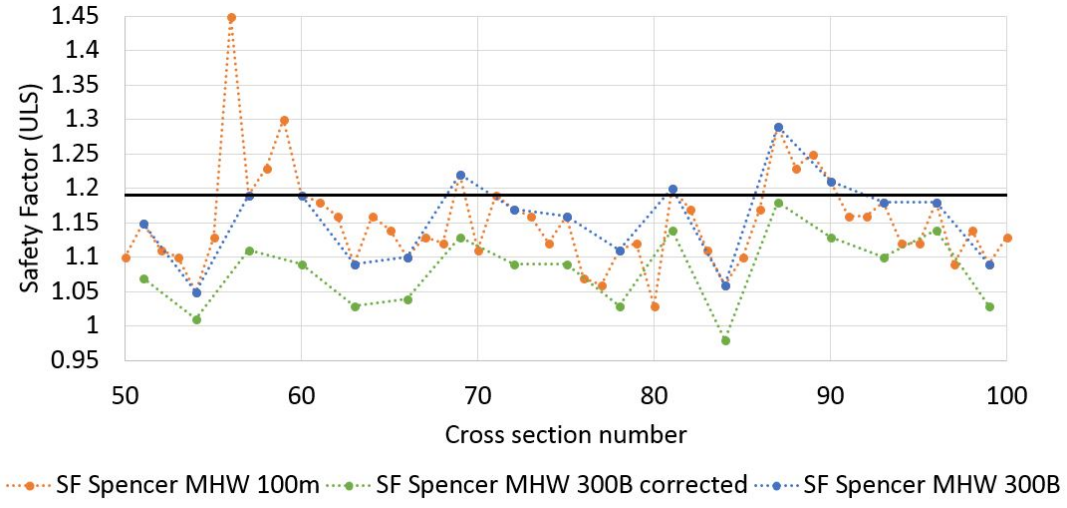

Figure D.5: Recalculated safety factor for an interval of 300B m based on adjusted undrained shear strength

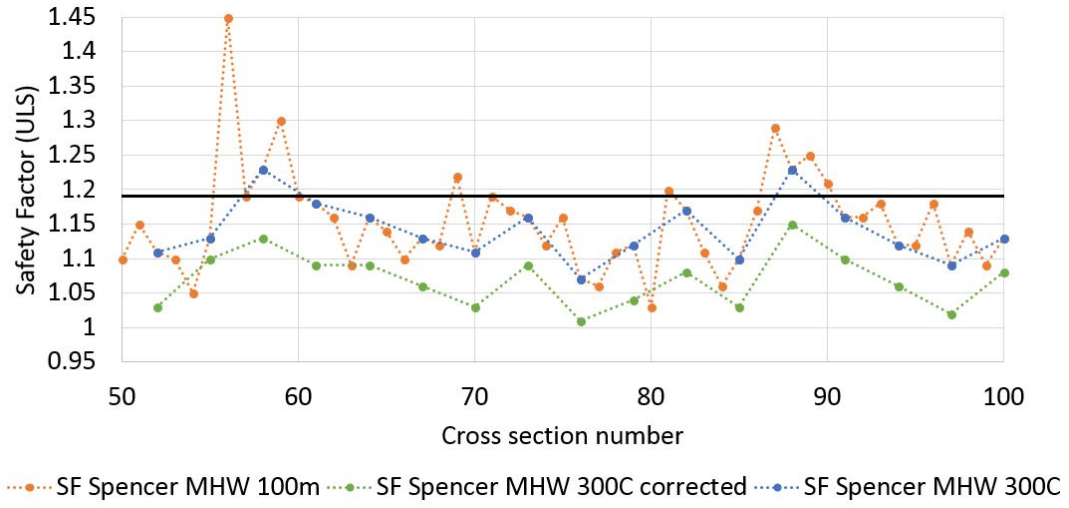

Figure D.6: Recalculated safety factor for an interval of 300C m based on adjusted undrained shear strength

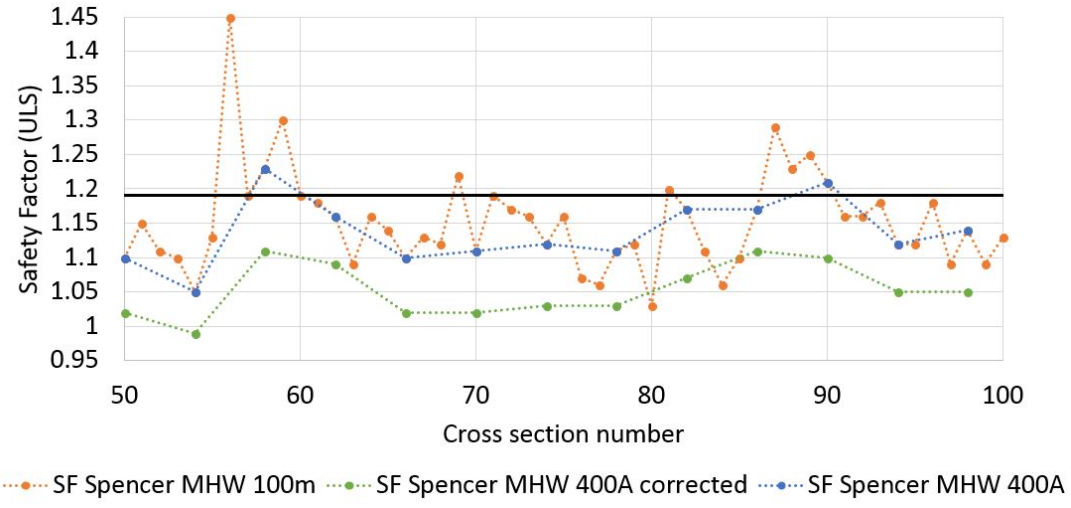

Figure D.7: Recalculated safety factor for an interval of 400A m based on adjusted undrained shear strength

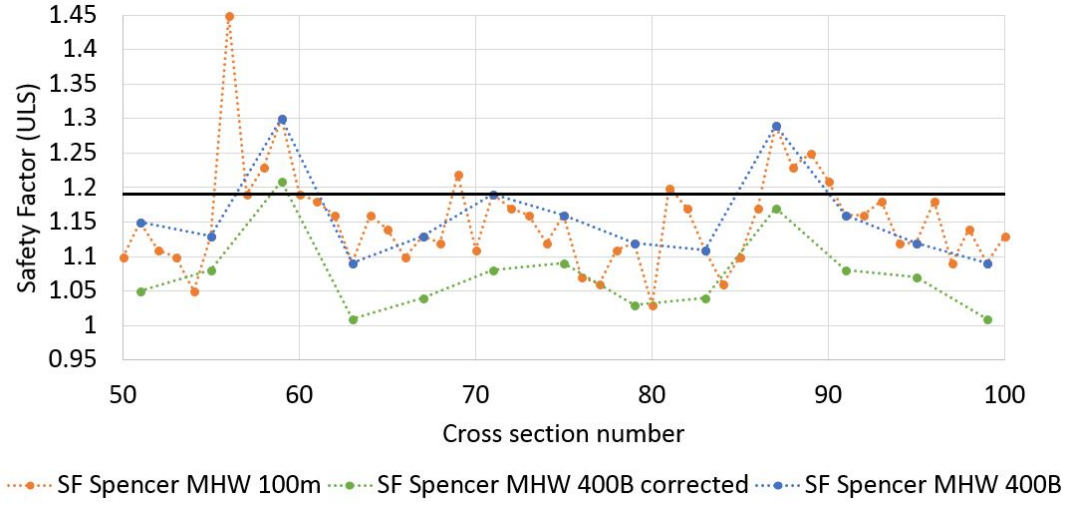

Figure D.8: Recalculated safety factor for an interval of 400B m based on adjusted undrained shear strength

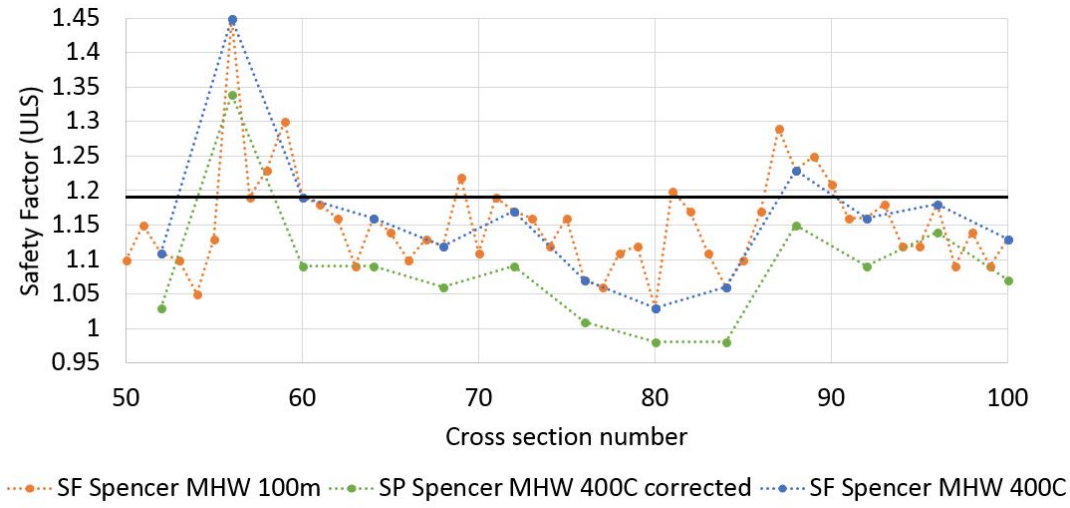

Figure D.9: Recalculated safety factor for an interval of 400C m based on adjusted undrained shear strength

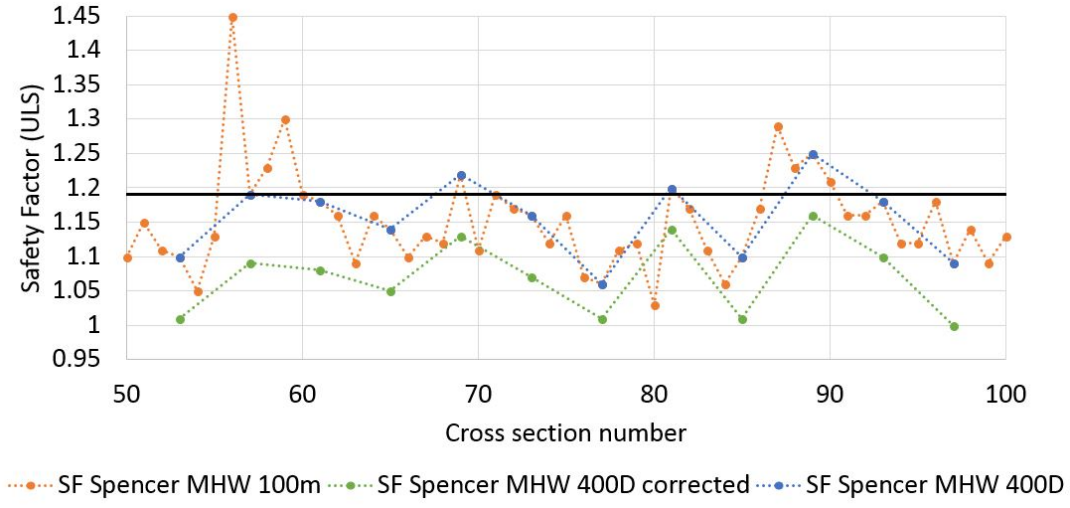

Figure D.10: Recalculated safety factor for an interval of 400D m based on adjusted undrained shear strength

E

Research Location

The content of this Appendix is confidential.